UNIVERSIDADE FEDERAL DE MINAS GERAIS

Using Computational Models and Clinical Data From Depth Electrode Implants to Evaluate Active Probing Paradigms in Epilepsy

Usando Modelos Computacionais e Dados Clínicos de Eletrodos Cerebrais Profundos Para Avaliar Paradigmas de Sondagem Ativa em Epilepsia

Vinícius Rezende Carvalho

Belo Horizonte

2021

UNIVERSIDADE FEDERAL DE MINAS GERAIS

ESCOLA DE ENGENHARIA

PROGRAMA DE PÓS-GRADUAÇÃO EM ENGENHARIA ELÉTRICA

Using Computational Models and Clinical Data From Depth Electrode Implants to Evaluate Active Probing Paradigms in Epilepsy

Vinícius Rezende Carvalho

Thesis presented to the Universidade Federal de Minas Gerais' Graduate Program in Electrical Engineering. In partial fulfillment of the requirements for the degree of PhD in Electrical Engineering.

Concentration Area: Signals and Systems

Advisor: Prof. Dr. Eduardo Mazoni Andrade Marçal Mendes

Co-advisor: Prof. Dr. Márcio Flávio Dutra Moraes

Belo Horizonte

2021

C331u

Carvalho, Vinícius Rezende.
Using computational models and clinical data from depth electrode implants to evaluate active probing paradigms in epilepsy [recurso eletrônico] / Vinícius Rezende Carvalho. - 2021.
1 recurso online (97 f. : il., color.) : pdf.

Orientador: Eduardo Mazoni Andrade Marçal Mendes.
Coorientador: Márcio Flávio Dutra Moraes.

Tese (doutorado) - Universidade Federal de Minas Gerais, Escola de Engenharia.

Apêndice: f. 97.

Bibliografia: f. 81-96.
Exigências do sistema: Adobe Acrobat Reader.

1. Engenharia elétrica - Teses. 2. Epilepsia - Teses. 3. Predição (Logica) - Teses. 4. Neurociência computacional - Teses. I. Mendes, Eduardo Mazoni Andrade Marçal. II. Moraes, Márcio Flávio Dutra. III. Universidade Federal de Minas Gerais. Escola de Engenharia. IV. Título.

CDU: 621.3(043)

Ficha catalográfica elaborada pela bibliotecária Roseli Alves de Oliveira CRB/6 2121
Biblioteca Prof. Mário Werneck, Escola de Engenharia da UFMG

"Using Computational Models and Clinical Data From Depth Electrode Implants To Evaluate Active Probing Paradigms In Epilepsy"

Vinícius Rezende Carvalho

Tese de Doutorado submetida à Banca Examinadora designada pelo Colegiado do Programa de Pós-Graduação em Engenharia Elétrica da Escola de Engenharia da Universidade Federal de Minas Gerais, como requisito para obtenção do grau de Doutor em Engenharia Elétrica.

Aprovada em 16 de setembro de 2021.

Por:

Prof. Dr. Eduardo Mazoni Andrade Marçal Mendes
DELT (UFMG) - Orientador

Prof. Dr. Márcio Flávio Dutra Moraes
(UFMG)

Prof. Dr. Antonio Carlos Roque da Silva Filho
Departamento de Fisica (FFCLRP, Universidade de Sao Paulo)

Prof. Dr. Jean Faber Ferreira de Abreu
Departamento de Neurologia/Neurocirurgia. (Universidade Federal de São Paulo)

Prof. Dr. Vinícius Rosa Cota
Departamento de Engenharia Elétrica (Universidade Federal de São João Del-Rei)

Leonardo A. B. Tôrres

Prof. Dr. Leonardo Antônio Borges Tôrres
DELT (UFMG)

This work was conducted at:

- Núcleo de Neurociências (NNC), Departamento de Fisiologia e Biofísica do Instituto de Ciências Biológicas), A4 168/240, Universidade Federal de Minas Gerais (UFMG), Belo Horizonte, Brasil.

- Cortical Physiology Laboratory. Thier Research Building, Massachusetts General Hospital, Boston, MA 02114

Funding was provided by the following:

- Coordenação de Aperfeiçoamento de Pessoal de Nível Superior – CAPES;
- Conselho Nacional de Desenvolvimento Científico e Tecnológico – CNPq;
- Fundação de Amparo à Pesquisa do Estado de Minas Gerais – FAPEMIG
- Pró-Reitoria de Pesquisa UFMG – PRPq/UFMG

Dedico este trabalho a meus pais, que tornaram tudo isso possível.

ACKNOWLEDGEMENTS / AGRADECIMENTOS

Tenho o privilégio de ser rodeado por pessoas que tornaram esse trabalho possível. A começar por minha família, minha fundação e âncora em todos os momentos de minha vida. Agradeço a meus pais, fonte inesgotável de carinho, orientação e apoio. Eu não seguiria este caminho se não fosse pelo suporte de vocês.

Como disse o Flávio depois de conhecer a Isabel: "Todo chinelo tem seu par MESMO, né?". Sou feliz de ter essa pessoa incrível como companheira, que esteve literalmente ao meu lado por todos os dias nos últimos anos (o que provavelmente faz dela a segunda pessoa que mais sofreu com essa tese). Obrigado pelo companheirismo, por me tranquilizar, e por topar a aventura de ir morar fora do país por um ano.

Agradeço à UFMG, minha casa há mais de 12 anos. Em tempos obscuros de ataques, cortes e desvalorização da educação e da ciência, a UFMG se mantém uma das maiores referências na América Latina em ensino e pesquisa. Sou grato por fazer parte desta balbúrdia.

Sou feliz em ter um "par" de orientadores que se complementam como yin e yang. Márcio, mestre enérgico e quem me instigou o interesse pela neurociência. Me mostrou a importância da interdisciplinaridade e que biologia e engenharia podem se relacionar de jeitos fantásticos. Me incentivou a buscar respostas e a rejeitar argumentos de autoridade. Sou grato a ele e a toda sua família pelo convívio e ensinamentos ao longo destes anos. Mas minha formação seria incompleta se não fosse a serenidade do Mazoni para me acalmar e colocar os pés no chão, com conversas frequentes que ajudaram a colocar no papel o caos de ideias que se fazem difíceis de serem capturadas. Conversas que também serviram para ganhar confiança em minha capacidade e a dar mais valor aos resultados, além de incentivar a busca por oportunidades (“o não você já tem”). Agradeço vocês dois por todos os ensinamentos, pela confiança durante todos esses anos, pelas oportunidades e portas abertas.

Sou grato e honrado por fazer parte da família que é o NNC. Esse grupo que reúne tantas pessoas brilhantes é uma das principais razões por eu ter decidido seguir uma carreira científica. Discussões nos journals e seminários, eventos comemorativos e conversas na copinha: todos foram parte de minha formação como pessoa e como cientista. Vocês fazem isso tudo valer a pena. Agradeço em especial a Profa. Grace e Prof. André por tudo isso.

Obrigado a todos colegas do Darkside, que compartilharam o vício pelo café, a Aritana com cerveja, o stress com setups de eletrofisiologia que parecem ter vontade própria, o desânimo que segue quando um experimento deu errado (às vezes comigo falando “hmmm” após analisar o LFP), até a salvação que eventualmente vinha pelas mãos do Flávio. Pedrão, Paulete, Hyo, Cayo, Letícia, Dan, Simões, Lari, Léo, Matheus,

Sérgio, e tantos outros. Vocês e todos que compartilharam a 240/168 merecem parágrafos e páginas inteiras de agradecimentos além da minha capacidade e eloquência. Espero em breve compensar isso e matar a saudade com uma cerveja na copinha ou no Language.

Flavitcho. Por todas as vezes que ajudou a mim e outros colegas a resolver todo tipo de perrengue no laboratório, por todas as recomendações de bandas, artigos, livros e HQs, por toda a tranquilidade, por todas as conversas, conselhos e risadas. Obrigado por tudo, meu amigo.

Agradeço a demais professores e colegas do ICB. Ao Prof. Cleiton pelas oportunidades, discussões e sugestões para a tese. Ao Prof. Bruno por todas as palhas italianas, sempre um ótimo pretexto para encontrar para bater um papo. Obrigado a ambos também por serem tão certeiros na escolha de alunos e alunas para orientação.

Agradeço aos professores e colegas do PPGEE, em especial à coordenação do programa. Além do empenho para que o PPGEE retome ao patamar que lhe é merecido, suas decisões foram fundamentais para que o meu programa de doutorado-sanduíche se concretizasse.

Aos colegas e organizadores do LASCON. Durante esse curso, fiz amigos e aprendi sobre neurociência computacional, o que eventualmente tornou possível a realização de grande parte desta tese.

Agradeço o trabalho e ativismo de A. Elbakyan em prol de uma ciência aberta, acessível e inclusiva.

Agradeço às agências de fomento. Em especial, à CAPES, responsável pelo auxílio ao longo de minha vida acadêmica.

Many thanks to Syd for hosting and advising me at MGH. The work being done at Cashlab is truly inspiring and shows an impressive synchrony between clinical practice and research. I'm glad to have been a part of that. I hope to have strengthened the collaboration between our groups and may it endure for the next years.

Before going to Boston, my initial expectations were that I would take a few months of adaptation before getting to have any data or doing any tasks. Thankfully, I had Angelique to help and guide me through everything. Her input was crucial to improve and make this project possible. She's a truly awesome person and a big influence for me and everyone at Cashlab.

Thanks to all colleagues at Cashlab for the warm welcome. The friendly environment, the discussions at lunch and lab meetings, and all the cheese made me feel at home. Special thanks to Kyle, Pariya, Gavin, Yangling (who was quick to support and help me whenever I needed something), Constantin (fellow companion at SfN), Senan for

the friendship and for the best possible Brosgiving ever, and to Dan for the all-around support.

Having the opportunity to meet with the participants that took part in this work gave me another perspective on what this is all about. I am immensely grateful to them for their kindness, altruism, and for generously sharing their time and attention during their treatment.

Thanks to everyone who made our stay in Boston such a remarkable experience. Cesar and Dima made the warmest welcome and the most delicious cuisine tours. To old and new friends who helped us adapt and made us feel in BH back again: Ana Luíza, Henrique, Luíza and Vinícius. To Fernando and Rita for the friendship.

ABSTRACT

Recurrent and spontaneous seizures are the hallmark of epilepsy, a neurological disease that affects around 1% of the world population and has higher incidence in developing countries. In general, seizure (or ictal) events are relatively easily identified due to their hypersynchronous and hyperexcitable nature, but the underlying neuronal mechanisms that give rise to such events are still unclear. One of the main ways of elucidating this involves the extraction of relevant features from electroencephalographic signals that are related to abnormal neuronal functioning. One promising strategy to highlight such features is the use of active probing paradigms. That is, the use of probing stimuli that would reveal information from a dynamical system, that would be otherwise inaccessible (or difficult to detect) through passive observation. This work evaluates the use of such probing strategies in two different contexts.

In the first part of this thesis, a modified version of a well-known neural mass model is used to test how low-frequency probing stimuli enhance the detection of approaching seizures. We show that, as parameters are shifted to bring the model towards seizure activity, features extracted from the simulated activity reflect these changes when probing stimuli are used. Furthermore, the changes revealed by the stimuli appear to reflect the phenomenon of critical slowing down, where increased recovery times from perturbations may signal the loss of a systems' resilience and are common hallmarks of an impending critical transition. Incorporating this strategy into early-warning systems may ultimately enable closing the loop for targeted seizure-controlling interventions.

In the second part of the work, an auditory task was used to evaluate sound processing in epilepsy patients undergoing presurgical monitoring with depth electrode implants. It was hypothesized that regions involved in the onset of seizures would display abnormal auditory steady-state responses (ASSR) to amplitude-modulated sounds. This could be in the form of abnormal hypersynchronous responses in regions not usually involved in primary auditory processing, or in impaired responses due to central auditory dysfunctions caused by epileptogenic circuits. Results show that ASSRs were rarely elicited in electrode contacts within seizure onset zones (SOZ), contradicting the first hypothesis. Accurately evaluating the second hypothesis (of impaired ASSRs within SOZ) was not possible due to the highly heterogeneous nature of the data and implant schemes from all participants.

This work showed the potential of low-frequency probing stimuli to highlight features and reveal underlying dynamics involved in the transition from interictal to ictal activity. However, the use of ASSRs for accurately identifying putative epileptogenic regions was limited. These responses are still promising for other diagnostics, such as identifying lateralization or seizure susceptibility, as may other types of stimuli be useful for identifying epileptogenic regions. Computational and experimental models will be

crucial for defining the best strategies and parameters of active probing approaches for the identification of abnormal and epileptic activity.

Keywords: Epilepsy. Critical slowing down. Seizure prediction. Active probing. Computational neuroscience. SEEG.

RESUMO

Crises espontâneas recorrentes são a marca registrada da epilepsia, uma doença neurológica que afeta cerca de 1% da população mundial e tem maior incidência em países em desenvolvimento. Em geral, os eventos de crise (ou ictais) são identificados com relativa facilidade devido à sua natureza hipersíncrona e hiperexcitável. Porém, os mecanismos neuronais subjacentes que dão origem a tais eventos não são totalmente esclarecidos. Uma das principais formas de elucidar isso envolve a extração de atributos relevantes de sinais eletroencefalográficos que estão relacionados ao funcionamento neuronal anormal. Uma estratégia promissora para ressaltar e auxiliar na identificação desses atributos é o uso de paradigmas de sondagem ativa. Ou seja, estímulos de sondagem revelariam informações de sistemas neurais, que seriam inacessíveis (ou difíceis de detectar) por meio da observação passiva. Este trabalho avalia o uso de tais estratégias de sondagem em dois contextos diferentes.

Na primeira parte desta tese, uma versão modificada de um conhecido modelo de massa neural é usada para testar como estímulos de sondagem de baixa frequência auxiliam na identificação de estados com alta suscetibilidade a crises. Mostramos que, conforme os parâmetros são alterados para trazer o modelo para a atividade ictal, os atributos extraídos da atividade neural simulada refletem essas mudanças quando os estímulos de sondagem são usados. Além disso, as mudanças reveladas pelos estímulos refletem o fenômeno de desaceleração crítica, no qual há um aumento nos tempos de recuperação a perturbações. Isso sinalizaria a perda de resiliência de um sistema e é uma marca comum de uma transição crítica iminente. A incorporação do método aqui avaliado em sistemas de previsão de crises poderia permitir o fechamento da malha de um sistema de intervenções para controle de crises.

Na segunda parte do trabalho, uma tarefa auditiva foi utilizada para avaliar o processamento auditivo em pacientes com epilepsia submetidos à monitorização invasiva pré-cirúrgica, com registros de estereoeletroencefalografia (SEEG). Partimos da hipótese que as regiões envolvidas no início das crises exibiriam potenciais evocados auditivos em regime permanente (PEARP, ou ASSR) anormais a sons modulados em amplitude (AM). Ou seja, circuitos epileptogêncicos influenciariam a resposta oscilatória induzida por sons AM. Esse efeito poderia ser (i) na forma de respostas hipersíncronas anormais em regiões que geralmente não estão envolvidas no processamento deste tipo de estímulo, ou (ii) em respostas comprometidas caso os circuitos epileptogênicos prejudicassem o processamento auditivo central. Os resultados mostram que os PEARPs

raramente foram observados em contatos dos eletrodos nas zonas de início das crises, contradizendo a primeira hipótese. Avaliar com precisão a segunda hipótese (de diminuição de PEARPs dentro de circuitos epileptogênicos) não foi possível devido à natureza altamente heterogênea dos dados e da grande variabilidade nos esquemas de implantes de todos os pacientes.

Este trabalho mostrou o potencial dos estímulos de sondagem de baixa frequência para ressaltar atributos eletrográficos e revelar dinâmicas envolvidas na transição da atividade neural de estados interictais para ictais. No entanto, o uso de PEARPs para identificar com precisão as regiões epileptogênicas foi limitado. Esses tipos de respostas auditivas ainda são promissores para outros diagnósticos, como a identificação de lateralização ou susceptibilidade a crises, assim como outros tipos de estímulos podem ser úteis para identificar regiões epileptogênicas. Modelos computacionais e experimentais serão cruciais para definir as melhores estratégias e parâmetros de abordagens de sondagem ativa para a identificação de atividade anormal e epiléptica.

Palavras-chave: Epilepsia. Desaceleração crítica. Predição de crises. Sondagem ativa. Neurociência computacional. Estereoeletroencefalografia.

LIST OF FIGURES

FIGURE 1: WNMM REPRESENTATION AND IMPULSE RESPONSE FUNCTIONS. 15
FIGURE 2: SIMULATED ACTIVITY TYPES AND MAPPING PARAMETERS TO ACTIVITY. 16
FIGURE 3: MODIFIED NEURAL MASS MODEL. 21
FIGURE 4: NEURONAL MASS MODEL OUTPUTS WITH AND WITHOUT ACTIVE PROBING STIMULI. 26
FIGURE 5: FEATURE SERIES AND PROBING EFFICIENCY FOR MODEL SETTING I-A. 27
FIGURE 6: FEATURE SERIES AND PROBING EFFICIENCY FOR MODEL SETTING I-B. 28
FIGURE 7: FEATURE SERIES AND PROBING EFFICIENCY FOR MODEL SETTING I-K. 29
FIGURE 8: FEATURE SERIES AND PROBING EFFICIENCY FOR MODEL SETTING II-A. 30
FIGURE 9: FEATURE SERIES AND PROBING EFFICIENCY FOR MODEL SETTING II-B. 31
FIGURE 10: FEATURE SERIES AND PROBING EFFICIENCY FOR MODEL SETTING II-K. 31
FIGURE 11: ONSET TIME OF ICTAL-LIKE ACTIVITY AS A FUNCTION OF STIMULUS AMPLITUDE. 32
FIGURE 12: AUDITORY STEADY-STATE RESPONSES. 41
FIGURE 13: INSERTION POINTS FOR ALL ELECTRODES FOR A SPECIFIC PARTICIPANT. 44
FIGURE 14: POST-SURGERY MRI RECONSTRUCTION. 44
FIGURE 15: OVERVIEW OF METHOD AND DATA PROCESSING PIPELINE. 46
FIGURE 16: ASSR TASK. 48
FIGURE 17: TRIAL PSD AND ASSR POWER MEASUREMENT. 50
FIGURE 18: REPRESENTATIVE LFP TRACES. 52
FIGURE 19: LFP TRACES FROM CHANNELS OF THE SAME ELECTRODE. 53
FIGURE 20: PSDS FROM ALL CHANNELS FROM TWO ELECTRODES, DURING THE AUDITORY TASK. 54
FIGURE 21: TIME-FREQUENCY PLOT HIGHLIGHTING THE EVOKED ASSRS DURING THE SOUND STIMULI. 54
FIGURE 22: SEEG CONTACT COVERAGE AND SOZS. 56
FIGURE 23: SIGNIFICANT 40 HZ ASSRS, MONOPOLAR MONTAGE. 57
FIGURE 24: DEPTH ELECTRODES IMPLANT TRAJECTORIES FOR EACH PARTICIPANT. 58
FIGURE 25: SIGNIFICANT 40 HZ ASSRS, BIPOLAR MONTAGE. 59
FIGURE 26: ASSRS WITH DIFFERENT MODULATION RATES, MONOPOLAR MONTAGE. 60
FIGURE 27: 40 AND 80 HZ ASSR PLVS BY REGION (BIPOLAR MONTAGE). 61
FIGURE 28: 40 HZ ASSR PLV BY REGION AND SOZ, WITH BIPOLAR MONTAGE. 62
FIGURE 29: ASSR WITH EYES OPEN AND EYES CLOSED, MONOPOLAR MONTAGE. 63
FIGURE 30: EYES-CLOSED – EYES-OPEN ASSR PLVS FROM SELECTED REGIONS (BIPOLAR MONTAGE). 64

SUPPLEMENTARY FIGURE 1: ALTERNATIVE MODEL SETTING I-A. 76
SUPPLEMENTARY FIGURE 2: ALTERNATIVE MODEL SETTING I-B. 76
SUPPLEMENTARY FIGURE 3: 40 HZ ASSR COVERAGE, LAPLACIAN MONTAGE. 77
SUPPLEMENTARY FIGURE 4: 80 HZ ASSR COVERAGE, MONOPOLAR MONTAGE. 77
SUPPLEMENTARY FIGURE 5: 80 HZ ASSR COVERAGE, BIPOLAR MONTAGE. 78
SUPPLEMENTARY FIGURE 6: 40 HZ ASSR PLV BY HEMISPHERE, MONOPOLAR MONTAGE. 78
SUPPLEMENTARY FIGURE 7: ASSR PLV DIFFERENCE (40 HZ – 80 HZ ASSRS) BY CONTACT DEPTH, MONOPOLAR MONTAGE. 79
SUPPLEMENTARY FIGURE 8: 40 HZ AND 80 HZ ASSR PLVS FOR ONE PARTICIPANT (P08). 79
SUPPLEMENTARY FIGURE 9: 40 HZ ASSR PLV RE-REFERENCING COMPARISONS FOR ONE PARTICIPANT (P08). 80

SYMBOLS & ABBREVIATIONS

AM	Amplitude-modulated
AP	Action potential
ASSR	Auditory steady-state response
CFC	Cross-frequency coupling
DBS	Deep brain stimulation
EEG	Electroencephalogram
EZ	Epileptogenic zone
f_c	Carrier frequency
f_m	Modulating frequency
FFT	Fast Fourier transform
FSI	Fast somatic inhibition
ERP	Event related potential
EZ	Epileptogenic zone
ILS	Interictal-like spikes
LFP	Local field potential
MEG	Magnetoencephalogram
MI	Mutual information
PAC	Phase-amplitude coupling
(e/i)PSP	(excitatory/inhibitory) Post-synaptic potential
PLV	Phase-locking Value
PSD	Power spectral density
SCANNM	Stochastic cellular automata neural network model
SEEG	Stereoencephalography
SDI	Slow dendritic inhibition
SOZ	Seizure onset zone

STFT	Short time Fourier transform
(m)TLE	(mesial) Temporal lobe epilepsy
WAR	Wistar audiogenic rat
WNMM	Wendling neural mass model

TABLE OF CONTENTS

1. INTRODUCTION 1

1.1. Rhythms and Oscillations in the Brain 1

1.2. Epilepsy 2

1.3. Seizures 3

1.4. Epileptogenesis, Ictonesesis and Seizure Focus 4

1.5. Neuronal networks and epilepsy 5

1.6. Seizure Forecasting 7

1.7. Active probing 8

1.8. Objectives 10

1.9. Thesis overview 11

2. ACTIVE PROBING ON A NEURAL MASS MODEL 12

2.1. Computational neural models 12

2.2. Probing *in-silico* neuronal models 14

2.3. Wendling neural mass model 15

2.4. Deep Brain Stimulation - DBS 18

2.5. Methods 20

2.5.1. Model parameters 20

2.5.2. Model settings 23

2.5.3. Feature extraction and probing effectiveness 24

2.6. Results 25

2.7. Discussion 32

2.7.1. Local effect of active probing and better effects stimulating both neuronal populations 33

2.7.2. Similar features and ILS serving as early-warning signals 34

2.7.3. Probing stimuli indicate critical slowing down prior to the transition to ictal activity 35

2.7.4. Comparisons with the EPILEPTOR model 36

2.7.5. Limitations 37

2.8. Conclusion 38

3. AUDITORY STEADY-STATE RESPONSES IN INVASIVE RECORDINGS 39

3.1. Introduction 39

3.2. Auditory Steady-State Evoked Potentials 40

3.3. Invasive monitoring by stereo-electroencephalography (SEEG) 43

3.4. Objectives 45

3.5. Methods 45

3.5.1. Ethics statement 46

3.5.2. Data acquisition 47

3.5.3. Auditory task 47

3.5.4. Data processing and analysis 49

3.5.5. SEEG signal referencing 51

3.6. Results 52

3.6.1. SEEG data overview and examples 52

3.6.2. ASSR by brain region and participants 56

3.6.3. 40 Hz and 80 Hz ASSR 59

3.7. ASSR was not evoked near seizure onset zones 61

3.7.1. Eyes-closed X eyes-open ASSR 62

3.8. Discussion 64

3.9. Conclusions 68

4. CONCLUSION AND PERSPECTIVES 70

4.1. Findings 70

4.1.1. Low-frequency stimulation enhances the predictability of upcoming seizures in a neural mass model 70

4.1.2. Low-frequency stimuli may reveal critical slowing down as an early-warning of upcoming seizures 71

4.1.3. ASSRs are promising diagnostic tools in epilepsy, but appear to have limited value on accurately localizing epileptogenic regions 72

4.1.4. 40 and 80 Hz ASSRs 73

4.1.5. Eyes-open x eyes-closed ASSR 73

4.2. Perspectives 73

4.2.1. Closing the loop 73

4.2.2. Evaluating active probing on other models and validating with experimental data 74

4.2.3. Evaluating ASSRs on longer timescales 75

4.2.4. Promising future for neuronal dynamics and epilepsy 75

5. SUPPLEMENTARY MATERIAL 76

REFERENCES 81

APPENDIX 97

1.INTRODUCTION

This thesis aims to evaluate active probing strategies to uncover brain dynamics involved in epilepsy. This chapter provides an overview of the current literature in the field, the rationale for using these approaches, and the main objectives of this work.

1.1.Rhythms and Oscillations in the Brain

Rhythms, oscillations, periodicity, and cyclic processes are terms that generally refer to the same principle of recurrent patterns, which are involved in several phenomena, in different systems and scales (BUZSÁKI, G, 2006). In the mid-’20s, the first Electroencephalography (EEG) recordings by Hans Berger showed the presence of rhythms of the brain, in the form of voltage deflections resulting from the coordinated activity of neuronal groups. The first robust oscillation type was coined Alpha, a rhythm around 10 Hz that was visible when individuals were in a relaxed state with eyes closed. Since then, rhythms in various frequency bands have been reported, ranging from 0.05 Hz to 600 Hz (BUZSÁKI; DRAGUHN, 2004), with different frequency bands and regions associated with specific functions. Remarkably, these rhythms are preserved and are similar across different mammalian species (BUZSÁKI; LOGOTHETIS; SINGER, 2013).

Several hypotheses propose that fundamental features of the brain, such as memory, action, and cognition, may emerge from the interaction of different neural circuits, brought together and coordinated through the interaction and synchrony between brain rhythms (BUZSÁKI, G, 2006; ENGEL, A. K.; SINGER, 2001; FRIES, 2015). These functions depend on the ability of the brain to codify and integrate an enormous amount of information in a temporally precise and coordinated way, which would hardly be explained only in terms of firing rate of action potentials (APs), a traditional coding mechanism for neurons. However, when this mechanism is combined with oscillations in different frequency bands, temporal information can be nested in specific rhythms, and synchronization between local and distant networks can be done in a dynamic and economic way (BUZSÁKI, G, 2006; BUZSÁKI; DRAGUHN, 2004). Neuronal circuits can also interact with different synchrony modes, which would be a flexible way to bind subsystems, allowing rapid changes in the topology of the networks, in contrast to the

rigidity of a traditional model based only on structural anatomical connectivity and activity-dependent changes (FRIES, 2015; MOSER *et al.*, 2010). Among the hypothesized synchrony mechanisms are communication through coherence (CTC, by (FRIES, 2015)), spike-timing-dependent plasticity (FELDMAN, 2012), phase synchronization (VARELA *et al.*, 2001), and cross-frequency coupling (CFC), which would be involved in cognition (TORT *et al.*, 2008), working memory (AXMACHER *et al.*, 2010) and odor recognition (PENA *et al.*, 2017). Thus, although it is still unclear what are the exact mechanisms ruling the coordination of neuronal groups that allow the execution of several brain functions, it is believed that synchrony plays an important role. The dysfunction of these mechanisms may result in pathologies such as sleep disorders, Parkinson's disease (HAMMOND; BERGMAN; BROWN, 2007), schizophrenia (BAŞAR, 2013), or epilepsy, a disease marked by hyperexcitability and hypersynchrony (BAŞAR, 2013).

1.2.Epilepsy

Epilepsy is defined by the ILAE (International League Against Epilepsy) as a brain disease, marked by one or more of the following conditions: (1) occurrence of at least two spontaneous or reflex seizures separated by at least 24h hours, (2) a spontaneous seizure with a high risk of recurrence, or (3) diagnosis of an epileptic syndrome (FISHER *et al.*, 2014). Epilepsy results in severe consequences for the patient and society, with an incidence rate of 0,5% to 1% of the world population, and higher in developing countries (ENGEL, J.; PEDLEY, 1989; WORLD HEALTH ORGANIZATION, 2012).

Epilepsy diagnosis is based mainly on the type of seizures and underlying causes, as well as clinical exams such as electroencephalography (EEG) monitoring. Other factors are also taken into account, such as medical background, imaging exams, blood, developmental, neurologic, and behavioral tests.

Treatment of this disease is predominantly pharmacological. When seizures are not controlled by these means (refractory epilepsy), surgical intervention by resection of putative seizure foci is a possible course of treatment (ROSENOW; LÜDERS, 2001). Alternative treatments include diets (MARTIN *et al.*, 2016) or stimulation devices, such as the vagus nerve stimulator or the recently FDA-approved NeuroPace RNS® System (FRIDLEY *et al.*, 2012).

Despite all research efforts to understand epilepsy, many problems still persist, such as high rates of erroneous diagnostics (CHOWDHURY; NASHEF; ELWES, 2008), poor seizure prediction algorithms performance (MORMANN *et al.*, 2007), and high rates of refractory epilepsy (FRENCH, 2007). The solution to these problems in epilepsy depends on the characterization of the mechanisms of various forms of this disease, and which factors could be common in most types.

1.3.Seizures

Seizures are the hallmark of epilepsy. They are defined as transient signs and/or symptoms arising from populations of brain cells in hypersynchronous and/or hyperexcitable firing states (ENGEL, J.; PEDLEY, 1989; PENFIELD, WILDER & JASPER, 1954). They can be characterized as partial (focal) or generalized seizures, depending on their nature and origin (DREIFUSS, 1989). Such events can begin locally, in specific regions from either cerebral hemispheres, or simultaneously in both hemispheres, in the case of generalized seizures. They can lead to various cognitive, sensorial, and motor symptoms, or even more severe ones as altered consciousness, complex automatic behaviors, or bilateral tonic-clonic movements (IASEMIDIS, LEON D, 2003).

Seizure events can be divided into stages, with different neuronal circuits more or less involved in each one of these (BERTRAM, 2013); (i) seizure initiation can be defined as the transition from an inter-ictal state into an ictal one, (ii) seizure buildup is the initial seizing activity and (iii) seizure spread is characterized by the recruitment of additional circuits and brain regions. Two more stages can be considered: (iv) seizure termination occurs often abruptly, but with observable dynamics such as slowing of rhythmic activity and increased synchrony. This can be a result of many possible mechanisms, such as glutamate depletion, changes in ion concentrations, reduced pH, changes in synaptic effectiveness, or modulatory effects from subcortical structures (KRAMER, M. A. *et al.*, 2012). Finally, the (v) post-ictal period is marked by refractoriness and depression of electroencephalographic activity (PITKÄNEN; SCHWARTZKROIN; MOSHÉ, 2006).

1.4.Epileptogenesis, Ictonesesis and Seizure Focus

The process in which the brain, by a series of structural, molecular, anatomic, and/or neuronal circuitry changes, becomes susceptible to seizures is called epileptogenesis (SCHARFMAN, 2007). These hypersynchronous or hyperexcitable network states may be brought by changes in intrinsic/synaptic excitability, or by alterations in anatomical structure, such as neuronal death or mossy fiber sprouting, one of the hallmarks of temporal lobe epilepsy (TLE) (BEENHAKKER; HUGUENARD, 2009).

On a smaller timescale, ictogenesis is the term usually used to describe the dynamics and mechanisms of seizure generation (PERUCCA; DUBEAU; GOTMAN, 2014). That is, the mechanisms and events involved in the transition of inter-ictal brain states to ictal ones. There are two main hypotheses about this transitions (PAZ; HUGUENARD, 2015); (i) In a more traditional view, all seizures, including generalized ones, are originated in localized microcircuits and propagate from this ictogenic focus, recruiting other regions, or (ii) seizures emerge from dysfunctions in distributed microcircuits, which would progressively coalesce and recruit further networks until a critical point, of activation of a ictogenic circuit which would lead to a seizure.

Traditionally, an epileptic focus is defined as a restricted cortical region that, due to the abnormal behavior of its cells, generates a series of phenomena related to hyperexcitability, such as seizures, interictal discharges, and pathological oscillations (JIRUSKA, PREMYSL; DE CURTIS; JEFFERYS, 2014). The region where clinical seizures are generated is called seizure onset zone (SOZ), generally identified through EEG (scalp or invasive) analysis. The SOZ is often related to the epileptogenic zone (EZ), a region necessary and sufficient for the occurrence of seizures, therefore the main target for surgical resection in refractory epilepsy (ROSENOW; LÜDERS, 2001). However, not all surgery outcomes are seizure-free; despite the common overlapping between these regions, the removal of a SOZ that is smaller than the whole EZ can result in the emergence of a different SOZ which triggers seizures again (FRAUSCHER *et al.*, 2017). Thus, while the exact definition of an epileptogenic zone is not possible, more accurate approximations can be done by the identification and delimitation of overlapping

pathological and pathophysiological regions involved or affected by epileptiform activity; the symptomatogenic zone (produces ictal symptoms when activated by an epileptiform discharge), irritative zone (an area that generates interictal electrographic spikes), SOZ, epileptogenic lesion (radiographic lesion that is the cause of the epileptic seizures) and functional deficit zone (an area that is functionally abnormal in the interictal period) (ROSENOW; LÜDERS, 2001).

More recent concepts about epileptic foci relate these to the presence of small neuronal clusters that generate pathological patterns locally, in the form of microseizures and pathological high-frequency oscillations (pHFOs), and/or globally, such as seizures and interictal discharges (JIRUSKA, PREMYSL; BRAGIN, 2011). These patterns can be initiated locally in separated clusters, resulting in macroseizures when these adjacent microdomains are eventually coalesced, recruiting larger-scale networks into hypersynchronous states (STEAD *et al.*, 2010). This is supported by findings such as the buildup of high-frequency activity (HFA) in an in-vitro model of CA1 (JIRUSKA, P. *et al.*, 2010), and the detection of low-voltage fast activity, usually used as biomarkers of SOZ and epileptogenic zone (WENDLING, FABRICE *et al.*, 2003), in regions of spread from patients with intracranial electrodes (PERUCCA; DUBEAU; GOTMAN, 2014).

Treating epilepsy as a network disorder brings promising strategies that may improve the outcome of surgical interventions (SINHA *et al.*, 2017). That is, instead of removing putative foci that are involved in the generation of seizures, interventions could be made on specific network nodes (or regions) that are critical for the generation of epileptogenic activity (GOODFELLOW *et al.*, 2016; SINHA *et al.*, 2017; WANG, Y. *et al.*, 2020).

1.5.Neuronal networks and epilepsy

With epilepsy being increasingly regarded as a network disorder (KRAMER, MARK A; CASH, 2012; VAN DIESSEN *et al.*, 2013), determining which alterations in the neuronal circuitry of the brain make it prone to seizures is crucial for understanding and treating it. In (BEENHAKKER; HUGUENARD, 2009), it is proposed that physiological neuronal circuits may act as templates, from which epileptic circuits use to generate seizures. That is, normal and epileptic circuits would share some inherent features. Two

oscillatory sleep circuits are described and their relation with specific seizure types or signatures is discussed. One involves the thalamus (thalamocortical circuit), is responsible for generating sleep spindles, but is also related to spike-wave discharges in seizures. Another one is in the hippocampus, where the generation of fast-ripples, oscillations present in patients with mesial temporal lobe epilepsy (mTLE) may be related to sharp-wave ripples.

In (PAZ; HUGUENARD, 2015), four microcircuit motifs that generate oscillations are described; (i) Feed-forward Inhibition, in which excitatory inputs recruit local inhibitory networks and regulate intensity and pattern of efferent signals (i.e. in the cortico-thalamic pathway), could be related to absence seizures and in TLE. (ii) Feedback inhibition, where locally activated inhibitory neurons regulate recurrent excitatory activity, may play a role in both suppressing (through chandelier cells) and promoting seizure activity. (iii) In Counter-inhibition (i.e. autaptic connections in parvalbumin-containing basket cells), local connections between inhibitory neurons can induce disinhibition or affect coupling. (iv) Local recurrent excitatory circuits are enhanced in most experimental epilepsies and are common in physiological cortical networks with the majority of excitatory synapses. From a dynamical systems point of view, it is intuitive how such a network, with positive feedback connections, can lead to the instability of a system. The authors suggested that alterations in any of these motifs, or the interactions between them, may lead to ictogenesis. Efferent projections, such as long-range interneurons or cortical axons composing the corpus callosum, would propagate abnormal activity from these altered microcircuits to distinct neuronal populations. Thus, critical chokepoints are proposed, not necessarily inside the SOZ, to be acted upon to suppress seizure activity. Aside from pharmacological interventions, electrical stimuli can also be used to achieve this, as reviewed in (FRIDLEY *et al.*, 2012) and (FISHER; VELASCO, 2014).

Some recent works also consider seizure onset dynamics as belonging to the class of critical transitions, with similarities among different systems, from economics and physics to tectonics (MEISEL *et al.*, 2012; SCHEFFER *et al.*, 2009). These transitions would

be preceded by changes such as critical slowing, flickering, increased correlation, variability, and lag-1 autocorrelation (SCHEFFER *et al.*, 2012).

1.6.Seizure Forecasting

Given the unpredictability of most seizures, achieving a way to predict their occurrence would ease part of the burden of patients with epilepsy, whether by serving as alarm systems or by enabling targeted interventions to prevent these events. However, identifying electrographic patterns that reliably indicate pre-ictal states is an enormous challenge in epilepsy research, as described by (MORMANN *et al.*, 2007), (SACKELLARES, 2008), and (FREESTONE; KAROLY; COOK, 2017). This problem, traditionally defined as seizure prediction, is more recently referred to as seizure forecasting to emphasize the probabilistic nature of the problem, although the terms are sometimes used interchangeably.

In most theories about ictogenesis, hyperexcitability and pathological neuronal synchronization play important roles (ENGEL, J., 1989). Therefore, many seizure forecasting or prediction methods are based on the exploration and quantification of features related to these properties, as well as their interaction between brain regions (SCHELTER; TIMMER; SCHULZE-BONHAGE, 2008). More complex measures may focus on system dynamics. In the ’90s, previous advances in non-linear systems theory were leveraged to develop seizure prediction methods (LEHNERTZ, KLAUS; ELGER, 1998; MARTINERIE *et al.*, 1998). Highly optimized algorithms achieved good performance using methods such as Lyapunov exponents (CHAOVALITWONGSE *et al.*, 2005; IASEMIDIS, LEONIDAS D. *et al.*, 1990; LEHNERTZ, K, 1999), correlation dimension (LEHNERTZ, KLAUS; ELGER, 1998), empirical mode decomposition (BAJAJ; PACHORI, 2013; MARTIS *et al.*, 2012), and dynamical similarity index (LE VAN QUYEN *et al.*, 1999). However, such optimistic findings were not replicated when faced with larger datasets – with an increased number of patients and long-term EEG recordings – and stricter statistical evaluations, especially in terms of specificity (MORMANN *et al.*, 2007). The following years were marked by improved methods that took in account some of the lessons learned during this period: use of long-term recordings and broader datasets for model evaluation, emphasis on the stochastic nature of the problem (which would be

more appropriately considered as regression problem with probabilities, as opposed to binary classification between interictal X ictal) and use of appropriate statistical methods for evaluation (FREESTONE; KAROLY; COOK, 2017). Other important factors and strategies that should play an important role are the use of individualized models (KAROLY *et al.*, 2018; RAMGOPAL *et al.*, 2014), the fact that seizures tend to cluster and usually display cyclic (circadian and multidien) components (BAUD *et al.*, 2018; BERNARD, 2020; KAROLY *et al.*, 2017), viewing the problem from a dynamical systems perspective (LOPES DA SILVA, FERNANDO H *et al.*, 2003), and the fast advances of machine learning in recent years (LECUN; BENGIO; HINTON, 2015) that has impacted nearly every field and are promising tools to be used for neural decoding and identification of pre-ictal and ictal states (CHAMPION *et al.*, 2019; FUMEAUX *et al.*, 2020; LHATOO *et al.*, 2020). Yet another promising strategy belongs to the class of perturbational approaches that are widely used in neuroscience, and consists of actively probing the brain; by applying stimuli and evaluating responses, more information could be obtained about the state of a system, which would be otherwise inaccessible with its passive observation. The use of such strategies has led to advancements in sensory-motor mapping (PENFIELD, WILDER & JASPER, 1954), identifying epileptogenic foci (VALENTIN, 2002), and evaluating states of consciousness (CASALI *et al.*, 2013; SANZ PERL *et al.*, 2021), among others.

1.7. Active probing

The concept of stimulating a system to better understand its properties is present in many research areas; from digital signal processing (DSP) filters (inferring transfer functions from impulse responses) to animal behavior (fear conditioning, with specific stimuli and freezing measures), more information can be assessed from a system by applying controlled inputs and recording the output response, instead of its passive observation. In general, it is desired that these perturbations should not drastically change the state of the system, whilst still enabling the identification of its dynamics. Such approaches, with the application of controlled and subtle stimuli to uncover a system's dynamics, highlighting otherwise noisy or hidden features, can be considered

as probing, or as defined in (KALITZIN, S. N.; VELIS; DA SILVA, 2010), active observation paradigms.

The use of a probing strategy to identify preictal states was pioneered by (KALITZIN, STILIYAN *et al.*, 2002), with the use of intermittent photic stimulation (IPS) to better detect dynamical changes preceding seizure activity in photosensitive patients. The use of IPS increased the relative phase clustering index (rPCI), which would reflect the hyperexcitability of the underlying state transition between inter-ictal and ictal activity and would indicate the presence of nonlinear dynamics. Since then, relatively few studies have used these probing approaches, despite promising results. These are briefly presented here and described with more details in subsequent sessions.

Despite its invasiveness, pre-ictal probing by electrical stimulation is the most studied stimulus type, with different papers applying either cortical or DBS (deep brain stimulation) to epilepsy patients (FREESTONE; KUHLMANN; *et al.*, 2011; KALITZIN, S. N.; VELIS; DA SILVA, 2010). DBS for pre-ictal probing was also used in canines (FREESTONE *et al.*, 2013) and with a pentylenetetrazol (PTZ) model in rats (MEDEIROS *et al.*, 2014).

Besides the applications in seizure forecasting, probing may also be applied to a range of problems. Direct electrical stimulation (DES) of cortical structures has contributed immensely to the mapping of brain functions, since the works of (PENFIELD, WILDER & JASPER, 1954). This approach has been used for the characterization of functional networks, the identification of the seizure onset zone, the study of brain plasticity mechanisms, and the anticipation of epileptic seizures (DAVID *et al.*, 2010). Single pulse electrical stimulation (SPES) was used for predicting seizure outcome after surgery in (VALENTÍN *et al.*, 2005).

Auditory steady-state responses (ASSR) were used in (PINTO, HYORRANA PRISCILA PEREIRA *et al.*, 2017) to evaluate auditory processing during inter-ictal and ictal periods in an audiogenic seizure model, showing enhanced and hypersynchronous responses in this model. In (CANCADO, 2016), the same ASSR was used to assess this enhancement of responses in patients with epilepsy.

In computational models, only two papers have been found to use probing approaches to evaluate inter-ictal to ictal transitions. In (SUFFCZYNSKI *et al.*, 2008), a

hippocampal lumped (or mass) model is used, showing that changes in parameters leading to seizure states can be better predicted with stimulation. Kuramoto oscillators are used in (O'SULLIVAN-GREENE *et al.*, 2017) to test a similar hypothesis.

This somewhat recent bibliography explores just a part of what could be done with probing approaches; there are multiple stimuli types (visual, DBS, auditory, TMS, etc.), different epilepsy types and seizure models to be evaluated. So, which methods are applicable to which problems?

1.8. Objectives

This thesis aims to evaluate the use of active probing as a tool for unveiling information about epilepsy. It is hypothesized that some stimuli would highlight features related to pathological states and reveal underlying dynamics, which would be inaccessible otherwise. Expected changes would be related to synchrony and excitability, relevant for the study of ictogenesis and region ictogenicity. To assess this, this thesis deals with different stimuli, in computational models, and data from tasks with participants who are epilepsy patients undergoing invasive presurgical monitoring.

Thus, the main objectives can be summarized:

I. Evaluate the potential of low-frequency probing stimuli for identifying pre-ictal states.
    - In a neural mass model, evaluate if low-frequency periodic stimuli aid in extracting features that allow the detection of an impending seizure state.

II. Evaluate the potential of auditory stimuli as tools for identifying epileptogenic regions and systems.
    - In epilepsy patients undergoing invasive SEEG presurgical monitoring, evaluate auditory processing with steady-state responses (ASSR).
    - Investigate if ASSRs can aid in identifying potential seizure foci. ASSRs may be enhanced and be elicited in brain regions not commonly involved in auditory processing, which would be due to epileptogenic neuronal circuits being prone to entrainment. Alternatively, reduced responses

can also be expected if epilepsy leads to dysfunctional central auditory processing.

1.9. Thesis overview

The text is divided into chapters, each one dealing with a different model or data to answer a specific hypothesis, describing the bibliographic references, methods, partial results, and following steps. Chapter 2 shows the application of low-frequency stimuli in a computational neural model to highlight features involved in the transition from inter-ictal to ictal activity in simulated neural signals. Chapter 3 shows ASSR distribution and assesses its relationship with region ictogenicity in a population of epilepsy patients that underwent presurgical evaluation with SEEG implants at the Massachusetts General Hospital in Boston, MA. Chapter 4 briefly summarizes the findings of the work with closing remarks.

2. ACTIVE PROBING ON A NEURAL MASS MODEL

This chapter aims to test the hypothesis that probing stimuli can highlight feature changes when the parameters of a seizure-generating computational neural model are shifted from inter-ictal (or normal) to ictal activity. We expect that, as the model becomes more prone to ictal activity, excitability and synchrony would be highlighted by probing. Some changes can also reveal underlying dynamics, with the appearance of hallmarks of impending critical transitions such as critical slowing, increased autocorrelation, and variance (SCHEFFER *et al.*, 2009, 2012). This part of the work has been published in (CARVALHO, VINÍCIUS REZENDE *et al.*, 2021).

2.1. Computational neural models

Epilepsy can be considered as a dynamic disease; both epileptogenesis and ictogenesis involve changes over time that can be quantified. This makes the use of dynamical systems theory and computational or *in-silico* models invaluable for uncovering its mechanisms (LYTTON, 2008).

Computational neuroscience is a field marked by the intersection between neurobiology, mathematics, physics, and neurophysiology (WENDLING, FABRICE *et al.*, 2012). To be useful, designed models need not be an exact representation of observed brain dynamics; to capture general behaviors and emerging properties derived from a set of (often simple) rules or elements can be enough to provide evidence about proposed hypotheses in neuroscience. This has been done increasingly in the last decades, such as in trying to uncover the mechanisms involved in neuronal oscillations (BERZHANSKAYA *et al.*, 2013; TRAUB *et al.*, 2005), neuronal dynamics (IZHIKEVICH, 2000), and synchronization (KUDELA; FRANASZCZUK; BERGEY, 1999), neural coding (BASTOS *et al.*, 2012), and used extensively in pathologies like epilepsy (JIRSA *et al.*, 2014; LYTTON, 2008; WENDLING, FABRICE *et al.*, 2016).

Just as studies about the mechanisms of the brain and its pathologies can be done from the micro-scale (with ion channels and neurons) to large-scale behaviors (with broad neuronal population activity as measured by the EEG), computational

modeling approaches can vary from microscopic to macroscopic (WENDLING, FABRICE *et al.*, 2012). Microscopic models may focus on detailing the equations ruling membrane potential and ion channel dynamics that determine the firing behavior of single neurons, such as the influential Hodgkin-Huxley (HODGKIN; HUXLEY, 1952) model. Diverse models can be built upon this formalism and extended to form networks of single detailed neurons that interact through synapses and gap junctions. However, the size and complexity of these models are limited by both computational costs and the dimension of their parameter space.

Mesoscopic models (sometimes referred to as lumped-parameter, mass models, mean-field or macroscopic), on the other hand, aim to describe the collective behavior of neuronal populations by representing their "mean activity" rather than detailing the activity of single neurons in a network. That is, instead of individual variables for membrane potentials, action potentials (APs), or post-synaptic potentials (PSP) for each neuron, the average of these attributes can be represented for specific sub-populations included in larger-scale networks (WENDLING, FABRICE *et al.*, 2012), which would be unfeasible to represent with detailed micro models. Pioneering works on these models include (WILSON; COWAN, 1972), (FREEMAN, 1964), and (LOPES DA SILVA, F H *et al.*, 1974). This work employs a model of this kind – one developed by (WENDLING, FABRICE *et al.*, 2002), which will be referred to from now on in this text as the Wendling neural mass model (WNMM).

A third type of modeling approach can be considered, which attempts to uncover putative invariant dynamical properties of brain phenomena (NAZE; BERNARD; JIRSA, 2015). The development of canonical models through sets of differential equations aims to replicate bifurcations observed in experimental data, such as the EPILEPTOR model developed by (JIRSA *et al.*, 2014), which reduces the vast diversity of seizure types into few classes determined by their seizure onset and offset bifurcations. This enables the identification of general rules of dynamic behavior, despite overlooking detailed representations of biophysical properties (JIRSA *et al.*, 2014).

While the emphasis on scale can be given when categorizing different types of neuronal computational models, there are multiple criteria to do this. A thorough

description of this and the decision process to choose fitting models to the right questions is given by (SCHRATER; KORDING; BLOHM, 2019)

2.2.Probing *in-silico* neuronal models

While the research literature regarding probing approaches in experimental models of epilepsy is limited, even fewer works study this approach on computational models. In (SUFFCZYNSKI *et al.*, 2008), the WNMM developed by (WENDLING, FABRICE *et al.*, 2002) – and the same used in the present chapter – is used to show that changes involved in the transition to seizure-like activity are reconstructed more accurately with an active probing approach, as opposed to a passive observation paradigm.

In (WENDLING, F. *et al.*, 2016), the impact of electrical extracellular, local, bipolar stimulation (ELBS) was evaluated with a simplified neural mass model consisting of principal excitatory cells coupled to inhibitory cells. When appropriately tuned, the stimuli enabled the preferential activation of GABAergic interneurons and, together with a proposed quantitative neural network excitability index (NNEI), allowed the identification of hyperexcitable neuronal populations. The results were validated with *in-vivo, in-vitro,* and data from 4 patients, reinforcing the value of ELBS and NNEI to reveal hyperexcitable brain regions.

With a more abstract approach, (O'SULLIVAN-GREENE *et al.*, 2017) used coupled Kuramoto oscillators to represent brain dynamics, showing that the underlying system synchrony is better observed when a combination of active probing and suitably dense electrode recordings is used. Another abstract model that focuses on capturing the dynamics involved in ictal activity is the EPILEPTOR (JIRSA *et al.*, 2014), which was used to evaluate an active probing approach in (CARVALHO, VINÍCIUS R.; MORAES; MENDES, 2019). The use of low-frequency stimuli in this model induced responses that changed gradually as the epileptogenicity of the model increased. Such changes were not visible with the passive observation of simulated activity, indicating the value of the active probing approach for seizure prediction.

A neuronal network model with interacting excitatory and inhibitory neurons referred to as stochastic cellular automata neuronal network model (SCANNM) was proposed by (LOPES, M A; LEE; GOLTSEV, 2017) to investigate the emergence of inter-

ictal and ictal activity. The stimulation of interictal-like spikes and the analysis of the progressively slower accompanying low-fluctuating activity showed early-warning signals that heralded the approaching transition to an ictal state. The model was also able to reproduce recurrent transitions to ictal states with adequate parameters.

2.3. Wendling neural mass model

The WNMM (WENDLING, FABRICE *et al.*, 2002) consists of 4 populations subsets representing neuron clusters in the CA1 region; excitatory main cells (pyramidal), excitatory interneurons, inhibitory neurons with slow kinetics (O-LM neurons, with IPSCs mediated by dendritic synapses) and with fast kinetics (soma-projecting basket cells). Projections between these groups are described in Figure 1a. Excitatory interneurons are implicitly represented as the feedback loop from Pyramidal Cells.

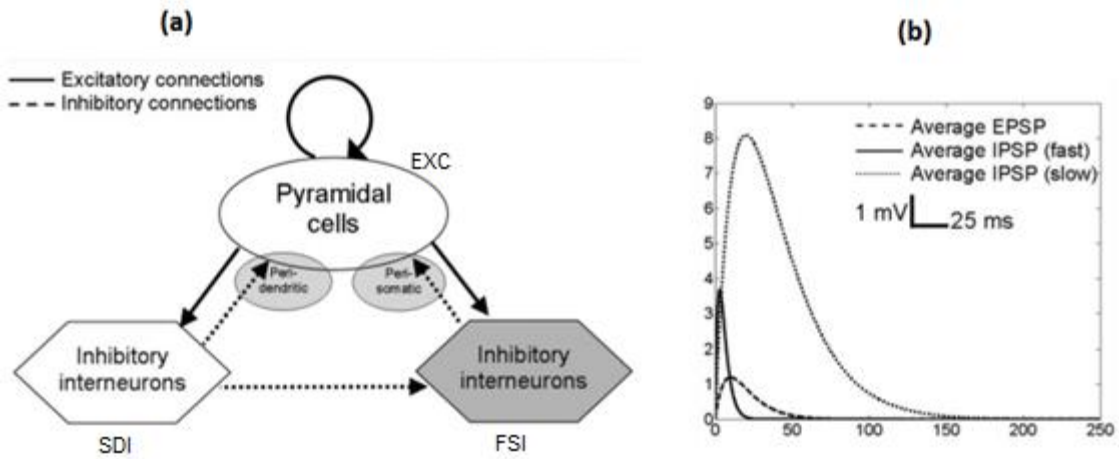

Figure 1: WNMM representation and impulse response functions. (a) Representation of each population subset and respective interactions. (b) Impulse responses of each synapse type; $\boldsymbol{h_e(t) = Aae^{-at}}$ for excitatory (EXC), $\boldsymbol{h_i(t) = Bbe^{-bt}}$ for slow dentritic inhibition (SDI) and $\boldsymbol{h_g(t) = Gge^{-at}}$ for fast somatic inhibition (FSI). A,B and G represent the respective synaptic gains. From (WENDLING, FABRICE *et al.*, 2005).

The dynamics of each population are represented by (i) AP density and (ii) PSP average. The “wave to pulse” function is an asymmetric sigmoid that takes as input the population average PSP and outputs the AP density fired by this population. The equation is given by:

$$S(v) = \frac{2e_0}{(1 + e^{r(v_0 - v)})} \tag{9}$$

Parameters of the sigmoid function are given as: $v_0 = 6\,mV, r = 0.56\,mV$, and $e_0 = 2.5\,s^{-1}$. A 2nd order linear transfer function relates the incoming AP density to efferent PSP average. Impulse responses are represented by $h_e(t) = Aae^{-at}$ for excitatory synapses (EXC), $h_i(t) = Bbe^{-bt}$ for slow dendritic inhibition (SDI) and $h_g(t) = Gge^{-gt}$ for fast somatic inhibition (FSI). *A, B,* and G are synaptic gains for each population. These are shown in Figure 1b.

The system input is **p(t),** a normally distributed random variable and represents afferent APs to pyramidal cells. The system output is the summated PSPs from pyramidal cells, which are the main contributors of EEG signals (WENDLING, FABRICE *et al.*, 2002).

Different types of activity can arise from this model, depending on the given parameters. The ones with the most interest are the synaptic gains of each population: A (excitatory), B (slow dendritic inhibition – SDI), and G (fast somatic inhibition – FSI). Figure 2a shows the six types of generated activity, while Figure 2b shows the set of parameters generating each one of them.

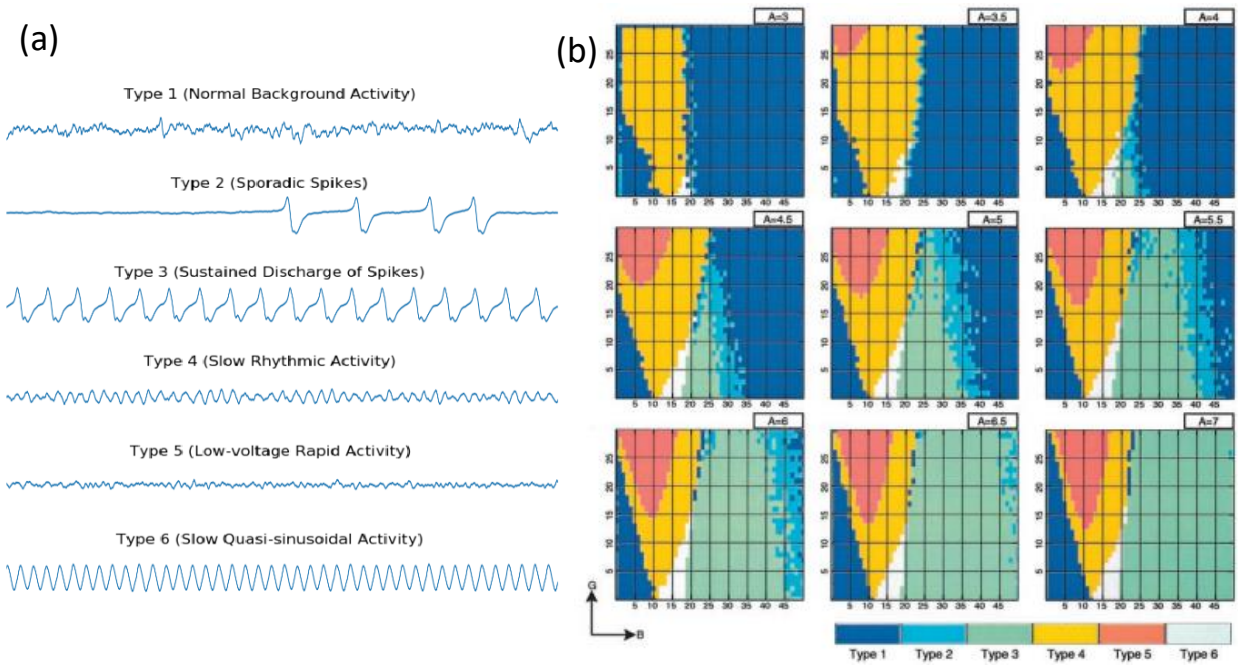

Figure 2: Simulated activity types and mapping parameters to activity. (a) Outputs representing each activity type generated by the model. (b) Activity map made by exploring the model's space parameter of synaptic gains; A for EXC, B for SDI, and G for FSI. In this work, most simulations were run from type 1 normal activity, as it approached type 3 activity (sustained discharges of spikes), which was considered to be the 'ictal' state. Figure adapted from (WENDLING, FABRICE *et al.*, 2002)

Different routes to seizures and parameters that give rise to epileptogenic activity are discussed in more detail (WENDLING, FABRICE *et al.*, 2002) and (WENDLING, FABRICE *et al.*, 2005). In general, the transition from normal to ictal activity can be best explained by SDI impairment (reduction in B). In physiological terms, this can refer to the selective loss of inhibitory interneurons that project to *stratum lacunosum moleculare*, increasing dis-inhibition of dendrites from pyramidal neurons (COSSART *et al.*, 2001).

The WNMM is an influential model that has enabled the investigation of several aspects of neuronal dynamics, ictogenesis, and the effects of perturbational approaches to control or probe neuronal activity. Some examples of this are given in the next paragraphs, emphasizing the latter.

In (SUFFCZYNSKI *et al.*, 2008), the WNMM was used to evaluate the potential of probing stimuli to identify changes in inhibitory-excitatory balance that precede the transition to a seizure. Stimulation affected equally all population subsets, shifting their membrane potentials toward depolarized states with monophasic quadratic pulses of 1 ms duration and frequency of 10 Hz. Increases in the relative phase-clustering index (rPCI) were found to occur when the neuronal activity – simulated and from some TLE patients – approached the ictal threshold.

A bifurcation analysis of the transition between normal and pathological responses in this model is given by (HEBBINK; VAN GILS; MEIJER, 2020), revealing two different dynamical regimes – fast and slow. The fast component is normally suppressed by normal inhibition but released by critical values of external stimulation.

With a data-driven approach, an extended version of the WNMM was used in (HEBBINK *et al.*, 2020) to confirm clinical observations about the value of using delayed responses to SPES as a biomarker for the epileptogenic zone. These responses depended not only on local excitability but were also influenced by network effects, with feedforward inhibition playing an important role.

The effects of local direct current stimulation (LDCS) on hyperexcitable neuronal populations were assessed in (MINA *et al.*, 2017). The rate of occurrence and duration of hippocampal paroxysmal discharges were reduced with the use of cathodal LDCS in

the *in-silico* model and validated with an experimental mouse model (kainic acid). Along with previous works, this further supported the use of computational models to assist in designing neuromodulation therapies. One of the most common types of these therapies, DBS, is detailed in the next section.

2.4.Deep Brain Stimulation - DBS

DBS consists of applying electric pulses directly to specific regions of the brain, through electrodes connected to pulse generators, usually contained in portable implantable devices. The insertion of electrodes can be done in conscious patients with local anesthesia to enable better mapping for accurate electrode placement. It has been used increasingly in clinical practice due to its use for both modulating and probing neuronal circuits (LOZANO; LIPSMAN, 2013). Applications include treatments for tremor, Parkinson's disease, dystonia, as well as neuropsychiatric disorders such as depression, Tourette's syndrome, and obsessive-compulsive disorder (WICHMANN; DELONG, 2006).

Since (PENFIELD, WILDER & JASPER, 1954), electrical brain stimulation is used to investigate mechanisms and possible treatments for epilepsy patients (FRIDLEY *et al.*, 2012; STACEY; LITT, 2008; VONCK *et al.*, 2013). One approach includes the use of DBS as a tool for evaluating epileptogenic circuits (LOZANO; LIPSMAN, 2013). In (VALENTÍN *et al.*, 2005) it was shown that, aside from being functional markers of epileptogenic structural abnormalities, single pulse electric stimulation (SPES) can also be used as predictors of surgery outcome. High excitability regions were correlated with longer-lasting responses and potential candidates for surgical resection.

Specific stimuli patterns can be anticonvulsive, by disrupting the mechanisms leading to a seizure, but can also facilitate or lead to ictal events; this all depends on its parameters, mainly the affected region or circuits, frequency, periodicity (regular, random, etc.) and amplitude (COTA *et al.*, 2016).

The first use of DBS as a seizure probing tool in epilepsy patients was done in (KALITZIN, S. *et al.*, 2005). Stimuli were used to evaluate the spatial distribution and temporal changes of the excitability state in patients with temporal lobe epilepsy (TLE). Measures of relative phase clustering index (rPCI) were correlated with putative SOZs,

further supporting the potential of this method in pre-surgical evaluation. Furthermore, it was found that, as seizures approached, rPCI values from specific locations were higher, showing the value of this method in seizure prediction. However, one of the main criticisms of this work is that the frequency used for stimulation (10 – 20 Hz) could be pro-ictal. That is, the stimulus itself could be the cause of the seizures, instead of just assisting as a predictor. In (KALITZIN, S. N.; VELIS; DA SILVA, 2010), a dynamical systems view of transitions involved in seizures is presented, while proposing the use of active observation paradigms to predict the approximation of these transitions. A pilot approach was done in a patient with refractory epilepsy, using the rPCI index. Results suggested that increased rPCI values in both hippocampi would be signs of increased seizure susceptibility.

In (FREESTONE; BURKITT; *et al.*, 2011), an active observation method is proposed to estimate cortical excitability, relating the measured index to ictal electrocardiographic events. Only 2 patients were analyzed, serving as proof-of-principle for the method, with results suggesting that changes in excitability may not be a sufficient condition for seizures, but may lead to a higher likelihood of seizures. The method used had some differences in relation to previous works. While (KALITZIN, S. *et al.*, 2005) used steady-state responses in the mesial temporal lobe, (FREESTONE; KUHLMANN; *et al.*, 2011) used repetitive single pulses to the Neocortex. Stimuli were delivered directly at the epileptic focus, more locally than the one used in (BADAWY, R. *et al.*, 2009), which applied transcranial magnetic stimulation (TMS) to the motor cortex to infer cortical excitability in peri-ictal states. Hippocampal responses to stimuli of the anterior nucleus of the thalamus were used in (WANG, Y. C. *et al.*, 2020) as a surrogate marker to predict DBS efficacy.

In canines, a fully implantable system was tested in (FREESTONE *et al.*, 2013). Probing was applied in the circuit of Papez, involved in mesial temporal lobe epilepsy. Animals were given anticonvulsive medication to manipulate network excitability, which would be estimated with the probing protocol; stimulation in the anterior nucleus of the thalamus (ANT), with local field potential (LFP, measured by intracortical electrodes, as opposed to the EEG, measured at the scalp with macro electrodes) recordings in the

hippocampus. Results showed changes of evoked potential morphology, according to circadian cycle and time of drug administration.

A seizure model was used in (MEDEIROS *et al.*, 2014), who delivered 0.5 Hz stimuli in the amygdaloidal complex of urethane anesthetized rats during PTZ injection. The very low stimulation frequency assures that no circuits are entrained, thus preventing pro-convulsive effects; no alterations in epileptiform activity were found. Results suggested that electrical stimulation induced the temporal rearrangement of pre-ictal activity in the form of evoked potentials before the seizure, reflecting the increasing coupling of reverberant neural networks. This was visible only with electrical stimuli, suggesting its potential for seizure prediction.

2.5.Methods

2.5.1. Model parameters

The original WNMM is available at ModelDB[1] in C. We coded a Python 3.7 port of the original and modified models. This and the code to generate all figures in this chapter are available at https://github.com/vrcarva/WNMM_probing. The following packages were used: NumPy (HARRIS *et al.*, 2020), Joblib, scikit-learn (PEDREGOSA *et al.*, 2012), statsmodels, pandas (MCKINNEY, 2010), Matplotlib (HUNTER, 2007), and SciPy (VIRTANEN *et al.*, 2019).

Two main modifications were made to the original WNMM, as represented in Figure 3. The first is the bidirectional coupling of two neuronal populations (or model subsets) through excitatory main cells. This aims to represent inter-hemispheric hippocampal coupling, where each model subset or population represents the CA1 region of one cerebral hemisphere. This interaction is influenced by a coupling factor K (varied across simulations) and a delay coefficient τ_d, set to 10 ms (SEGAL, 1978).

The second modification to the original model is the addition of low-frequency periodic stimuli. These probing stimuli are represented by $s_i(t)$ and summed to the model's Gaussian noise input $p_i(t)$, which is the incoming density of action potentials to

[1] https://senselab.med.yale.edu/modeldb/ShowModel.cshtml?model=97983

the main excitatory cells of the neuronal population *i*. That is, the simplified modeling of the probing stimuli consists of an additional input function that represents incoming AP bursts due to the electrical stimulation of afferent regions such as the dentate gyrus or Schaffer collaterals. In the model, this is defined as periodic pulses with a duration of 10 ms and amplitude E_{stim}, delivered every 2 seconds. This stimulation paradigm differs from (SUFFCZYNSKI *et al.*, 2008) in three important ways: instead of using a stimulation frequency of 10 Hz, that might be pro-convulsive (COTA *et al.*, 2016; MIRSKI *et al.*, 1997), probing stimuli were given at every 2 s (0.5 Hz, 10 ms duration and amplitude 4 APs/s), in a way that should not entrain neuronal networks into proictal states. And while all population subsets are influenced equally (as in an electrode is placed in the CA1 region) in the referenced paper, this work stimulates the model input p_i(t), which would be equivalent to the perforant pathway. Moreover, in addition to comparing 'passive' vs stimuli conditions, different stimulation amplitudes were evaluated in the present work.

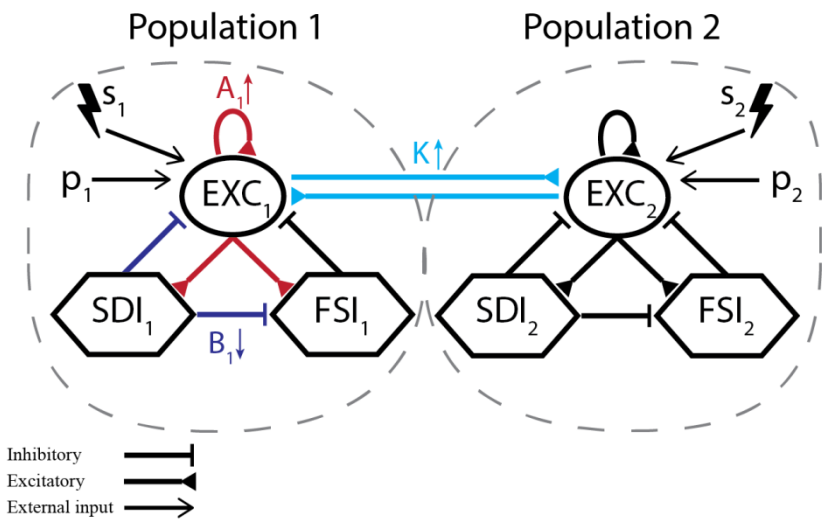

Figure 3: Modified neural mass model. (a) Representation of each coupled neuronal population and corresponding subpopulations. Excitatory interneurons are implicitly represented as the self-feedback loop from main pyramidal cells (EXC_i to itself). Each model settings consists of either (I) unilateral (s_2) or (II) simultaneous bilateral low-frequency probing stimulation (s_1 and s_2), while slowly changing one parameter towards ictal activity – A_1, B_1 or K.

The following set of 10 differential equations rule the activity of each neuronal population $i \in [1,2]$. In addition to adding the *i* subscript for different populations, highlighted terms indicate changes from the original WNMM.

$$\dot{y}_{i,0}(t) = y_{i,5}(t)$$

$$\dot{y}_{i,5}(t) = A_i a S\left[\boldsymbol{K_{i,j} y_{j,1}(t - \tau_d)} + y_{i,1}(t) - y_{i,2}(t) - y_{i,3}(t)\right] - 2a y_{i,5}(t) - a^2 y_{i,0}(t)$$

$$\dot{y}_{i,1}(t) = y_{i,6}(t)$$

$$\dot{y}_{i,6}(t) = A_i a\left(\boldsymbol{s_i(t)} + r_i(t) - C_2 S\left[C_1 y_{i,0}(t)\right]\right) - 2a y_{i,6}(t) - a^2 y_{i,1}(t)$$

$$\dot{y}_{i,2}(t) = y_{i,7}(t)$$

$$\dot{y}_{i,7}(t) = B_i b C_4 S\left[C_3 y_{i,0}(t)\right] - 2b y_{i,7}(t) - b^2 y_{i,2}(t)$$

$$\dot{y}_{i,3}(t) = y_{i,8}(t)$$

$$\dot{y}_{i,8}(t) = G_i g C_7 S\left[C_5 y_{i,0}(t) - C_6 y_{i,4}(t)\right] - 2g y_{i,8}(t) - g^2 y_{i,3}(t)$$

$$\dot{y}_{i,4}(t) = y_{i,9}(t)$$

$$\dot{y}_{i,9}(t) = B_i b S\left[C_3 y_{i,0}(t)\right] - 2b y_{i,9}(t) - b^2 y_{i,4}(t),$$

where s_i is the probing stimulus applied to population $i \in [1,2]$, and $K_{i,j}$ is the coupling factor between populations i and j, with $j \in [1,2]$ and $j \neq i$. In this work, bidirectional equal coupling was used, with $K_{1,2} = K_{2,1} = K$. Values and descriptions of model parameters are given in Table 1.

Table 1. Parameter descriptions and values (WENDLING, FABRICE *et al.*, 2002). A, B, and K values are either fixed or varied linearly throughout the simulations. (CARVALHO, VINÍCIUS REZENDE *et al.*, 2021)

Name	Description	Value
A_i	Average excitatory synaptic gain of population *i*	4.0 or [2.5 4.6]
B_i	Average slow dendritic inhibitory gain of population *i*	40 or [45 30]
G_i	Average fast somatic inhibitory gain of population *i*	20
K	Inter-population coupling factor	0.3 or [0 0.5]
a	Dendritic average time constant in the feedback excitatory loop	100 s^{-1}
b	Dendritic average time constant in the slow feedback inhibitory loop	50 s^{-1}
g	Somatic average time constant in the fast feedback inhibitory loop	350 s^{-1}
C1, C2	Mean number of synaptic contacts in the excitatory feedback loop	C1 = 135, C2 = 0.8 C1
C3, C4	Mean number of synaptic contacts in the slow feedback inhibitory loop	0.25 C1
C5, C6	Mean number of synaptic contacts in the fast feedback inhibitory loop	0.1 C1
C7	Mean number of synaptic contacts in between slow and fast inhibitory interneurons	0.8 C1
v0, e0, r	Parameters of the sigmoid (wave to pulse, or average PSP into average AP density) function	6mV, 2.5 s^{-1}, 0.56 mV^{-1}
μ, σ	Mean and standard deviation of noise input function p(t)	90, 1.3 APs/s
E_{stim}	Periodic probing stimuli amplitude, applied to the input of neuronal population *i*	[0 200] APs/s

The next section explains how parameters were varied according to different model configurations or settings.

2.5.2. Model settings

To simulate an increasing propensity to seizures in the model, parameters were set initially to generate normal activity, but gradually shifted to bring the activity towards the ictal state. As shown in Figure 3, this was done with different model settings, by varying which neuronal populations were externally stimulated, and which parameter was altered – increasing A_1 (EXC gain of population 1), decreasing B_1 (SDI gain of population 1), or increasing K (inter-population coupling gain). More specifically, the following parameters were used for each model setting:

I. **Probing neuronal population 2**

   A. Increasing A_1: A_1 = 2.5 to 4.6, A_2 = 4.0, B = 40, K = 0.3

   B. Decreasing B_1: A = 4.0, B_1 = 45 to 30, B_2 = 40, K = 0.3

   K. Increasing K: A = 4.0, B = 40, K = 0 to 0.5

II. **Probing neuronal populations 1 and 2**

   A. Increasing A_1: A_1 = 2.5 to 4.6, A_2 = 4.0, B = 40, K = 0.3

   B. Decreasing B_1: A = 4.0, B_1 = 45 to 30, B_2 = 40, K = 0.3

   K. Increasing K: A = 4.0, B = 40, K = 0 to 0.5

That is, model setting I consists of probing population 2 while parameters of the other population are shifted towards ictal-like activity. This aims to evaluate if applying stimuli to different regions that are not ictogenic (but coupled to ictogenic ones) allows for the identification of impending ictal transitions. The use of bilateral probing is evaluated in model setting II, where both populations receive stimuli simultaneously. Figure 3 highlights the interactions between neuronal populations and subpopulations of the proposed model settings, and each model setting diagram is shown in the respective results figures (Figures 5 - 10). Additional model settings with a single

population stimulated (ictogenic instead of “normal”) are shown in Supplementary Figure 1 and 2.

2.5.3. Feature extraction and probing effectiveness

Each simulation yields one signal for each of the two neuronal populations (or model subsets), as parameters are shifted from normal towards ictal activity, as shown in Figure 4. With 400 ms epochs delimited by stimuli onsets, different features were extracted from the output of each neuronal population: variance, skewness, kurtosis, and lag-1 autocorrelation (lag-1 AC). The mutual information between the activity of both coupled populations is also calculated to assess synchronization (QUIAN QUIROGA; PANZERI, 2009; ROSS, B. C., 2014).

In each simulation, the dynamics of the extracted features may indicate if the system is approaching the transition to an ictal state. In addition to visual inspection, where increasing or decreasing feature trends could indicate increased seizure susceptibility, it is important to quantify how good a predictor a feature is and compare this quantitative measure with and without probing stimulation. This can be done by assessing the relationship between the shifted parameter and the selected feature. The Spearman’s rank correlation coefficient (ZWILLINGER; KOKOSKA, 2000) was used for this to account for non-linear correlations. It is defined by:

$$\rho = \frac{\sum_{k=1}^{n}(x_k - \bar{x})(y_k - \bar{y})}{\sqrt{\sum_{k=1}^{n}(x_k - \bar{x})^2}\sqrt{\sum_{k=1}^{n}(y_k - \bar{y})^2}},$$

with k being the paired score, x and y the ranks of extracted features (variance, skewness, kurtosis, Lag-1 AC, and mutual information), and shifted parameters (A_1, B_1, or K), respectively.

Simulations were done for increasing values of stimulus intensity: from 0 (corresponding to the “control” or passive observation with no stimulus) to 200 APs/s, with steps of 20. In each of these, fifteen realizations were run and resulted in distributions for each extracted feature time-series, from which correlations measures were calculated. This enables statistical comparison between the effects of increasing probing stimuli amplitude through Tukey's honestly significant difference (HSD) method,

accounting for pairwise comparisons of probing efficiency between increasing stimulation amplitudes and the passive observation case (stimulus amplitude = 0).

Additional assessments should be done to ensure that the probing stimuli do not have pro-ictal effects. That is, probing stimuli should not elicit the seizure events that are trying to be predicted. Thus, additional tests were done using the same model settings and varying degrees of stimulus amplitude but shifting parameters further to elicit ictal activity. Criteria for defining seizure onset was the first time in the simulation where spike discharges occurred in succession – five spikes with an inter-spike interval of at least 4 seconds occur in succession. Spikes were detected if a peak was found in the simulated signal with an amplitude greater than 5 mV. To exclude stimuli responses, peaks 200 ms periods post-stimuli were discarded. Multiple comparisons testing with Tukey's HSD were made to test if stimulation of increasing amplitudes resulted in significantly different seizure onset times in relation to the passive case with no stimuli.

2.6.Results

Representative simulations are shown in Figure 4, showing the transition from normal to ictal activity with and without stimulation of both neuronal populations. A_1 was varied linearly from 4.3 to 4.95 throughout the simulation, eliciting ictal activity at the end. The shape of the evoked responses changed slightly, up to a point in the vicinity of the transition to the ictal state, where these are drastically increased and resemble interictal-like spikes (ILS) (LOPES, M A; LEE; GOLTSEV, 2017). Despite this, there was no activity in the form of sustained series of spontaneous discharges elicited by the stimuli.

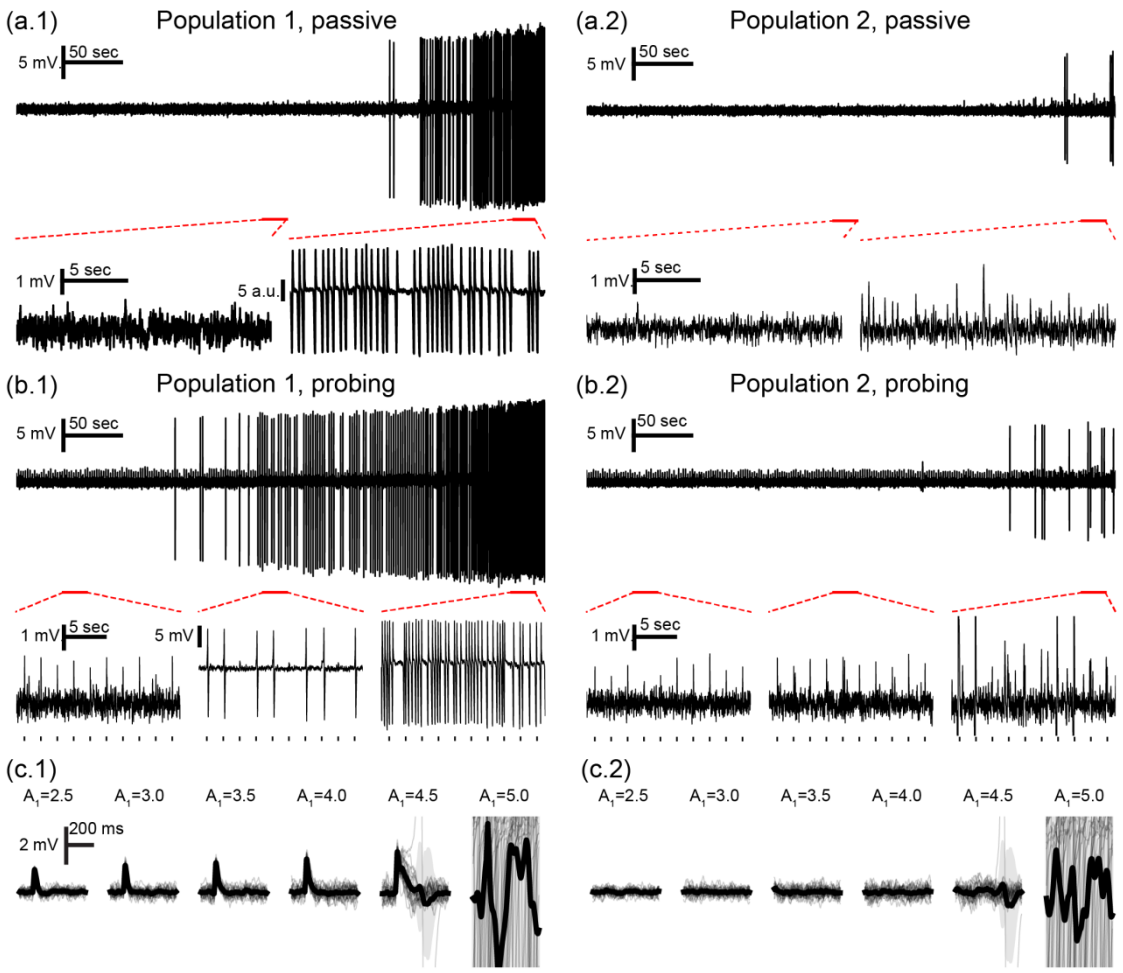

Figure 4: Neuronal mass model outputs with and without active probing stimuli. Simulation changing parameter A_1 from 4.30 to 4.95 (B = 40, G = 20) to elicit ictal activity in the end, with (a) passive observation or (b) active probing of both populations. Outputs are shown for population 1 (a.1 and b.1) and population 2 (a.2 and b.2), with tick marks showing stimuli onsets for (b). Ictal-like activity in the form of sustained discharges of spikes is observed for population 1 at the end of both simulations. ILS appear before this transition and are elicited even further in advance by stimulation. (c) Bottom plots show overlapped and mean response waveforms for increasing values of A_1 for (c.1) population 1 and (c.2) population 2. Gradual response changes are observed until the appearance of ILS for A_1=4.5 and ictal activity at A_1=5.0.

Active probing strategies are first evaluated with model setting I, in which a population is made ictogenic (but without crossing the threshold to ictal activity) by shifting a parameter linearly throughout each simulation – increasing A_1 (I-A), decreasing B_1 (I-B), or increasing K (I-K) – while perturbation stimuli are applied to the input of population 2. The following figures show a similar scheme, with (a) a template of the current model setting, (b-f) feature series from each population, for varied stimulation amplitude values, in addition to the corresponding Spearman's correlation ρ values at the bottom. Trends in a feature series result in increased absolute values of ρ and indicate that the underlying parameter change towards ictal activity is viable to detect

– if this happens only for increased stimulation amplitudes, the active probing approach is shown to have predictive value. Results for setting I-A are shown in Figure 5.

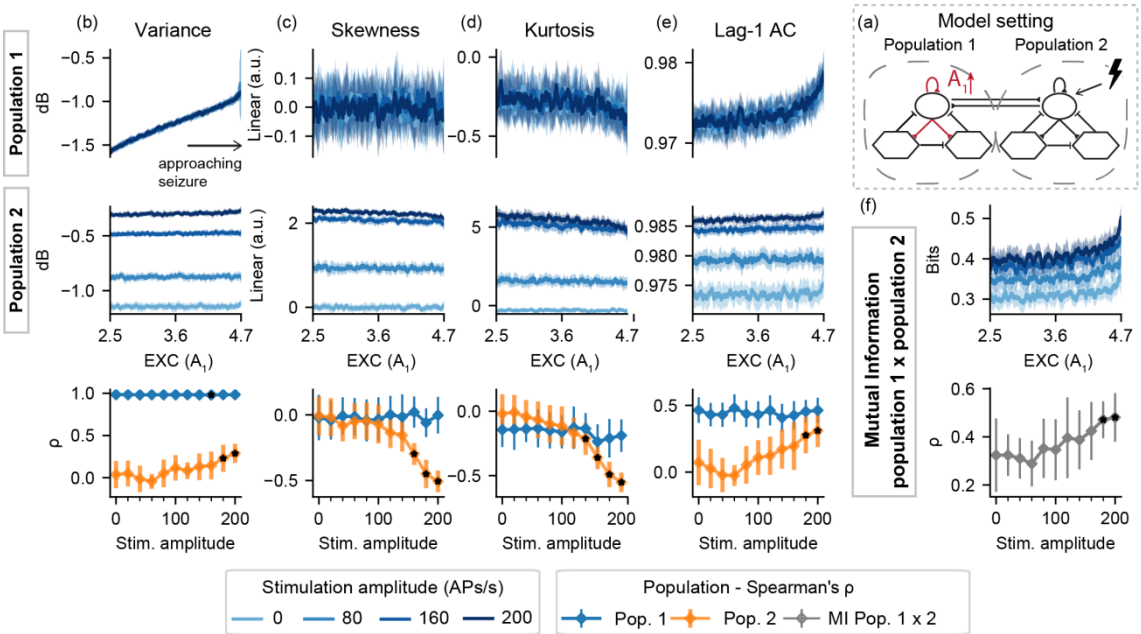

Figure 5: Feature series and probing efficiency for model setting I-A. For population 1, excitability increase is correlated with variance even with passive observation. However, increased amplitude probing responses from population 2 reflect gradual changes of A_1 towards ictogenesis. (a) shows a simplified illustration of the model setting. For (b) variance, (c) skewness, (d) kurtosis and (e) lag-1 AC features, top rows show feature values extracted from the output of each population, as the excitability gain parameter (A_1) is increased. (f) shows the inter-population synchronization as measured by the mutual information feature. The bottom row shows Spearman's rank correlation between each feature series and the shifted parameter (A_1), as stimulus amplitude is increased. Black dots indicate significant differences from passive observation (stim. Amplitude = 0) according to Tukey's HSD.(CARVALHO, VINÍCIUS REZENDE *et al.*, 2021)

For I-A, as observed from feature series and ρ from the bottom row of Figure 5b, the approaching transition to ictal activity is observed in the output of population 1 even without stimuli – with a notable increase in signal variance, as previously described in (SUFFCZYNSKI *et al.*, 2008). However, increasing stimulus amplitude (greater than 140 APs/s) affects other features for the "normal" population 2. Slight decreases in skewness and kurtosis can be observed with the increase in A_1, but only when probing stimuli are used. This suggests a predictive effect of the perturbational approach in this setting if only the activity of the 'normal' population is available. The increasing synchronization between neuronal activity of both populations is also slightly highlighted by increased stimuli amplitudes, as shown in Figure 5f.

Figure 6 shows results for model setting I-B. For decreasing values of slow inhibition B_1, slight increases in Lag-1 AC and variance of population 1 output are

observed, regardless of stimulation. That is, no predictive effects of active probing are observed in the activity of the neuronal populations when B_1 is decreased while population 2 is stimulated.

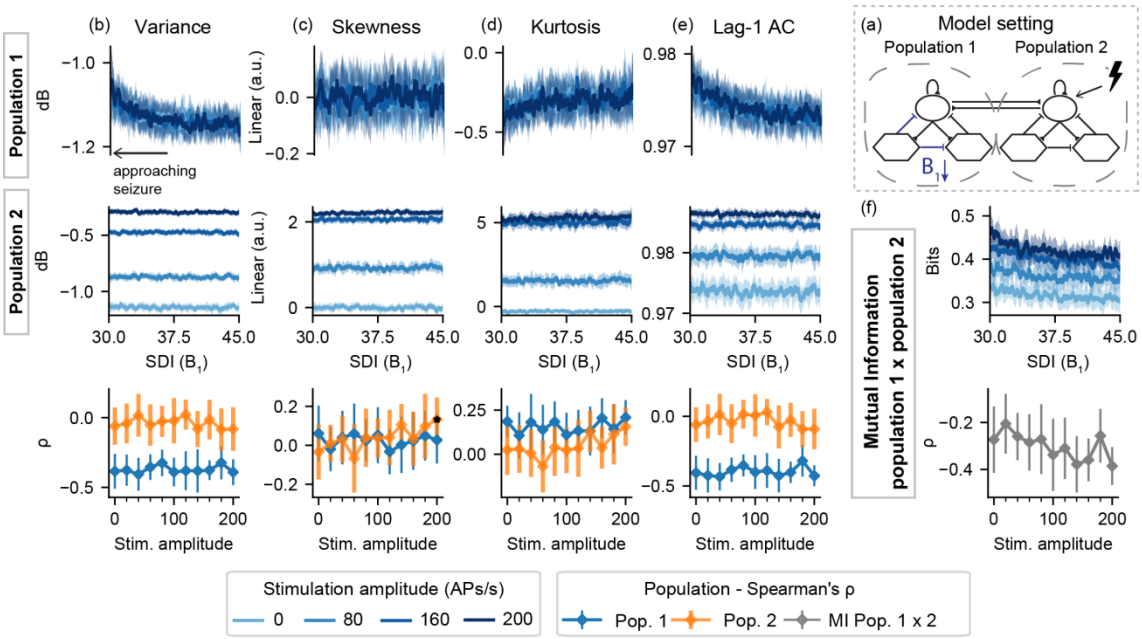

Figure 6: Feature series and probing efficiency for model setting I-B. Decreased slow inhibition of population 1 is not highlighted by the extracted features if only the "normal" neural mass (set 2) is stimulated. (a) shows a simplified illustration of the model setting. For (b) variance, (c) skewness, (d) kurtosis and (e) lag-1 AC features, top rows show feature values extracted from the output of each population, as the slow inhibition gain parameter (B_1) is decreased. (f) shows the inter-population synchronization as measured by the mutual information. Bottom row shows Spearman's rank correlation between each feature series and the shifted parameter (B_1), as stimulus amplitude is increased.

Figure 7 shows results for model setting I-K. Feature trends with increased correlation with the ictogenic parameter K are observed for population 1, but only when stimuli are used. This is also evident with the mutual information between population activities, with an increase correlated with approaching ictal threshold that is highlighted by the probing stimuli. However, these changes are not observed with the un-perturbed population 1. Altogether, the results for setting I indicate that the effectiveness of active probing to highlight preictal changes is limited to the model subset being perturbed.

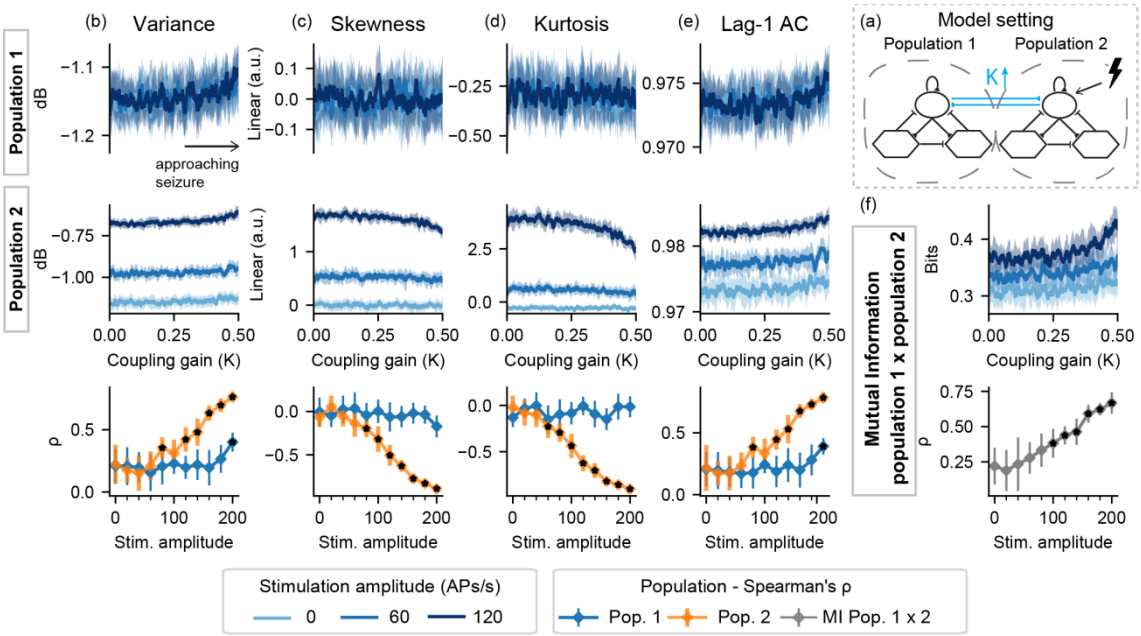

Figure 7: Feature series and probing efficiency for model setting I-K. Coupling gain increase is highlighted by features extracted from the stimulated population and by the mutual information between activities of both model subsets. (a) shows a simplified illustration of the model setting. For (b) variance, (c) skewness, (d) kurtosis and (e) lag-1 AC features, top rows show feature values extracted from the output of each population, as the coupling gain gain parameter (K) is increased. (f) shows the inter-population synchronization as measured by the mutual information feature. Bottom row shows Spearman's rank correlation between each feature series and the shifted parameter (K), as stimulus amplitude is increased.

Results are now shown for model settings II, where both populations are simultaneously probed while one parameter is shifted towards ictal activity. Figure 8 shows the specific model II-A. Increasing A_1 results in evident feature changes in the activities of both populations, when high stimulation amplitudes are used. The evident variance increase is still visible for population 1 even without stimuli, but the changes for population 2 are highlighted only when bilateral probing is used. The same holds for the synchrony measure between both populations, as shown in Figure 8f. The sharp increase in signal variance for higher stimulation amplitudes reflects enhanced responses or ILS shown in Figure 4.

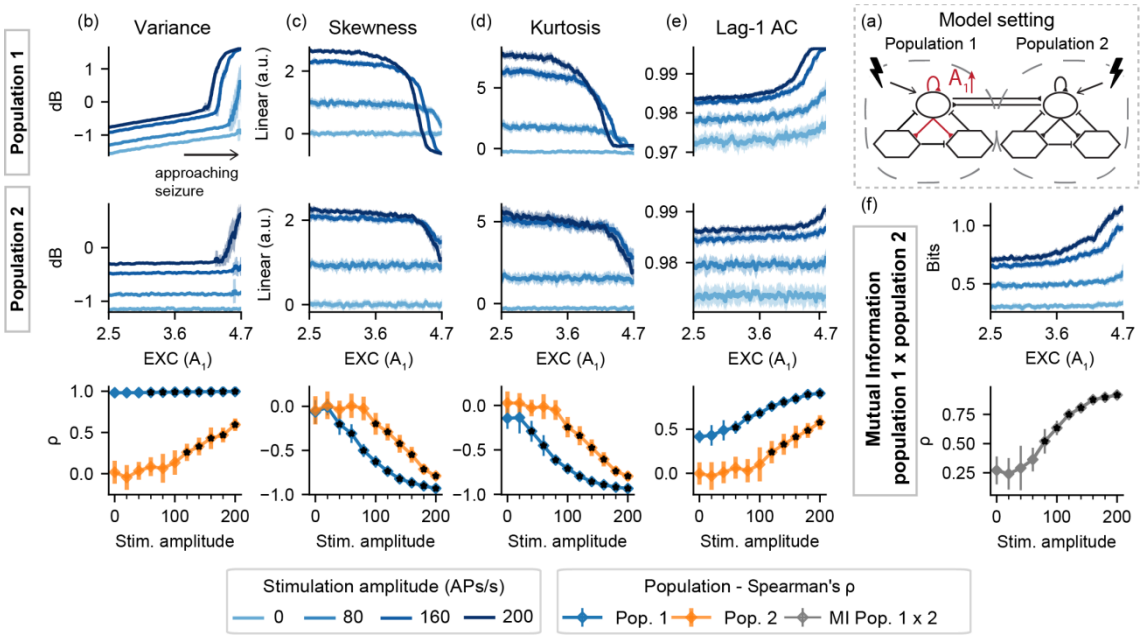

Figure 8: Feature series and probing efficiency for model setting II-A. Active probing effects are visible for population 2, but only for increased stimulation amplitudes. (a) shows a simplified illustration of the model setting. For (b) variance, (c) skewness, (d) kurtosis and (e) lag-1 AC features, top rows show feature values extracted from the output of each population, as the excitability gain parameter (A_1) is increased. (f) shows the inter-population synchronization as measured by the mutual information feature. Bottom row shows Spearman's rank correlation between each feature series and the shifted parameter (A_1), as stimulus amplitude is increased

Model setting II-B results in Figure 9 show that significant feature changes are correlated with decrease in B_1 when probing stimuli are used. This is observed for univariate features extracted from each population and from the mutual information between both population activities.

Similar feature profiles are visible in Figure 10 for with model setting II-K. Sharp increases in variance, lag-1 AC, and mutual information, while skewness and kurtosis decreased – but only when probing stimuli >= 60 APs/s are used.

Stimulating a single ictogenic population also leads to clear predictive features, as shown by Supplementary Figure 1 and 2.

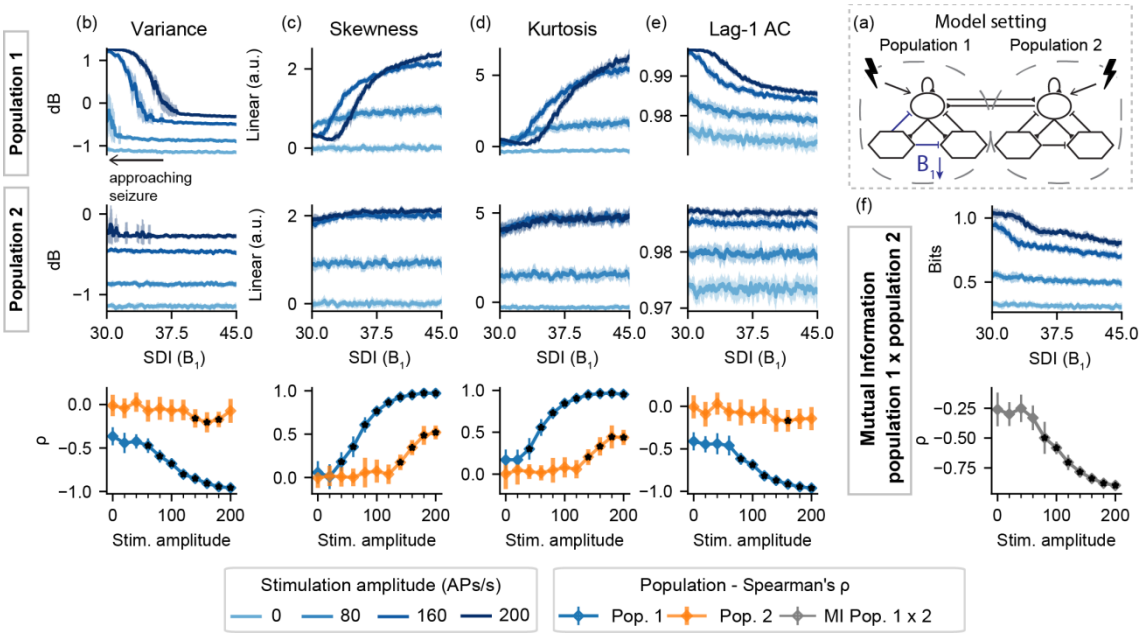

Figure 9: Feature series and probing efficiency for model setting II-B. Active probing provides predictive value for features extracted from both populations, but the effect is limited to increased stimulation amplitudes for population 2. (a) shows a simplified illustration of the model setting. For (b) variance, (c) skewness, (d) kurtosis and (e) lag-1 AC features, top rows show feature values extracted from the output of each population, as the slow inhibitory gain parameter (B_1) is decreased. (f) shows the inter-population synchronization as measured by the mutual information feature. Bottom row shows Spearman's rank correlation between each feature series and the shifted parameter (B_1), as stimulus amplitude is increased.

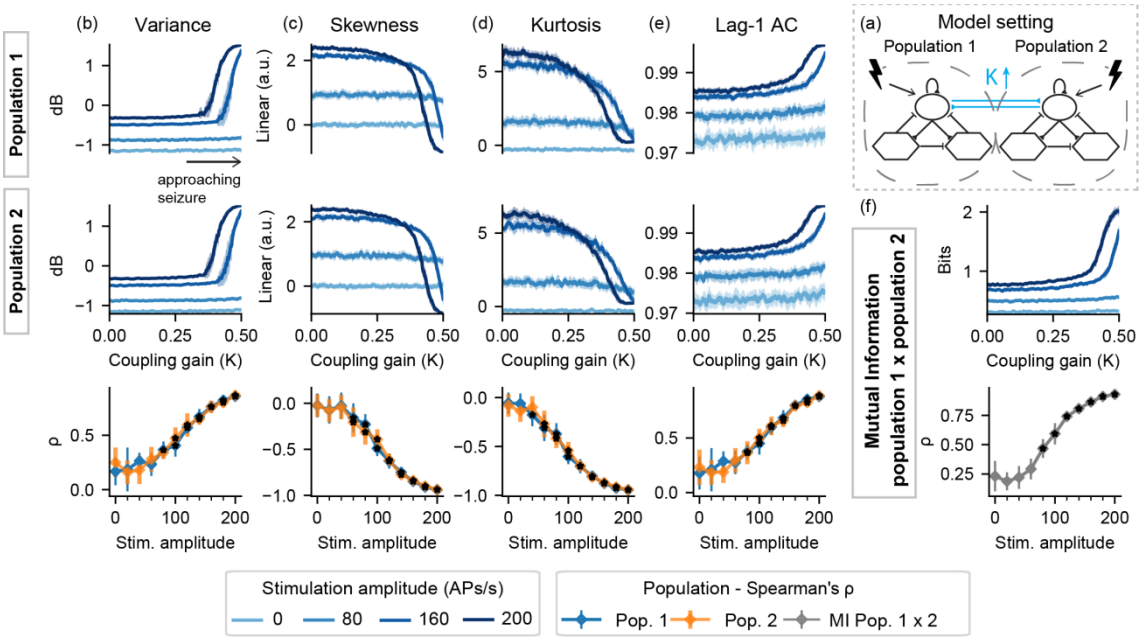

Figure 10: Feature series and probing efficiency for model setting II-K. Probing provides predictive value for both stimulated populations. (a) shows a simplified illustration of the model setting. For (b) variance, (c) skewness, (d) kurtosis and (e) lag-1 AC features, top rows show feature values extracted from the output of each population, as the coupling gain parameter (K) is increased. (f) shows the inter-population synchronization as measured by the mutual information feature. Bottom row shows Spearman's rank correlation between each feature series and the shifted parameter (K), as stimulus amplitude is increased

Finally, additional simulations are run to evaluate if the occurrence of ictal-like activity is precipitated by the probing stimuli. The same model settings were used, but shifting parameters beyond the point that ictal activity in the form of sustained spike discharges are elicited. The onset time of occurrence of these transitions is measured for each simulation, for increasing values of stimulation amplitudes and shown in Figure 11. Tukey's HSD of all stimulation amplitudes versus the passive observation case (amplitude = 0) did not result in any significant differences in any model setting. That is, the occurrence of sustained discharges of spikes was not anticipated when stimuli were used, compared with the passive observation simulations.

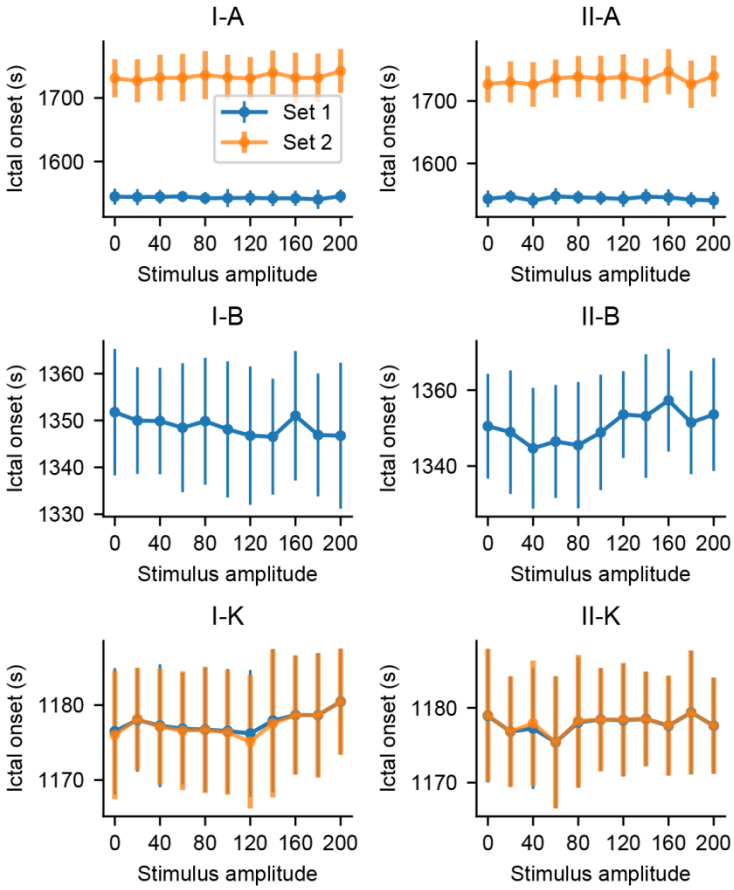

Figure 11: Onset time of ictal-like activity as a function of stimulus amplitude. Simulations with increased amplitudes did not affect the onset latencies of sustained spike discharges in any model setting.

2.7.Discussion

Using coupled neuronal populations of a well-known neural mass model, the results here provide support to using probing stimuli as a method to highlight features

that herald incoming seizures. When stimuli were used, it was possible to infer shifts in different parameters (A_1, B_1 and K) leading to seizure states, which could not be achieved with only the passive observation of the system in the majority of the model settings evaluated.

2.7.1. Local effect of active probing and better effects stimulating both neuronal populations

In model setting I, passive observation of the first neuronal population is enough to infer the increase in A_1 due to the marked increase in signal variance, as shown previously in (SUFFCZYNSKI *et al.*, 2008). To a lesser extent, this is also true for setting I-B, where the activity of the first ictogenic population is not better able to predict the incoming ictal state. However, features extracted from the activity of the probed population 2, the effects depended on which parameter was being altered. That is, no detectable changes were found in setting I-B, but increases in the coupling factor (K) and excitability (A_1) were correlated with features extracted from the perturbed population 2. This local effect of probing efficiency highlights the importance of spatial coverage of ictal activity, reaffirming the findings of (O'SULLIVAN-GREENE *et al.*, 2017) that suitably dense recordings are important for the success of an active probing approach in extracting relevant system information.

With the simultaneous stimulation of both neuronal populations, better results were found for model settings II regardless of which parameter was used to bring the model towards ictal activity. That is, the extracted features from stimuli responses are consistently correlated with the increasing excitability (A_1), coupling strength (K), and decreasing slow inhibition (B_1). Together with the fact that changes heralding the approach of ictal activity were visible not only in the ictogenic population activity, but also in the coupled neuronal populations with fixed parameters (as in the case of model setting II-A), these results indicate that the coordinated stimulation of more than one area may enhance the predictive power of the active probing approach. This goes in line with the increasing notion that epilepsy should be regarded as a neuronal network disorder (ZWEIPHENNING *et al.*, 2019), with network topology playing a major role in seizure generation. This perspective has been used to plan optimal surgery strategies –

e.g., scale-free and rich-club networks display specific nodes that are critical for seizure generation and should be good candidates for removal (LOPES, MARINHO A. *et al.*, 2017). Future work could show how different active probing configurations and parameters should be tailored for specific network topologies, leveraging the predictive power while assuring that seizures are not precipitated by stimulation.

2.7.2. Similar features and ILS serving as early-warning signals

Regardless of the seizure route taken by the changing parameters (decrease in B_1, increase in A_1 or K), feature changes serving as early-warning signals were consistent. Increased lag1-AC and signal variance were observed, suggesting states of hyperexcitability, which is in accordance with the results in (BADAWY, R. A. B. *et al.*, 2012) and (FREESTONE; KUHLMANN; *et al.*, 2011). There were also marked decreases in Skewness and Kurtosis, which could indicate greater neuronal reorganization and slower dynamics, resulting in more salient event-related potentials (ERPs) as one of the findings in (MEDEIROS *et al.*, 2014). In this 2014 paper, evoked responses were mostly visible only up to seconds before a seizure, whereas in the current work, these are visible after every stimulus, with changes in morphology as a seizure state gets nearer. In some cases such as the model setting II-A, drastic changes occurred in the vicinity of the transition to the ictal state, where stimuli responses evoked ILS. This can be related to the responses observed in (MEDEIROS *et al.*, 2014) and to the findings in (LOPES, M A; LEE; GOLTSEV, 2017). The latter work proposed a stochastic cellular automata neural network model (SCANNM), showing that the required external stimulation to evoke ILS became smaller as the model's activity approached the ictal state. Optimal stimuli intensities could then be tuned to serve as early-warning signals of incoming seizures according to the desired minimum period.

Despite evoking ILS right before the transition to ictal activity, the stimuli did not elicit sustained discharges of spikes when compared to the "control" simulations with no stimuli. That is, there were no pro-ictal effects due to stimulation using this model. However, while the evoked sharp responses could serve as clear early-warning signs of impending seizures, the role of interictal discharges in epilepsy is still unclear, including whether these events are anti or pro-ictal (AVOLI; DE CURTIS; KÖHLING, 2013; KAROLY

et al., 2016; STALEY; DUDEK, 2006). Thus, despite the lack of pro-ictal effects of the active probing approach in this work and others (FREESTONE; KUHLMANN; *et al.*, 2011; MEDEIROS *et al.*, 2014; WENDLING, F. *et al.*, 2016), more experimental evidence is needed to ensure that the use of long-term low-frequency probing stimuli would not induce pro-ictal effects while still providing seizure-forecasting value.

2.7.3. Probing stimuli indicate critical slowing down prior to the transition to ictal activity

Some of the features serving as early-warning signals may reveal underlying dynamics involved in the transition from normal/inter-ictal to ictal activity. The increased synchronization, signal variance, and lag-1 AC observed in this work reflect increased response amplitudes and longer recovery times from perturbations, which can be interpreted as markers of decreasing system resilience and critical slowing down. These are common signatures of approaching critical transitions (SCHEFFER *et al.*, 2009), which are sudden shifts in dynamical states that have been reported in several complex systems (BRETT *et al.*, 2020) and are marked by common hallmarks (SCHEFFER *et al.*, 2012).

It has been shown that the process of seizure termination in humans involves critical transitions (KRAMER, M. A. *et al.*, 2012), but it is still unclear if that is also the case for the initiation of seizures. Several computational models indicate that this might be the case (BREAKSPEAR *et al.*, 2006; JIRSA *et al.*, 2014; KALITZIN, S. N.; VELIS; DA SILVA, 2010; NEGAHBANI *et al.*, 2015), but conflicting evidence is found in patient data. Comparing human epileptic seizures data with models exhibiting self-organized criticality (SOC), deviations from a power-law were observed during seizures and could indicate a shift of dynamics toward an ordered phase during ictal events in (MEISEL *et al.*, 2012). Increased lag-1 AC was observed in 4 of 12 patients in (CHANG *et al.*, 2018), suggesting that critical slowing down should be evident in periods leading up to seizures in at least specific populations of epilepsy patients. However, long-term iEEG from 28 epilepsy patients did not reveal evidence for critical slowing down before epileptic seizures in (WILKAT; RINGS; LEHNERTZ, 2019). A minority of patients displayed the classical hallmarks or critical transitions before seizure onset in (MILANOWSKI;

SUFFCZYNSKI, 2016). Part of this conflicting evidence might be explained by the results in (MATURANA *et al.*, 2020), which found evidence that seizure onsets involve critical transitions by analyzing common signatures over different timescales in long-term iEEG data from epilepsy patients, which was not possible with previous works that used data from clinical settings.

These results further support the potential of active probing strategies to reveal underlying dynamics involved in the onset of seizures. Previous works have provided evidence for this in different models. Increased variance and longer recovery times from perturbations were found to highlight critical slowing in (NEGAHBANI *et al.*, 2015), using periodic stimulation and even noise inputs. Critical slowing down was also evidenced by low-frequency stimuli before PTZ-induced seizures in rats (MEDEIROS *et al.*, 2014).

2.7.4. Comparisons with the EPILEPTOR model

In (CARVALHO, VINÍCIUS R.; MORAES; MENDES, 2019) similar methodology of using low frequency stimuli to probe for preictal states was evaluated in another seizure (or ictal-like activity) generating computational model: the EPILEPTOR developed by (JIRSA *et al.*, 2014). This is a generic phenomenological model that aims to capture dynamical transitions involved in ictal activity and is composed by two subsystems (one fast and another slow) coupled by a slow permittivity variable.

By gradually changing the epileptogenicity parameter of the EPILEPTOR, “normal” background activity shifts to ictal-like activity. The approaching of this transition could not be observed with features such as variance, Lag-1 AC, Skewness, or Kurtosis. However, when low-frequency stimuli were used, trends in these features were observed, in similar way that what was found in this chapter. This provides more evidence, using another model, that active probing approaches facilitate or enable the detection of impending transitions from normal (or inter-ictal) to ictal activity. Furthermore, some hallmarks of critical slowing down were observed in (CARVALHO, VINÍCIUS R.; MORAES; MENDES, 2019), with an increase of lag-1 AC as the epileptogenicity parameter increased. However, response amplitudes and variance were decreased, contrary to what was expected. A possible reason for this is the abstract

nature of the EPILEPTOR, which makes it harder to interpret its parameters and output signal (EL HOUSSAINI *et al.*, 2015), including the shape of its responses to stimulation.

2.7.5. Limitations

One of the limitations of the model includes the inability to generate high-frequency oscillations (HFOs). Pathological versions of these oscillations are found to be involved in epilepsy in animal models (BRAGIN; ENGEL; WILSON; FRIED; MATHERN, 1999) and in patients (BRAGIN; ENGEL; WILSON; FRIED; BUZSÁKI, 1999), and have received increased interest in clinical research. These might work as spatial Biomarkers for Epileptogenic Zones (FRAUSCHER *et al.*, 2017; ZIJLMANS *et al.*, 2012) and temporal biomarkers for Epileptic intensity (ZIJLMANS *et al.*, 2012), as well in basic research, helping to uncover mechanisms of ictogenesis (ENGEL, J. *et al.*, 2009; JIRUSKA, PREMYSL *et al.*, 2017). Additional research in computational and experimental models should be done to evaluate the use of active probing strategies to enhance the use of these oscillations as predictors – or how to use them to elucidate mechanisms involved in ictogenesis and generation of ILS.

Another limitation is the simplification made to represent the nature of the probing stimuli. These consisted of low-frequency pulses summed to the input of the model in the form of density of action potentials. Thus, the dynamics of the incoming effects of external signals were simplified. This could be overcome by (i) adding another population that receives direct external stimuli and projects to the “main” model input, or (ii) changing the probing target to affect the membrane potential of all subpopulations, representing local electrode placement for stimulation as done in (MINA *et al.*, 2017; SUFFCZYNSKI *et al.*, 2008).

Finally, active probing approaches may be viable but not be required for accurate seizure forecasting in some cases. In this work, for instance, increased variance of the “ictogenic” population was found when the excitability parameter was increased, even without stimulation. Intrinsic measures were used by (MEISEL *et al.*, 2015) to show reduced cortical excitability due to antiepileptic drugs, and increased excitability across the wake period in patients – and were correlated with stimulations-evoked responses

2.8. Conclusion

By using a modified version of a well-known neural mass model, it was shown that a low-frequency active probing approach provides predictive value that correlates with different parameter changes that led to seizures. Furthermore, the parameter changes revealed by the stimuli are consistent with the phenomenon of critical slowing down. This indicates that in addition to serve as a tool for feature extraction, active probing approaches may reveal underlying dynamics involved in the transition from inter-ictal to ictal activity.

3. AUDITORY STEADY-STATE RESPONSES IN INVASIVE RECORDINGS

Following the rationale of using active probing strategies to investigate abnormal and epileptogenic activity, this chapter aims to evaluate auditory steady-state responses in epilepsy patients undergoing presurgical evaluation with invasive depth brain electrodes. We hypothesized that abnormal ASSRs would be evident in epileptogenic regions, with either: (i) enhanced ASSR due to neuronal circuits being prone to entrainment, or (ii) impaired responses due to dysfunctional central auditory processing (CAP).

Activities described here were conducted during a one-year visiting researcher program at the Neurology department of the Massachusetts General Hospital (Boston, MA), under the supervision of Dr. Sydney S. Cash. The program *Programa de Doutorado-sanduíche no Exterior* (*PSDE*), was sponsored by the *Coordenação de Aperfeiçoamento de Pessoal de Nível Superior* (CAPES).

3.1. Introduction

For patients with refractory epilepsy (around 30% of epilepsy patients), surgical resection of the putative seizure focus is a viable treatment option. Seizure-free outcomes in these cases are estimated as 52% (5 years after surgery) and 47% (10 years after surgery) (KWAN *et al.*, 2012). This motivates further research on methods to identify candidate regions for resection, as well as the reevaluation of concepts such as the epileptogenic focus and other regions like SOZ, irritative zone, etc.

Some of the widely used methods for localization of candidate regions for resection include brain imaging (MRI, SPECT, CT), direct electrical stimulation, and the implantation of invasive brain electrodes (probes, grids, or stereo-EEG) for obtaining higher spatial resolution electrophysiological data. In conjunction with these methods, alternative approaches can be used, some of which have shown promising results, such as the use of patient-specific computational models (PROIX, T. *et al.*, 2014; PROIX,

TIMOTHÉE *et al.*, 2017; SINHA *et al.*, 2017). In line with the main topic of this thesis, we propose that different probing stimuli may be used for assisting the identification of epileptogenic foci, or candidate regions for surgical resection of patients with refractory epilepsy. This chapter presents the use of the auditory steady-state response (ASSR) to assess auditory processing and how it is affected by epileptogenic regions.

3.2. Auditory Steady-State Evoked Potentials

Sound stimuli elicit electrical activity in the order of 10 µV across structures along the auditory pathway (SILVA; NIEDERMEYER, 2010). Specific sounds are commonly used in clinic and research to elicit two main types of auditory evoked responses (AER): (i) Transitory evoked responses are elicited by short-duration sounds (such as clicks or bursts) and presented at relatively low rates, such that the evoked response vanishes before another stimulus is presented (PICTON, T.W. *et al.*, 1974). (ii) Auditory steady-state responses (ASSRs) are sustained evoked potentials, which can be elicited by amplitude-modulated (AM) tones. That is, a carrier frequency f_c is enveloped by a lower modulating frequency f_m. This results in the activation of neurons responding to the carrier frequency along the auditory pathway, in an oscillatory pattern which follows the modulating frequency as shown in Figure 12. Besides being used in clinical settings for anesthesia monitoring and evaluation of hearing threshold (PICTON, TERENCE W *et al.*, 2003), responses of this kind are being increasingly used in research (KOZONO *et al.*, 2019). Since oscillatory neuronal activity is pervasive across the brain and likely involved in several aspects of cognition and information processing (BUZSÁKI, G, 2006), it is likely that oscillations evoked by stimuli in the form of ASSRs may reveal neuronal dysfunctions of diverse types.

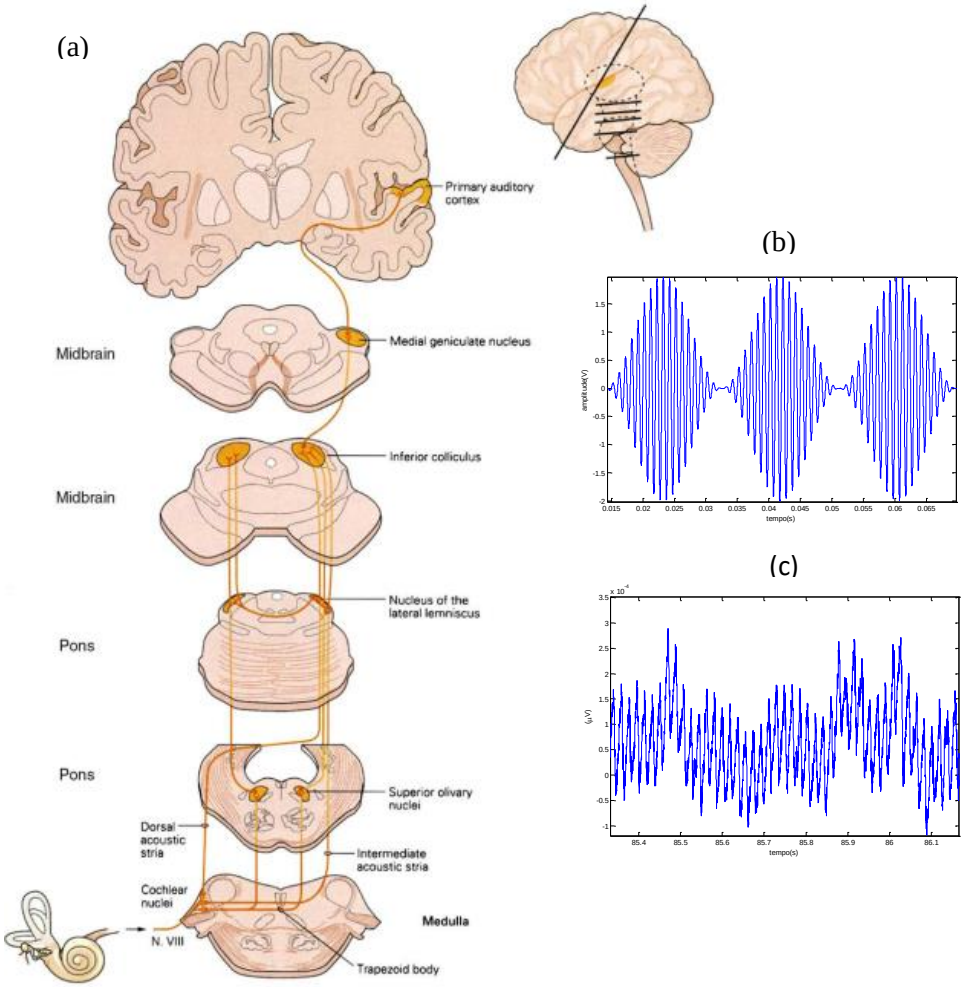

Figure 12: Auditory steady-state responses. (a) Human auditory Pathway (BRODAL, 1981). (b) AM tone, with $\boldsymbol{f_m} = \mathbf{53.71}\ \boldsymbol{Hz}$ and $\boldsymbol{f_c} = \mathbf{10}\ \boldsymbol{kHz}$. (c) Resulting ASSR of a Wistar Audiogenic Rat in the form of 53.7 Hz oscillations.

The evaluation of ASSR features such as amplitude or degree of coupling with the stimulus can provide information about the way sound is processed along the auditory pathway. But these responses may also reveal underlying pathologies that are at first, not exclusively related to auditory processing. Pioneering examples of this are the converging results showing reduced ASSRs elicited by either clicks or AM tones in patients with schizophrenia, as reviewed by (O'DONNELL *et al.*, 2013). Similar findings were reported for patients with bipolar disorder (ODA *et al.*, 2012). Reduced responses to rhythmic stimuli around 30 Hz (a band optimal for phonemic analysis) in the left auditory cortex of dyslexics was found with magnetoencephalography (MEG) in (LEHONGRE *et al.*, 2011).

Since the ASSR reflects neuronal entrainment to external stimuli, it is possible that it may prove useful as a tool to be used to investigate epilepsy. Using pure tones first, promising results were found in (MATSUBARA; OGATA; *et al.*, 2018), which showed altered neural synchronization in patients with unilateral mTLE. Stimuli responses and their synchronization between auditory cortices could differentiate not just between mTLE patients and healthy controls but indicate the degree of laterality of the seizure focus. A follow-up study of the same group (MATSUBARA *et al.*, 2019) used monoaural ASSRs and MEG, finding that healthy controls displayed clear contralateral temporal dynamics (in line with the contralateral predominance of the auditory pathway), while patients with unilateral mTLE showed a lack of contralaterality of the affected hemisphere. That is, stimuli to the right ear should induce increased responses to the left hemisphere (and vice-versa), but left mTLE patients did not display this type of predominant contralaterality (and vice-versa). This clarified the relationship between central auditory processing disfunction and the epileptic focus in patients with mTLE. Recently, impaired responses to chirp-modulated auditory stimuli were found in epileptic children (SANCHEZ-CARPINTERO *et al.*, 2020). In this study, children with Dravet syndrome were found to have weak or no ASSRs, while non-Dravet epileptic children had impaired responses when compared with healthy controls. Different results were found by (CANCADO, 2016), who observed that epileptic patients tended to present higher amplitude ASSRs when compared with controls. It was hypothesized that epileptogenic regions would be related to increased responses. However, due to the low number and heterogeneity of patients, statistical differences could not be found regarding response topology.

In an animal model of seizures, (PINTO, HYORRANA PRISCILA PEREIRA *et al.*, 2017) showed that Wistar audiogenic rats, a genetic strain susceptible to audiogenic seizures (triggered by loud sounds), displayed increased ASSR amplitude and synchrony for subthreshold AM tones (85 dB). Furthermore, when seizures were later elicited by suprathreshold AM tones (110 dB), ASSRs tended to decrease in the pre-ictal phase, but increase sharply in the post-ictal phase – which is usually characterized as a refractory period to external stimuli. The auditory processing in this rat strain was further investigated in (PINTO, HYORRANA PRISCILA PEREIRA *et al.*, 2019), with WARs showing

a corruption of the inferior colliculus synchronization that impaired performance in a classical fear conditioning task while preserving motor and hippocampus-related functions.

3.3.Invasive monitoring by stereo-electroencephalography (SEEG)

In patients with pharmaco-resistant epilepsy, removal or disconnection of the putative epileptogenic regions can be an option for treatment. However, pinpointing the exact locations involved in triggering and maintaining seizures is not always a straightforward task that may not be accomplished with only non-invasive methods such as brain imaging, MEG, or EEG. Electrocorticography (ECoG) is an invasive procedure that requires craniotomy for the placement of electrode grids or strips and provides a good spatial sampling of the activity near the cortical surface but is limited for finding seizure activity in deeper brain structures. Another alternative that is being increasingly used in clinical practice is stereoelectroencephalography (SEEG) (GONZALEZ-MARTINEZ; CHAUVEL, 2020; TALAIRACH *et al.*, 1961), a minimally invasive surgical procedure where depth electrodes are implanted in the brain. SEEG recordings may provide evidence to delineate regions of interest (such as EZ, SOZ, irritative zone) needed to guide clinical decisions. Each electrode has a number of contacts (8 to 16, in general) spaced by 2 mm throughout its shaft. Succinctly, the method consists of: choosing the brain regions to be covered based on initial hypotheses of EZ location, defining the number and type of electrodes, fusion of angiotomography and MRI to guide insertion of the electrodes, stereotaxic surgery for implants of the depth electrodes, followed by brain tomography that is fused with MRI to confirm the placement of each electrode. This reconstruction is essential to label exactly which region is covered by each contact. Figure 13 shows an example of mapping of the insertion points, followed in Figure 14 by the post-surgery imaging reconstruction of a specific contact.

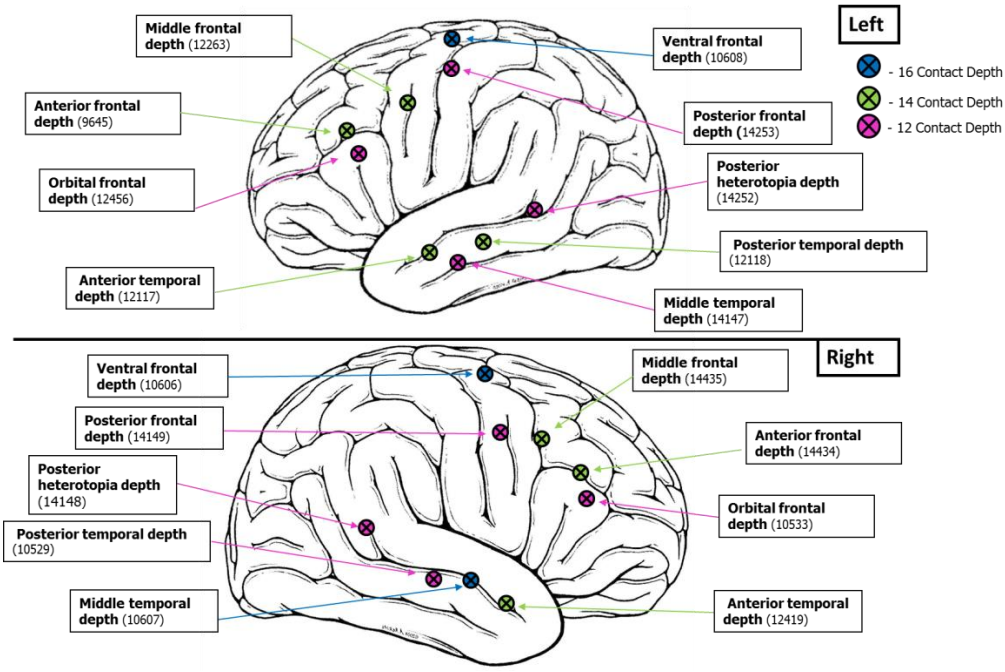

Figure 13: Insertion points for all electrodes for a specific participant. Detailed for left and right hemispheres, with each electrode having from 12 to 16 contacts along the shaft.

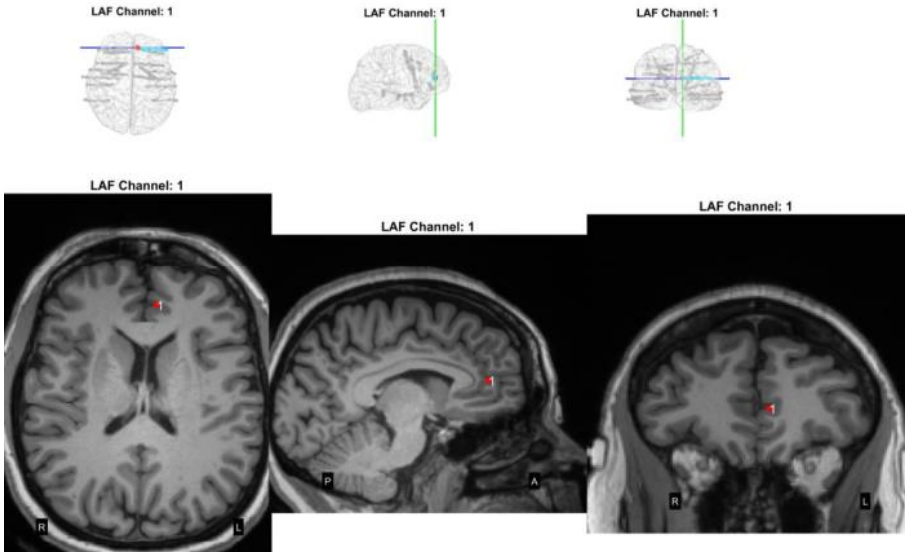

Figure 14: Post-surgery MRI reconstruction. Upper plots show transverse, sagittal and coronal views of electrode locations, highlighting the LAF (Left Anterior Frontal) one. Bottom plot shows MRI with the location of the first, deepest contact of this electrode.

Electrode labels are 3-5 letter identifiers that refer to the insertion points. In general, the letters refer to:

- 1st Refers to the side (R for Right, L for Left).
- 2nd: O (Orbital), A (Anterior), V (Ventral), M (Mesial), P (Posterior)
- 3rd: F (Frontal), T (Temporal), H (Hippocampus)

Thus, electrode LAF would be left anterior frontal, as shown in Figure 13 and Figure 14.

After the implant surgery, the patient is monitored for days – how long depends on the number and nature of the ictal events observed. The inter-ictal and ictal events of interest captured by the SEEG recordings provide evidence of putative regions involved in triggering seizures, hence guiding the course of surgical intervention. The SEEG recordings of rarely explored deep brain regions also provide unique opportunities to assess brain functioning. Simple tasks can be designed and executed to investigate not only how epilepsy impairs specific brain functions, but also reveal mechanisms of memory, cognition, auditory/visual/olfactory processing, etc.

3.4. Objectives

The main goal of this chapter is to evaluate if abnormal ASSRs are related to seizure-generating regions in patients with depth electrode implants. The two main hypotheses are that (i) ASSRs could be enhanced due to neuronal circuits being prone to entrainment, and that (ii) reduced responses can also be expected due to dysfunctional central auditory processing.

Another goal is to evaluate the topography of ASSRs, assessing which brain regions consistently generate responses to AM auditory stimuli. Furthermore, responses to different modulation rates (40 Hz and 80 Hz) are compared.

Finally, we aim to evaluate the ASSR under different conditions: when participants remain relaxed with their eyes closed and compare to responses elicited when the eyes are open. This is intended to support a next objective that was not able to be accomplished: to evaluate if ASSRs elicited by stimuli presented throughout the day would have predictive value for identifying periods of increased seizure susceptibility.

3.5. Methods

Figure 15 outlines the main steps of the methodology, from the auditory task, data preprocessing, analysis and visualization. Each step is detailed in the next sections.

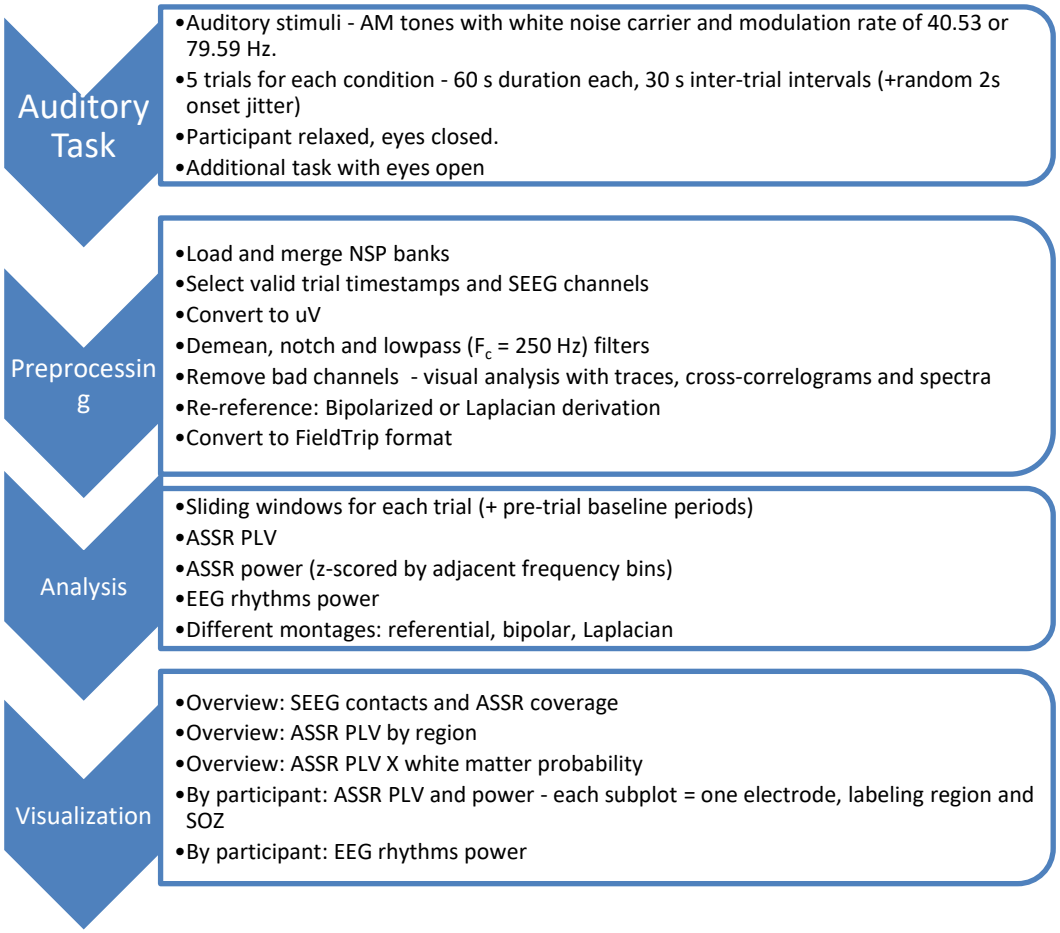

Figure 15: Overview of method and data processing pipeline.

3.5.1. Ethics statement

All participants were patients from the Massachusetts General Hospital (MGH) and Brigham and Women's Hospital (BWH), who had refractory epilepsy and underwent invasive continuous monitoring to confirm the location of the EZ and SOZ. The choices of implanting electrodes (how many, electrode types, and trajectories) of each one were defined by clinical criteria only, by a team of clinicians independent of this study. Participation of all volunteers was conditioned by fully informed consent according to NIH guidelines, and procedures were approved and monitored by Partners/MGH Institutional Review Board (IRB). This includes communicating that participation in the study would not alter any aspects of their clinical treatment and that this participation could be interrupted anytime if wanted – again with no impact on clinical care.

3.5.2. Data acquisition

SEEG data were acquired with a Blackrock Cerebus system (Blackrock Microsystems), sampled at 2000 Hz, and initially referenced to one of midline contacts (FZ, CZ, or PZ) of the 10-20 system scalp electrodes. The scalp EEG data was not used in this project. Two amplifiers were used, depending on availability: a Front-end amplifier or a CerePlex A. LFP signals were digitized by a Blackrock NeuroPort Biopotential neural signal processing (NSP) unit (or two units, if the number of channels exceeded 128) and stored on a hard disk. Triggers for onset and offset of stimuli were also recorded.

After the implant surgery and 3D reconstruction of electrode/contact locations, an automatic labeling algorithm is used to map electrode contacts to corresponding brain regions (FELSENSTEIN *et al.*, 2019; PELED *et al.*, 2017) according to the Desikan–Killiany–Tourville (DKT) atlas (KLEIN; TOURVILLE, 2012). The algorithm also computes the probability of each contact to be surrounded by white matter. Additional labels were assigned according to clinical reports made during the presurgical monitoring; a SOZ label was assigned to contacts that appeared to be within seizure onset zones, and EZ labels were assigned to contacts involved in seizure spread.

3.5.3. Auditory task

The auditory task consists of using AM sound stimuli to elicit ASSRs in participants undergoing invasive epilepsy evaluations with SEEG. The participant is asked to remain with eyes closed while auditory stimuli are delivered in 8-10 trials of 60 s duration with 30 s between trials, with up to 2 seconds of a random onset jitter. In some patients, trial and inter-trial durations were changed to 45 and 20 seconds, respectively. Sounds consist of AM modulated white noise, with modulation rates f_m of 40.53 Hz or 79.59 Hz (4-5 trials each, randomly ordered), and 100% of modulation depth. White noise was chosen to exclude response differences due to tonotopic mapping of the auditory cortex. In other words, since specific regions of the auditory cortex are activated by specific carrier frequencies, having a stimulus that covers all possible frequencies should avoid confounding factors from this. Two modulation frequencies were chosen to assess ASSRs that involve different brain structures as generators – lower rates would involve cortical structures, while brainstem would be more involved in 80 Hz responses

(HERDMAN *et al.*, 2002; LEROUSSEAU *et al.*, 2019; ROSS, B. *et al.*, 2003). Auditory cortex disturbances should be reflected in 40 Hz responses (O'DONNELL *et al.*, 2013), while 80 Hz ASSRs would have reduced background 1/f noise (BUZSÁKI, GYÖRGY; WATSON, 2012) and reduced effects of laterality (POELMANS *et al.*, 2012).

Sound stimuli are delivered through speakers (Creative Pebble 2.0) placed on a tray in front of the participant (or in some cases, in two trays around the participant). Ideally, sound stimuli should be presented with headphones or earbuds instead of a speaker, but this would involve a more invasive procedure for running the task (since it would require partial removal or adjusting head bandages to insert the earbuds). Volume was set initially around 75dB but changed according to values that were comfortable to each participant.

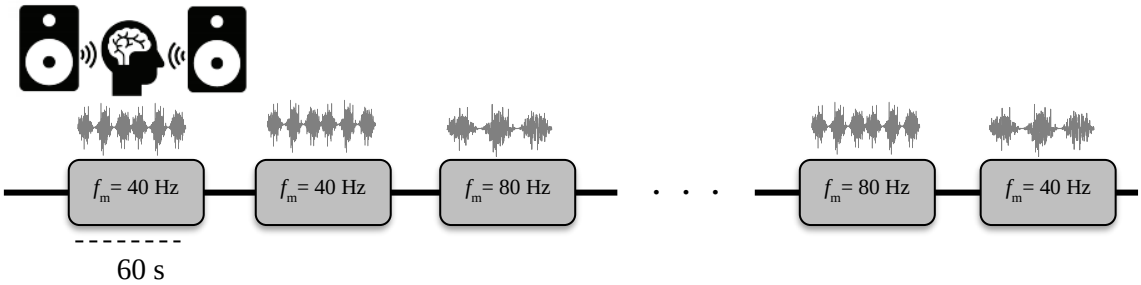

Figure 16: ASSR task. In each trial, an AM tone is played during 60 s with a pair of speakers facing the participant, with volume set to a comfortable level. White noise with amplitude enveloped by a slower frequency – either 40.5 Hz or 79.6 Hz.

An additional task was run with 13 participants. This consisted of using the same sounds and parameters mentioned previously, but asking the participant to remain with eyes open. This allowed evaluating the robustness of the responses under a different attentional condition.

A custom MATLAB (r2019b) script was used for running the tasks. The Psychophysics Toolbox Version 3[2] was used for interfacing between MATLAB and the computer hardware, including setting the output for the speakers and the input triggers.

[2] http://psychtoolbox.org/

3.5.4. Data processing and analysis

The first step in preprocessing consists of aligning the two Blackrock's Neural Signal Processor (NSP) banks, when applicable – this is done by taking the lag corresponding to the largest correlation between trigger channels from both NSP banks. Next, trials are identified based on selected triggers and modulating stimuli signals are reconstructed. SEEG channels are selected and rejected based on visual inspection of (i) each raw signal, (ii) autocorrelation matrixes, and (iii) signal spectra. Line noise notch filter is applied to all channels (zero-phase Butterworth, 4th order). When applicable, signals are re-referenced and then converted to Fieldtrip[3] format. Re-referencing is discussed in section 3.5.5.

The analysis is focused on the ASSR, which consists of oscillations centered at the modulation frequency (and harmonics) of the auditory stimuli – 40.53 Hz or 79.59 Hz. Baseline and trial periods were divided with sliding windows of 5s duration and 50% overlap, from which response was quantified both in terms of amplitude and phase-locking.

The ASSR amplitude was quantified by taking the spectral power around the modulation frequency and z-score normalizing it with spectral power from neighboring frequency bins around the modulation rate, as shown in Figure 17. Power spectral density (PSD) was calculated with Welch's method (WELCH, 1967), with 5-second Hanning-tapered windows, and 50% overlap.

[3] https://www.fieldtriptoolbox.org/

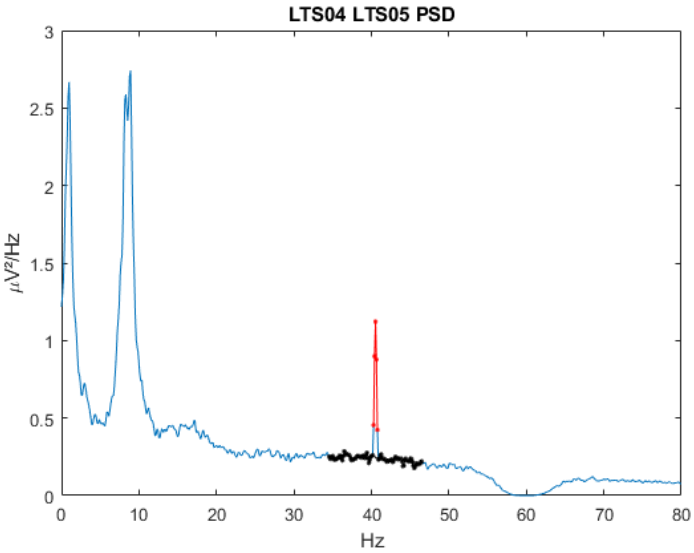

Figure 17: Trial PSD and ASSR power measurement. The elicited ASSR power is measures by the spectral magnitude in a narrow band at the modulation rate f_m (in red) and z-score normalized by values from neighboring frequency bins.

Phase synchrony is hypothesized to play a role in neuronal communication (FRIES, 2015), and can be inferred with the Phase-Locking Value (PLV) (LACHAUX *et al.*, 1999). The PLV is a measure of how dispersed is the relative phase between two time series. The first step for its calculation is filtering both signals in the desired frequency band. In this work, zero-phase 4th order Butterworth filters were used with cutoff frequencies around the modulation rates (40.53/79.59 ± 3 Hz). Phases $\psi_1(t)$ and $\psi_2(t)$ are extracted from each filtered signal through the Hilbert transform, obtaining the relative phase as the phase difference between them. The PLV is then calculated from this relative phase series $\psi_{1,2}(t)$:

$$PLV = \frac{1}{N}\left|\sum_{j=1}^{N} e^{i\psi_{1,2}(t_j)}\right|,$$

where N is the total number of time samples in $\psi_{1,2}$. Thus, PLV tends to 1 if the phase in the selected frequency band is coupled between two signals (even if there is a lag between them, as long as the lag is constant, they are phase-locked), and 0 if the phases are uncorrelated. The PLV is calculated between each SEEG contact and the modulating component of the auditory stimulus.

Thus, the ASSR is quantified in terms of two measures: power, and PLV. Both measures are taken for every sliding window in each trial. An ASSR is considered to be

evoked if the mean PLV value is greater than 0.16, AND the ASSR power is greater than 3.

3.5.5. SEEG signal referencing

The acquired LFP signals are initially referenced to a common electrode, usually the same used by the clinical recording system that is placed on the patient's chest. In some cases, the reference was changed to one of the midline contacts (FZ, CZ, or PZ) of the scalp electrodes. However, these signals may contain common-mode interference, be affected by changes to the reference electrode, and display voltage deflections due to field effects from far-reaching sources – this is an obstacle if these signals are used to evaluate hypotheses that rely on localizing features, such as the proposed one of comparing auditory responses and contacts near the SOZ. One way to overcome these limitations is through signal re-referencing, which can be done with several strategies, as discussed in detail in (LI *et al.*, 2018). In this chapter, we chose to use two methods: bipolar (or differential), which is widely used with SEEG recordings in research and clinical practice, and Laplacian, which is found to be an optimal referencing method in (LI *et al.*, 2018).

Bipolar re-referencing consists of subtracting the signal from two adjacent contacts from the same electrode shaft. For instance, re-referencing channels from an electrode LA (with contacts LA01, LA02, LA03, …, LA08) results in channels LA01-LA02, LA02-LA03, …, LA07-LA08.

Laplacian re-referencing also consists of subtracting adjacent channels, but this is done with surrounding contacts from the same electrode shaft, on both sides. That is, the Laplacian re-referenced signal from contact *i* is given by:

$$S_{iLapl} = S_i - \frac{(S_{i-1} + S_{i+1})}{2}$$

3.6.Results

3.6.1. SEEG data overview and examples

First, representative signals and spectra are shown to demonstrate the nature of the signals and evoked responses. SEEG traces from one participant are shown in Figure 18.

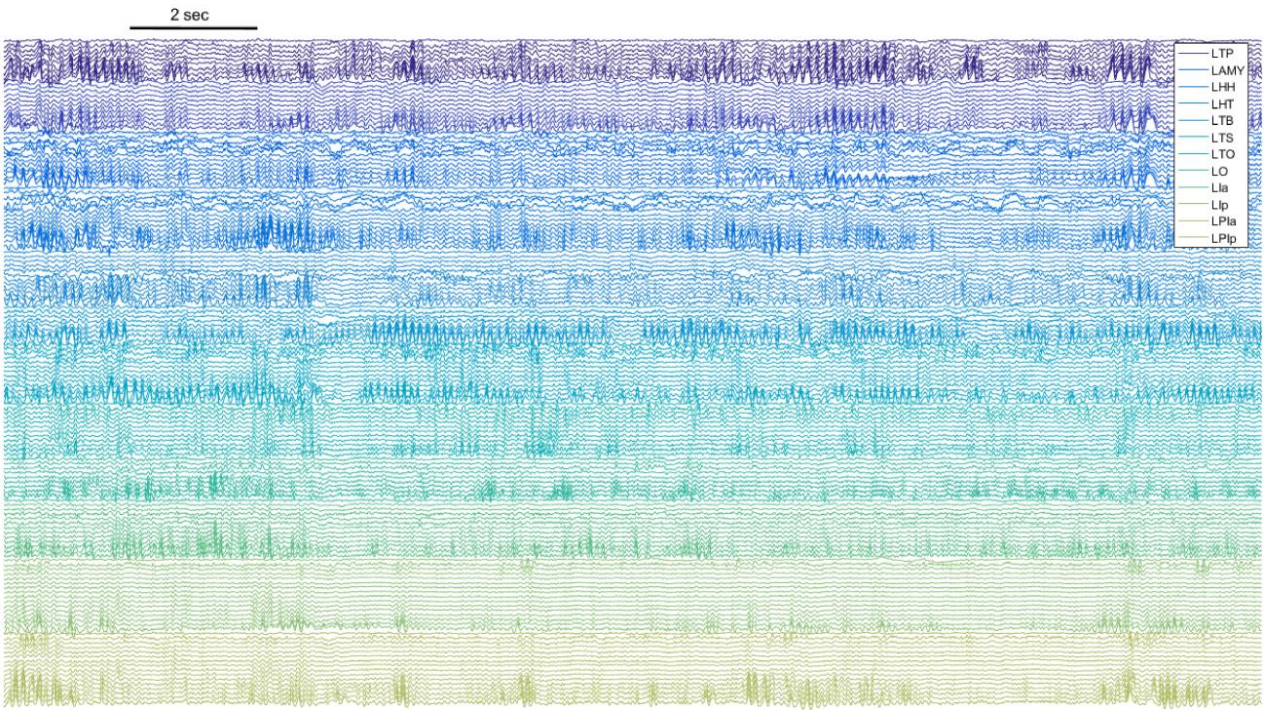

Figure 18: Representative LFP traces. A 20-second segment of all LFP signals recorded from P08. Each electrode is coded as a different color.

Plots of this kind, showing the time course of the LFP from each electrode contact, are commonly used for clinical diagnosis. Specialists (sometimes aided by algorithms) identify abnormal rhythms and electrographic signatures, inter-ictal discharges, and ictal activity that will guide the course of the clinical treatment. However, analyzing the evoked responses from the auditory task in this way is not recommended, since the scale of the ASSR is small compared to other components of the raw signal. This is exemplified by Figure 19, which highlights the referential/monopolar signals and the bipolarized derivations from contacts of one electrode.

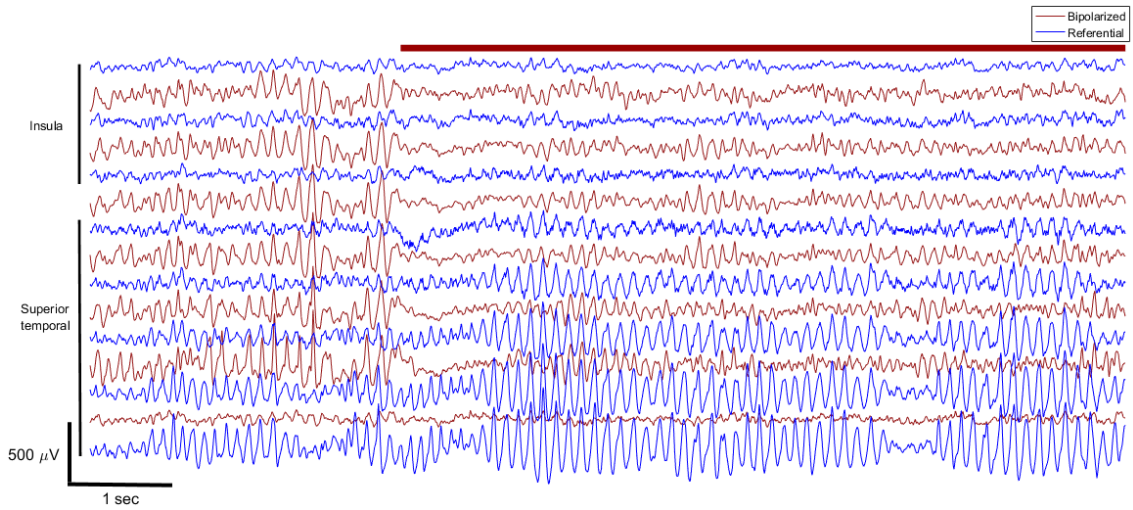

Figure 19: LFP traces from channels of the same electrode. Comparing monopolar and bipolarized signals from the same electrode from P08. Red trace indicates the initial period with the sound stimulus.

When analyzing the power spectral densities (PSD) of each contact, the evoked ASSRs are easily highlighted, appearing as high coefficients from oscillations around the modulating frequency of the stimuli – with either 40 or 80 Hz. This is evident in Figure 20, which shows the resulting PSDs from contacts across two electrodes from one participant during the task. Different re-referencing schemes are shown; both electrodes have contacts with the ASSR with monopolar recordings. However, in the LTO electrode, the ASSR vanishes when re-referencing with bipolar or Laplacian derivation, while the LTS electrode still has large responses. Probably, the former reflects field effects from a response generated elsewhere, while the latter (LTS) has contacts near the auditory cortex region responsible for generating the ASSR.

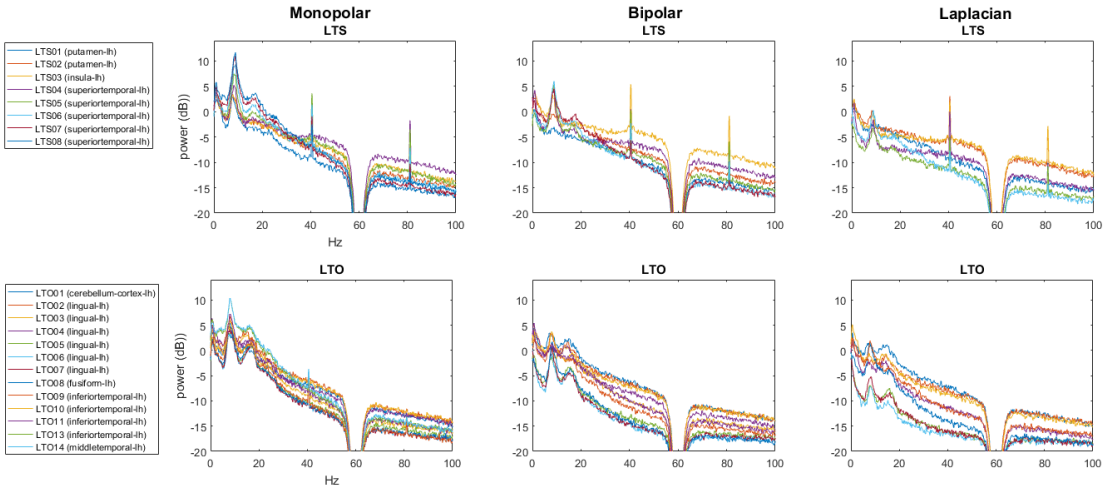

Figure 20: PSDs from all channels from two electrodes, during the auditory task. The ASSR is evident as oscillations around 40 Hz, visible in channels from both electrodes. However, re-referencing causes the vanishing of these oscillations in the LTO electrode, while contacts from LTS still display elevated responses.

A time-frequency representation of one of the contacts displaying the ASSR is shown in Figure 21.

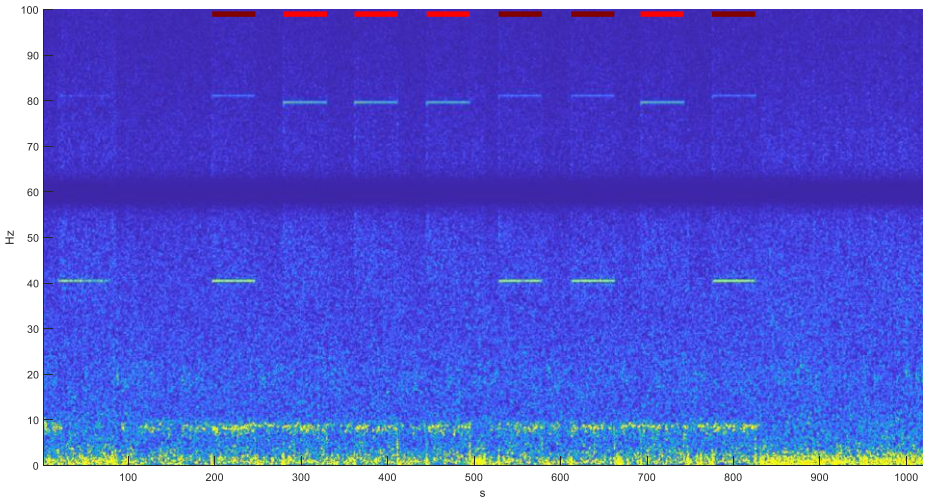

Figure 21: Time-frequency plot highlighting the evoked ASSRs during the sound stimuli. Spectrogram from the bipolarized LTS03-LTS04 derivation (P08) throughout the task. Sound stimuli of 40 Hz Trials in dark red, and 79 Hz trials in red. ASSRs are evident as oscillations around the modulating frequency of the respective stimulus. A 9 Hz rhythm is also evident throughout the task when the participant stays with the eyes closed but is suppressed at the end when the eyes are opened.

Next, a general overview from the data across participants is shown. The ASSR task was presented to 25 participants that comprised a very heterogeneous population with different implant schemes, epilepsies, and seizure etiology, as shown in Table 2:

Table 2: Overview of participant profiles. Age range is [22, 67] with median 37, and epilepsy onset age range [1, 65] and median 18.

P	Gender	Hand.	Prev. surgery	Seizures during monitoring	Seizure onset
01	F	R	Y	40	Left Frontal Lobe
02	F	R	N	19	Superior temporal
03	M	L	N	8	Multifocal seizures
04	F	R	Y	6	Insula
05	F	R	N	2	Inferior parietal, inferior temporal, lateral-occiptal
06	F	R	Y	2	Middle & superior temporal, other extratemporal locations (R orbital frontal, R insula, R frontal and parietal operculum)
07	F	R	N	5	Hippocampus
08	F	R	N	25	Onset at Left Hippocampal Tail and Head
09	M	R	N	7	Hippocampus, rostal middle frontal,lat. orb. frontal, amy, pars orbitalis, caudate
10	F	R	Y	2	Right posterior frontal seizure focus. Possibly, broad spatial areas are capable of ictogenesis
11	F	R	N	12	Left Mesial Occipital, Right Mesial Temporal
12	M	R	Y	7	Somewhat Unclear and Broad, LFIa
13	F	R	N	7	Inferior parietal and hippocampus
14	M	R	Y	3	Hippocampus
15	F	R	N	7	Inferior temporal
16	M	L	Y	5	bilateral mesial and posterior orbitofrontal cortex
17	M	R	N	12	right anterior inferior insular
18	F	R	N	10	Inferior parietal
19	M	R	Y	9	left posterior frontal region (electrographically, with delay)
20	F	L	N	2	Left mesial temporal structures
21	M	R	N	23	right mesial temporal lobe
22	F	R	N	19	Hippocampus
23	M	R	Y	>15	Superior frontal, hippocampus
24	M	R	N	-	-
25	F	R	N	-	-

Figure 22 shows the contact coverage for each brain region across participants, according to the assigned region for each contact by the electrode labeling algorithm (PELED *et al.*, 2017). Thus, for each participant and brain region, displaying the number of contacts and how many were considered as belonging to the SOZ.

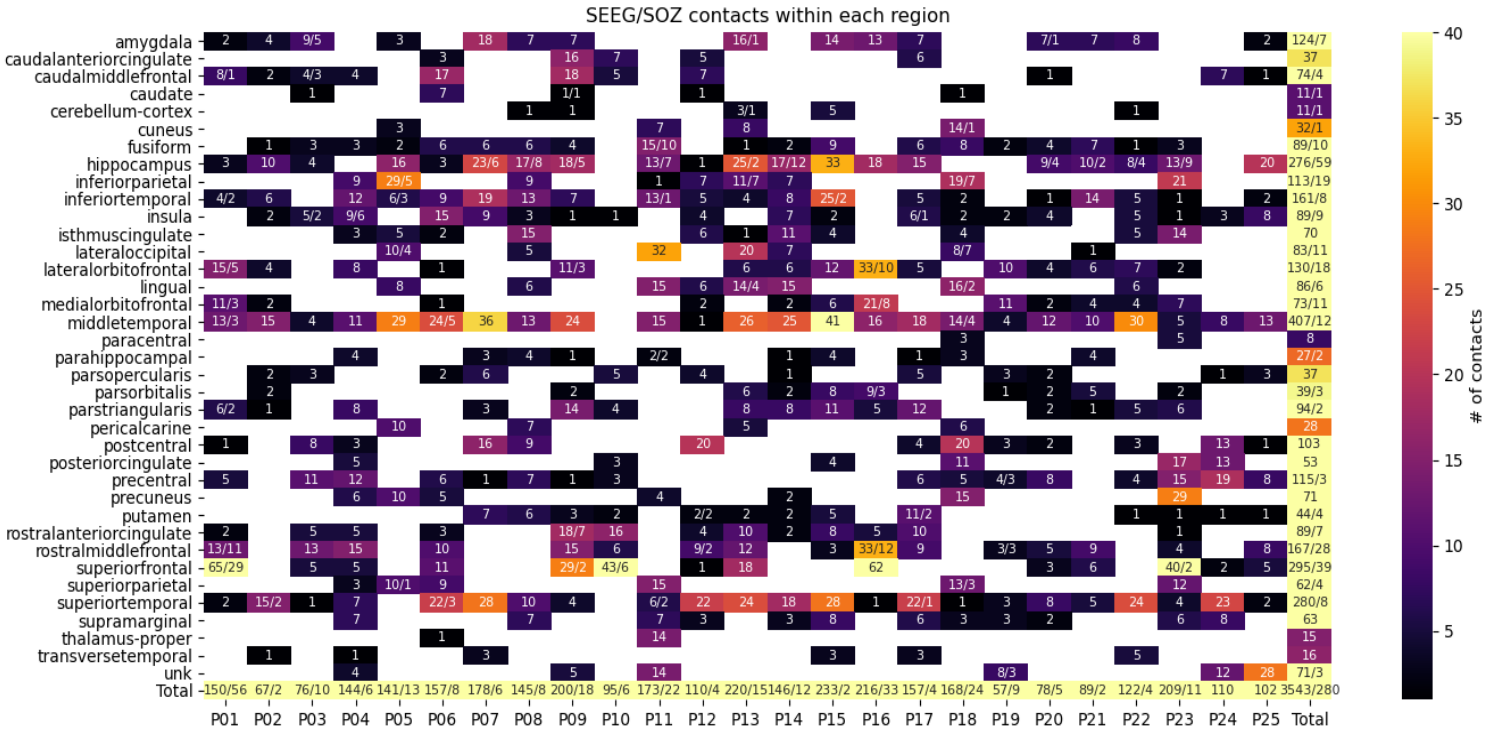

Figure 22: SEEG contact coverage and SOZs. Heatmap color scale shows the total number of contacts within each region, for each participant (P01-P25). Annotations within each cell show the exact number of total and SOZ contacts within each region.

The most common form of epilepsy is reflected by the majority of contacts near or within the temporal lobe: 276 (59 of these SOZ contacts) in the hippocampus, 124 (7 SOZ) in the amygdala, 407 (12 SOZ) middle temporal gyrus, and 280 (8 SOZ) in superior temporal. All participants have at least a few contacts in one of these regions. Frontal contacts are also abundant but concentrated on fewer participants: 295 (39 SOZ) in superior frontal gyrus, and 167 (28 SOZ) in rostral middle frontal.

3.6.2. ASSR by brain region and participants

Next, the coverage of the contacts with a detectable ASSR is show. Mean PLV and ASSR power values across trials and sliding windows were taken for each contact. A response is considered significant if the mean ASSR power is greater than 3, AND the PLV is greater than 0.16. Results for 40 Hz trials with monopolar montage are shown in Figure 23.

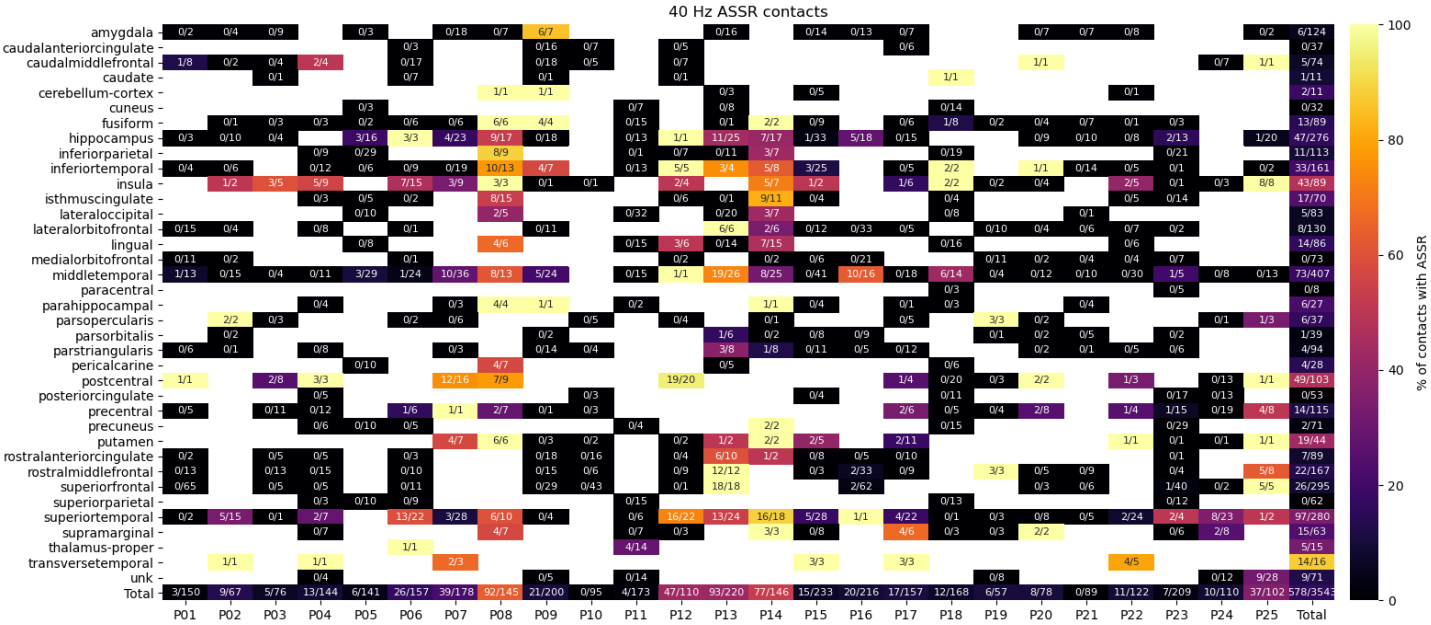

Figure 23: Significant 40 Hz ASSRs, monopolar montage. Across patients and brain regions, the color scale shows the percentage of contacts that display the ASSR. Annotations show the exact number of contacts with ASSR, followed by the total number of implanted contacts.

From Figure 23, it can be seen that responses are heterogeneous between participants. A certain discrepancy is expected, considering the differences in the population and in the implant schemes, and the slightly different sound intensities used in each case. However, while some participants display the ASSR in more than half of the implanted contacts, responses were not evoked at all in two participants, and in less than ten contacts in seven participants. Most of these cases had few to no contacts within regions that responded more consistently. Despite being covered in only six participants, the region that most reliably had evoked ASSRs was the transverse temporal gyrus (or Heschl's gyrus) – which belongs to the primary auditory cortex and is one of the main generators of auditory evoked responses (GODEY *et al.*, 2001; LIÉGEOIS-CHAUVEL, C. *et al.*, 1994). Nearby regions such as superior and middle temporal and postcentral gyri also show robust responses. The insula is also recruited in the majority of participants, probably due to its highly integrative role in sensory information. Regions that no response was elicited include superior parietal gyrus, cuneus, posterior cingulate and caudal anterior cingulate gyri, pars orbitalis, and medial orbito frontal gyrus.

Participants showed good tolerance to the task, with all trials being carried out with no interruptions. However, the task evoked mixed feelings among participants – a few found the task to be pleasant, some were not bothered by it, but others found the sound annoying – in two cases, fatigue was reported, and the eyes-open block was chosen not to be run. Different sensations were also evoked by the task in some participants. P06 reported being awake but daydreaming during the task. P08 reported having liked the task and felt a tingling/pressure sensation on the left side of the body during the sound – and is perhaps the participant with the most widespread response from all. P17 felt anxious and a sense of déjà vu from the sound.

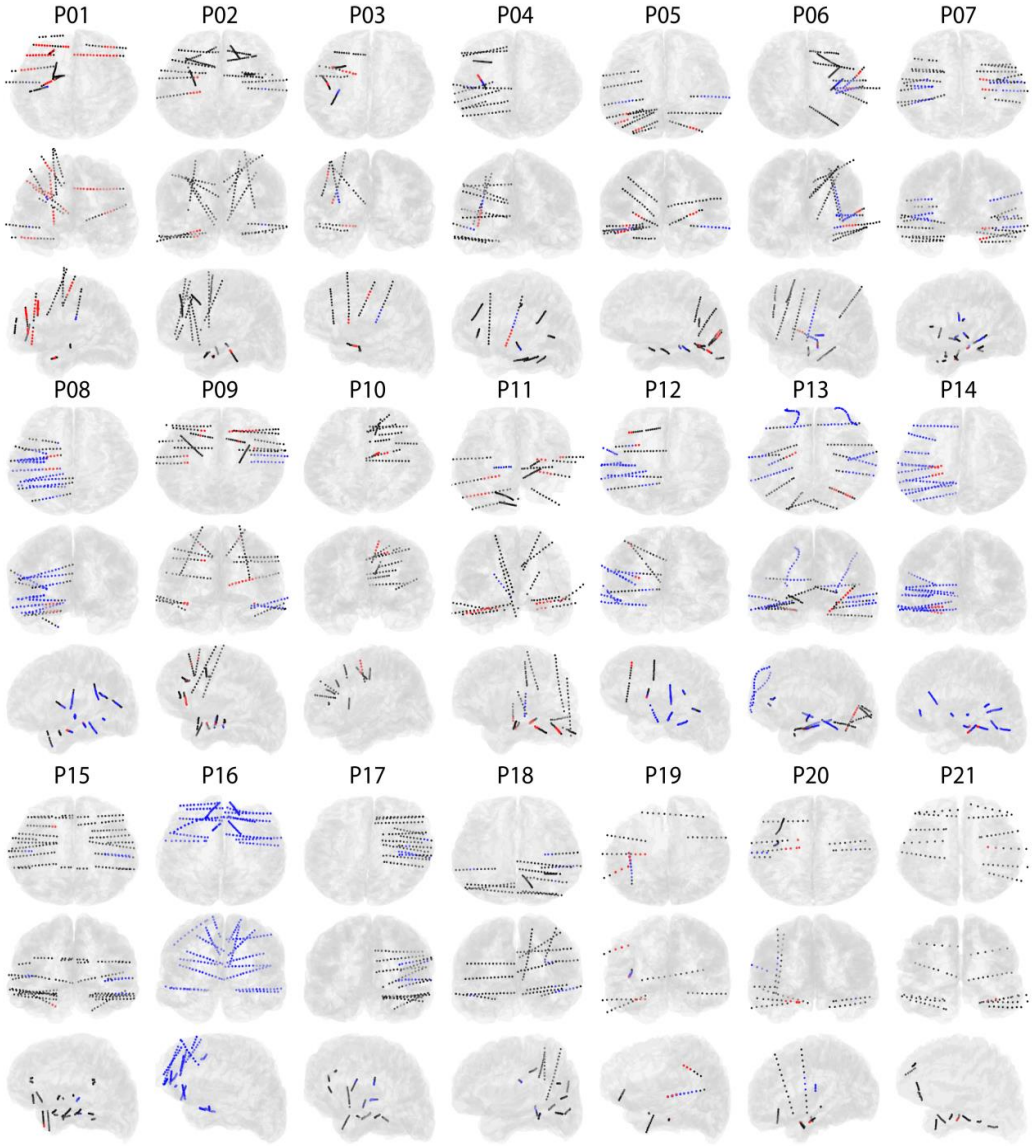

Figure 24: Depth electrodes implant trajectories for each participant. Each dot is a contact, showing from axial, coronal, and sagittal planes reconstructed from MRI and RAS coordinates. SOZ contacts are shown in red, and blue contacts show significant ASSR with referential montage.

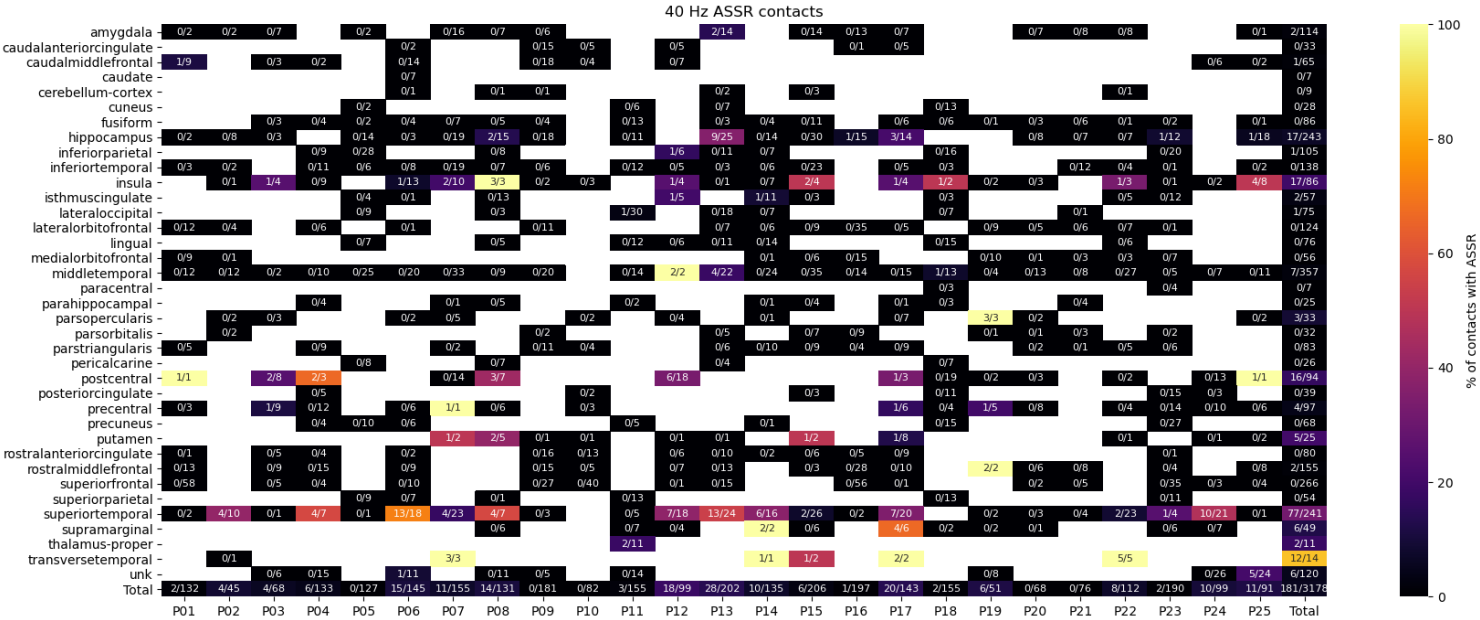

Figure 25: Significant 40 Hz ASSRs, bipolar montage. Across participants and brain regions, the color scale shows the percentage of contacts that display the ASSR. Annotations show the exact number of contacts with ASSR, followed by the total number of implanted contacts.

As mentioned previously, re-referencing is required to have a better localization of the source of the evoked responses. Thus, a similar ASSR coverage heatmap is shown in Figure 25 with responses from bipolarized channels.

Bipolar re-referencing the SEEG signals drastically reduced the number of channels with the ASSR: 181 total contacts, and five participants with no response in any channel. Brain regions directly involved in generating the ASSR are highlighted, especially the transverse temporal gyrus, with 12 from 14 channels showing responses. The superior temporal and the postcentral gyrus are also involved in most responses, followed by the insula, hippocampus, and (perhaps surprisingly) the putamen. Middle and inferior temporal gyri, which had a good share of the responses with the monopolar montage, show few to no contacts with responses after bipolarizing. Re-referencing with Laplacian results in an even bigger drop in responding contacts.

3.6.3. 40 Hz and 80 Hz ASSR

Contacts with ASSR in 80 Hz trials were reduced, when compared to 40 Hz. Supplementary Figure 4 and 3 show the results for 80 Hz trials using monopolar and bipolar montages, respectively. The difference is clearer on Figure 26, which shows ASSR

PLV values, for each participant, on 40 Hz and 80 Hz trials, in addition to the difference between those.

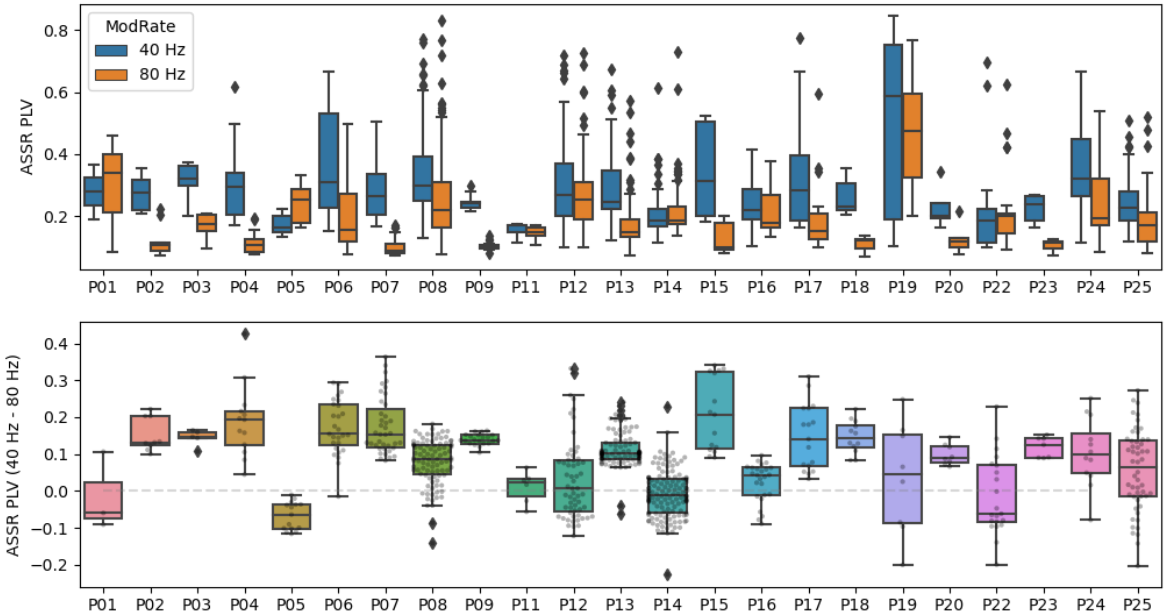

Figure 26: ASSRs with different modulation rates, monopolar montage. Comparing absolute values of ASSR PLV for 40 Hz and 80 Hz trials, across participants. Bottom plot shows difference between 40 Hz and 80 Hz ASSR PLVs (values > 0 indicate greater responses for 40 Hz trials), only for contacts with significant ASSR.

Despite some heterogeneity between responses, ASSR tended to be greater for 40 Hz trials, as previously shown in (HERDMAN *et al.*, 2002). But for some participants, this was not the case, such as P05, and part of the contacts from P12, P14, P22, and P25.

Investigating response differences are related to specific regions, Figure 27 shows ASSR PLVs for 40 and 80 Hz trials across different regions, with bipolarized channels.

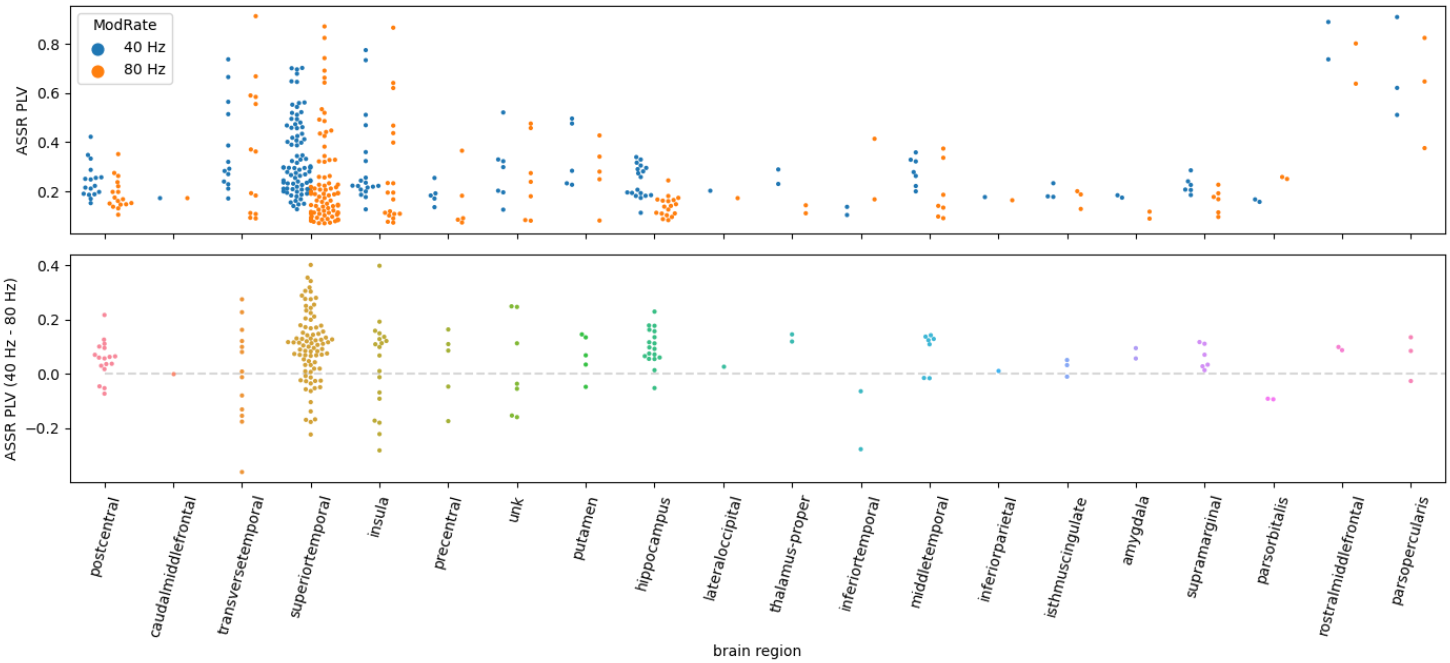

Figure 27: 40 and 80 Hz ASSR PLVs by region (bipolar montage). First plot shows ASSR PLV values for 40 and 80 Hz trials, across brain regions. Bottom plot shows the ΔASSR PLV = 40 Hz ASSR – 80 Hz ASSR. Only significant responses (either 40 OR 80 Hz) were considered.

From Figure 27, most regions tend to have higher values for 40 Hz ASSRs. However, a proportion of contacts within cortical temporal regions respond more to 80 Hz trials (namely transverse and superior temporal gyri). This was not expected, since the literature suggests that 80 Hz generators are mostly of subcortical origin (HERDMAN *et al.*, 2002). The thalamus, a region hypothesized to be involved in the generation of 40 Hz ASSRs in (HERDMAN *et al.*, 2002), also showed responses, but only one participants had contacts within this region.

3.7. ASSR was not evoked near seizure onset zones

Next, we evaluate the ASSR across brain regions and see if regions involved in generating the seizures (SOZ contacts) are related to abnormally enhanced responses. Of interest are regions that display ASSR, but normally would not display this response, or regions that should normally respond and have visible ASSRs but do these are not elicited by the AM tones.

Pooling results from all participants, Figure 28 shows 40 Hz ASSR PLV values with bipolar re-referencing, by labeled region and highlighting channels marked as belonging to the SOZ. However, only one participant (P19, with two channels) showed overlap

between the SOZ and ASSRs, in the rostral middle frontal gyrus – and one of the highest ASSR PLVs of the whole dataset. However, a careful look at the MRI images of these contacts (not shown here) shows that these contacts were mislabeled by the parcellation algorithm (probably due to the removal of a wide cortical region in a previous surgery, which affected the accuracy of the algorithm). In fact, these 2 contacts are located within the transverse temporal gyrus, which is expected to have a high ASSR value. Thus, in principle, this contributes to the refusal of the initial main hypothesis that SOZ regions would display abnormally enhanced steady-state responses to AM sounds. Even when including the labels of seizure spread contacts, the overlap is low, as shown by Figure 28.

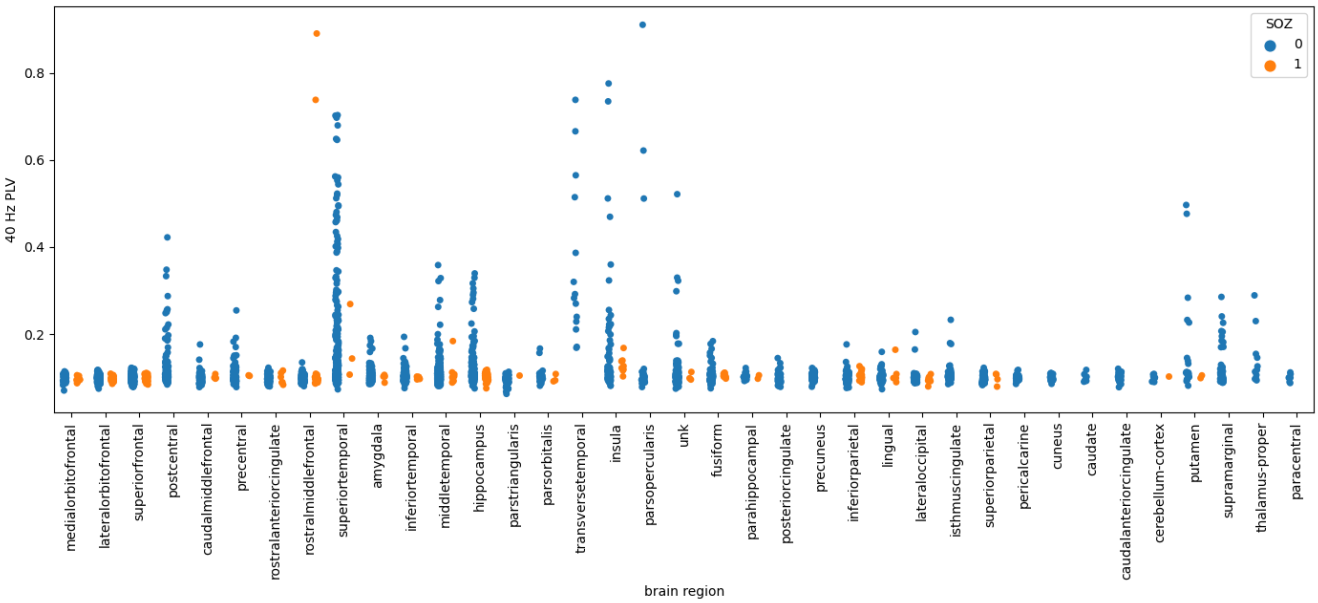

Figure 28: 40 Hz ASSR PLV by region and SOZ, with bipolar montage. A select few of regions have significant values for the ASSR, but with very low overlap with SOZ contacts.

3.7.1. Eyes-closed X eyes-open ASSR

The additional task with the “eyes-open” condition was executed by thirteen participants (P02, P09, P12, P14-18, P20, P22-25). Results are shown in Figure 29 for the monopolar montage.

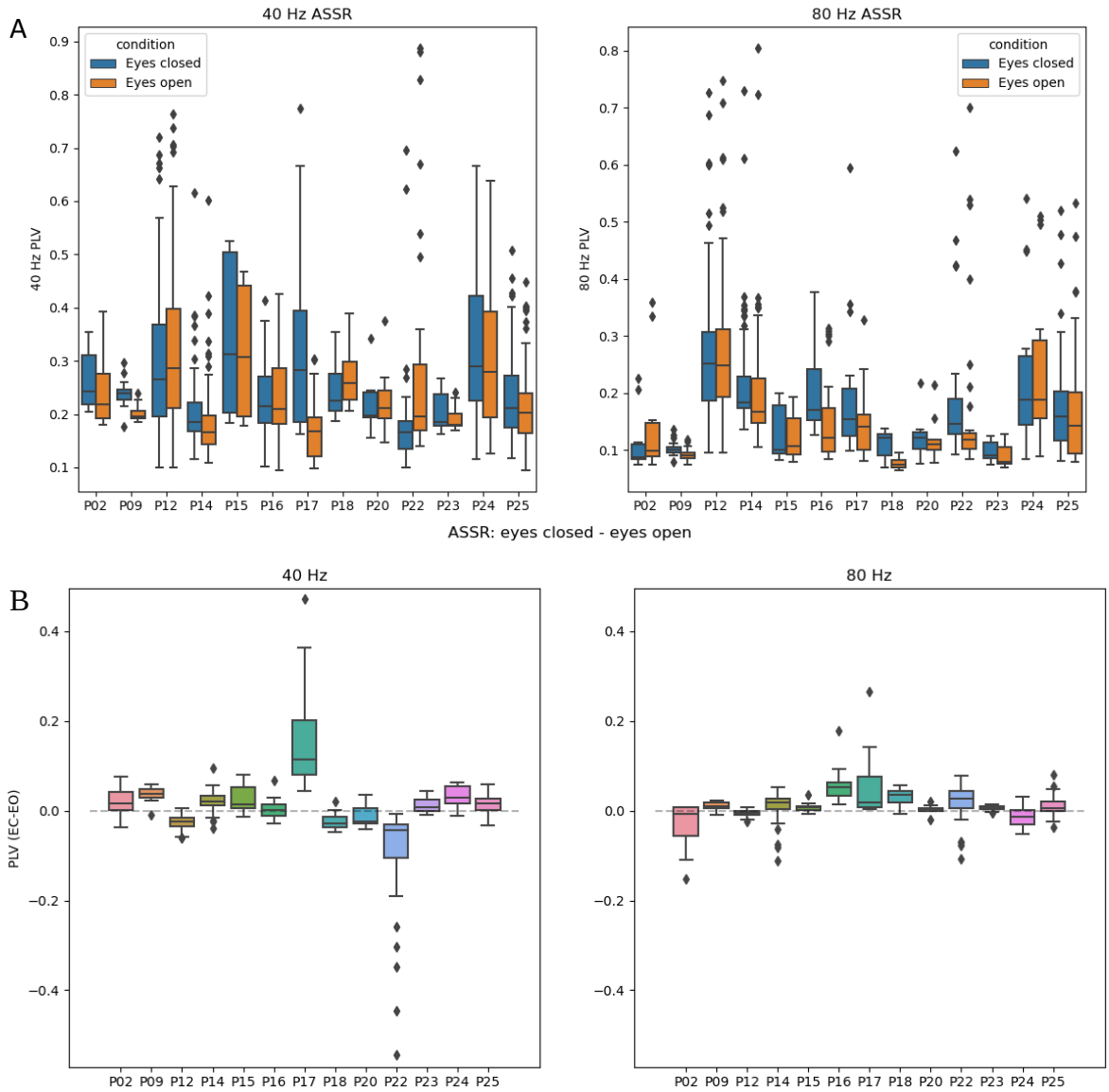

Figure 29: ASSR with eyes open and eyes closed, monopolar montage. For 40 and 80 Hz, (A) shows ASSR PLV for eyes-closed and eyes-open conditions, by participant. (B) shows ASSR PLV difference between both conditions (PLV eyes-closed - PLV eyes-open). Only contacts with significant responses are considered

Significant differences between conditions were found in only some participants, and some with the opposite relationship to what was expected. That is, in P09, P14, P15, and P17, response with eyes-closed was greater than eyes-open, while the opposite was observed for P12 and P22 – the latter showed the greatest difference between conditions.

In Figure 30, ASSR PLV differences (from bipolarized montages) are shown between selected brain regions (the ones that displayed more consistent responses).

That is, ASSR PLVs from contacts with significant ASSR values under the two conditions (EC x EO) were paired and subtracted – for 40 Hz and 80 Hz trials.

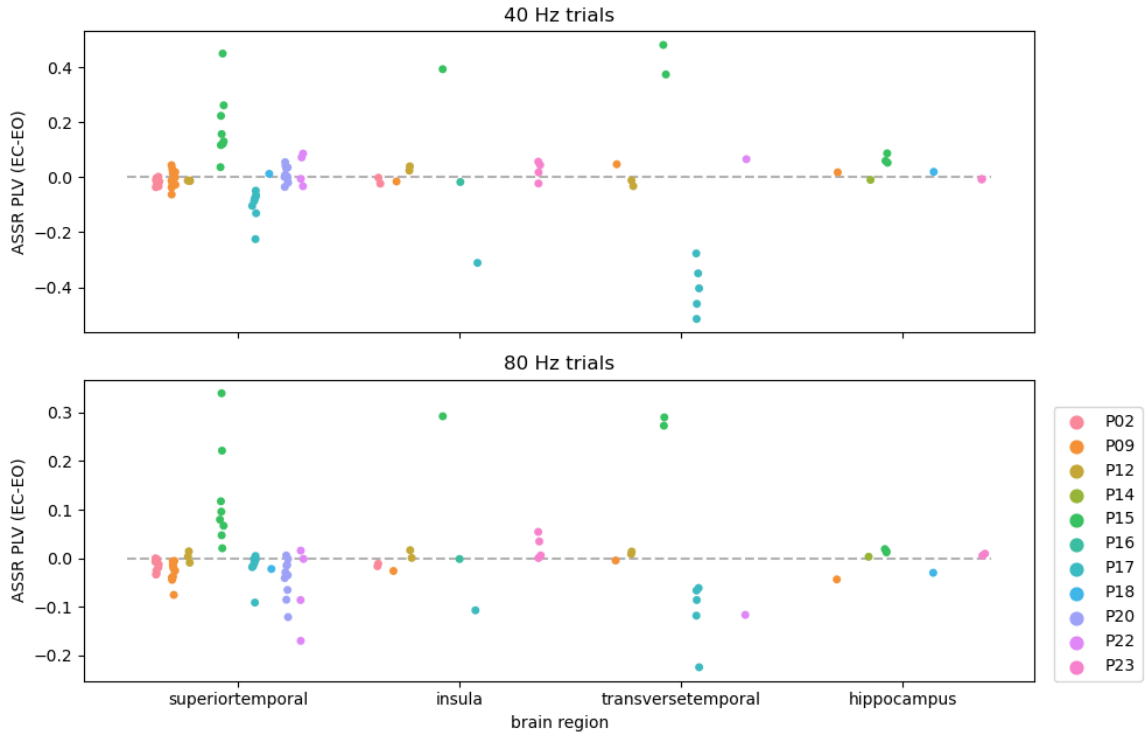

Figure 30: Eyes-closed – Eyes-open ASSR PLVs from selected regions (bipolar montage). For 40 Hz (upper plot) and 80 Hz (bottom plot) trials, ASSR PLV differences between EC and EO conditions

As indicated by Figure 29 and Figure 30, there is a greater variability among participants, and not so much between regions. For contacts within superior temporal gyrus, there is a tendency of greater 80 Hz ASSR PLV values for the eyes-closed condition (except for P15), but not so much for 40 Hz trials.

3.8. Discussion

Motivated by recent findings on the use of ASSRs in detecting neurological disorders, we evaluated if abnormal responses are correlated with epileptogenic regions in epilepsy patients undergoing invasive SEEG monitoring. Contrary to one of the main proposed hypotheses of epileptogenic regions being associated with increased ASSRs, we found that ASSRs were not elicited within SOZ/EZ, nor within regions that responses were in principle not expected (such as frontal or occipital lobes). The former could be evidence of the alternative hypothesis – that impaired auditory processing is present in epileptogenic circuits – but accurately assessing this is difficult due to the limitations of

this study. Namely, the heterogeneity of participants and implantation schemes, besides the fact that we lack some kind of control, makes it hard to assess with confidence if a response is “abnormal” or not. Furthermore, the sound was presented in a less-than-ideal way, with speakers (with varying amplitudes) instead of headphones or earbuds, which elicits significantly smaller ASSRs. Altogether, these results do not seem to provide evidence for using ASSRs to assist in delineating epileptogenic regions. This does not preclude the use of other kinds of stimuli for this purpose, as previously shown with SPES in (VALENTIN, 2002), or using ASSRs as probing stimuli for assessing other aspects in epilepsy and ictogenesis. These auditory responses may play a role in helping to identify lateralization of epileptic focus (MATSUBARA *et al.*, 2019), epilepsy diagnosis (CANCADO, 2016), or seizure susceptibility for seizure forecasting purposes. The latter would be evaluated in this work using a modified task with auditory stimuli interspaced throughout the day but could not be carried out due to the COVID-19 pandemic. A pilot run of such a task was done and was well received by the participant, who mentioned not being bothered by the sound stimulus.

Auditory responses to AM-modulated sound stimuli with SEEG implants have been measured previously in (LIÉGEOIS-CHAUVEL, CATHERINE *et al.*, 2004). However, this is the first time a thorough description of brain regions eliciting ASSRs with this type of recording is done. Thus, in addition to evaluating the main hypotheses about probing effectiveness of ASSRs in highlighting epileptogenic regions, the results in this chapter provide an overview of the brain regions involved in ASSRs evoked by auditory AM stimuli. Using raw monopolar signals, ASSRs were observed in widespread brain regions, not only in the auditory cortex. Bipolar re-referencing highlights the few regions that are involved in generating such responses, by filtering oscillations in the ASSR range that might be due to field effects of distant brain regions. The well-known role of the transverse temporal gyrus (or Heschl’s gyrus) in auditory processing and generation of both transient (GODEY *et al.*, 2001; LIÉGEOIS-CHAUVEL, C. *et al.*, 1994) and steady-state auditory responses (ROSS, B. *et al.*, 2003) is reflected in the high percentage of contacts within this region responding with high PLV values. Neighboring regions within the temporal lobe also tended to elicit responses, especially the superior temporal gyrus. ASSRs also tended to be elicited near the insula, which was expected due to its

integrative role (GUÉGUIN *et al.*, 2007). In some participants, responses were elicited in regions that were not expected initially, such as pre and postcentral gyrus, and putamen. However, none of these contacts were within epileptogenic regions.

The effect of the stimuli modulation rates in generating ASSRs has been discussed extensively in the literature (O'DONNELL *et al.*, 2013; POELMANS *et al.*, 2012; SANCHEZ-CARPINTERO *et al.*, 2020), with several works comparing 40 Hz and 80 Hz ASSRs (HERDMAN *et al.*, 2002; MATSUBARA; UEHARA; *et al.*, 2018). However, to the best of our knowledge, this is the first time this is done using invasive depth recordings. These different modulation rates elicit responses by different brain structures; 80 Hz ASSR would be primarily generated by the brainstem, whereas 40 Hz ASSRs are mainly related to speech perception and are cortically evoked (GIRAUD; POEPPEL, 2012; HERDMAN *et al.*, 2002; POELMANS *et al.*, 2012). Both 40 and 80 Hz ASSRs were found to be bilaterally reduced in patients with bipolar disorder (ODA *et al.*, 2012). Differences between 40 Hz and 80 Hz ASSRs were more participant-specific than region-specific. That is, using a modulation rate of 40 Hz tended to elicit ASSRs with increased amplitude and PLV when compared with 80 Hz for most, but not all participants. No specific regions displayed consistent 80 Hz responses greater than 40 Hz.

The choice of the referencing method can drastically influence the results in SEEG analyses; different referencing montages can enhance or suppress measured activity from distant sources, differently influence correlations between channels within gray and white matter, among other effects (MERCIER *et al.*, 2017). This work is also the first time a comparison between referencing methods is done when evaluating ASSR responses from SEEG recordings. Other works evaluate SEEG referencing methods but dealing with different objectives and types of responses. In (LI *et al.*, 2018), the Laplacian method was found to be optimal for broadband gamma and low-frequency activity during a motor task, but it is highlighted that it might not be the case for other tasks that involve ERPs. In cortico-cortical evoked potentials, it is suggested in (PRIME *et al.*, 2018) that bipolar montages are preferred when metrics involve higher frequency components, but monopolar recordings should be favorable when working with low-frequency signals and coherence metrics. Previous work with ASSR and SEEGs used

monopolar recordings (GUÉGUIN *et al.*, 2007; LIÉGEOIS-CHAUVEL, CATHERINE *et al.*, 2004). But since the main hypothesis of this chapter is about using ASSRs to better identify epileptogenic regions, the original common-referenced signals may not be suitable enough. This is because the ASSR oscillations measured from each channel may be due to field effects that are related to neuronal activity generated by distant sources (LI *et al.*, 2018). Thus, we evaluated ASSRs with Laplacian and bipolar montages, finding that both methods drastically reduce ASSR amplitude and PLV in most contacts, as expected. However, the Laplacian montage resulted in an even smaller proportion of responding channels and this did not differ significantly between different modulation rates (40 Hz and 80 Hz). While the bipolar montage seems to be a more adequate tradeoff between detectable responses and localizing power (suppressing effects from distant sources), more work is needed to define the best referencing method for evaluating ASSRs. Since these responses involve entrainment of neuronal activity, phase-locked oscillations with 0 lag between neighboring channels may not necessarily mean that these are capturing activity from distant sources. So, local re-referencing, in this case, may 'cancel' an oscillatory ASSR component that is spread through a few contacts. Disentangling this from remote-generated oscillatory sources may be done by recording with additional micro-electrode contacts or by combining ASSR with auditory ERPs.

A possible next step of this work involves evaluating ASSRs when applying data-driven spatial filters to SEEG signals through spatio-spectral decomposition. This method is used to enhance signal-to-noise ratio for oscillations in specific frequency bands (SCHAWORONKOW; VOYTEK, 2021).

An additional task compared ASSRs between two conditions: eyes-open and eyes-closed. It is well-known that ASSRs are modulated by attention and arousal (GRISKOVA-BULANOVA *et al.*, 2011; PICTON, TERENCE W. *et al.*, 2003; POCKETT; TAN, 2002). ASSRs elicited by click trains with 40 Hz and 20 Hz were evaluated in (GRISKOVA-BULANOVA *et al.*, 2011). This work first compared responses during eyes-closed with eyes-open, finding that 40 Hz ASSR was enhanced in the eyes-closed condition. Furthermore, 40 Hz ASSRs were attenuated when attention to the stimulation was low.

During sleep, 40 Hz ASSR is attenuated, but not 80 Hz ASSR (PICTON, TERENCE W. *et al.*, 2003). However, no investigations about this have been made in the literature with SEEG recordings. In this work, a slight difference between modulation rates was observed with eyes-open X eyes-closed, with a greater decrease of 80 Hz ASSR in the eyes-open condition. However, this response decrease did not occur in all participants (and in two participants, eyes-open responses were greater than eyes-closed), and is apparently not related to any specific region. The task fulfilled another objective, which is to confirm that robust ASSRs are still elicited with the current setup (using speakers) while participants remain with eyes open. This is an encouraging step to evaluate the use of ASSRs as a surrogate marker for excitability. That is, assessing the ASSR with shorter trials throughout the day to investigate if significant changes occur in the proximity of seizure events.

3.9. Conclusions

The ASSR is a promising tool for investigating and diagnosing neuronal pathologies such as schizophrenia, bipolar disorder, dyslexia, and epilepsy. This work provided a rare opportunity to investigate auditory processing with these steady-state responses in epilepsy patients with depth electrode implants undergoing invasive presurgical evaluation. The potential of ASSRs to assist in identifying epileptogenic regions was evaluated. No evidence was found to support this specific use, considering the two evaluated hypotheses of (i) abnormally high responses in SOZ regions that were not expected to generate ASSRs, and (ii) impaired responses in contacts within the SOZ. That is, very few contacts with ASSR within epileptogenic regions were found. This low overlap between contacts with ASSRs and within SOZs could possibly be a result of impaired responses in epileptogenic circuits. However, the highly heterogeneous data (with different implant schemes and epilepsy types between participants) and the overall low percentage of contacts with ASSRs using re-referenced montages make it difficult to accurately assess this. Even though the localizing power of ASSRs could not be demonstrated, this does not preclude the use of this tool for diagnosing lateralization, as previously demonstrated by (MATSUBARA *et al.*, 2019), specific epileptic syndromes (SANCHEZ-CARPINTERO *et al.*, 2020), or assessing changes in

excitability and synchrony that may herald the occurrence of seizures (PINTO, HYORRANA PRISCILA PEREIRA *et al.*, 2017). The latter is a promising next step for this work.

4. CONCLUSION AND PERSPECTIVES

This chapter summarizes the findings of this work and discusses possible future steps, in light of the recent literature.

4.1. Findings

Perturbational approaches have been used extensively in neuroscience for decades. Among these approaches are active probing paradigms, in which relatively subtle stimuli are used to uncover more information about the integrity and dynamics of neuronal activity. This work aimed to contribute to the relatively recent literature that investigates the use of these paradigms in epilepsy. Different hypotheses and models were evaluated, providing insights into the problems of seizure forecasting and identification of epileptogenic regions.

4.1.1. Low-frequency stimulation enhances the predictability of upcoming seizures in a neural mass model

An implantable device that can predict or indicate an increased probability of seizures would have a big positive impact on the quality of life of epilepsy patients, allowing the use of early-warning systems, or by enabling closed-loop systems to prevent or suppress the occurrence of these events. However, this is a problem yet unsolved, despite decades of research (MORMANN *et al.*, 2007).

A one potentially effective way to tackle the hard problem of forecasting epileptic seizures is the use of stimuli to highlight features involved in the initiation of these events. Since pioneering works by (KALITZIN, STILIYAN *et al.*, 2002), the feasibility of this approach has been indicated in different models (FREESTONE; KUHLMANN; *et al.*, 2011; MEDEIROS *et al.*, 2014; O'SULLIVAN-GREENE *et al.*, 2017; PINTO, H.P.P. *et al.*, 2017; WANG, Y. C. *et al.*, 2020). However, there is still much more to be explored, considering the diversity of epilepsies and seizures, and the wide array of possible stimuli types and parameters.

In this work, low-frequency pulses were shown to improve the predictive power of extracted features from simulated neuronal activity, as model parameters were

gradually shifted from normal towards ictal states. As hypothesized, excitability and synchrony between the neuronal populations were shown to increase when stimuli were used while parameters increased the model's ictogenicity. Most importantly, stimuli did not anticipate the time to onset of sustained discharges of spikes. That is, just like experimental seizure models (MEDEIROS *et al.*, 2014), results here indicated no pro-ictal effect of low-frequency stimulation.

4.1.2. Low-frequency stimuli may reveal critical slowing down as an early-warning of upcoming seizures

It has been shown that critical transitions rule the self-termination of human seizures through spatial scales (KRAMER, M. A. *et al.*, 2012). It still remains an open question if similar dynamics are involved in the onset of seizures, with several works with positive evidence from computational models (CHANG *et al.*, 2018; JIRSA *et al.*, 2014; NEGAHBANI *et al.*, 2015), but some works not finding evidence of this for human data (MILANOWSKI; SUFFCZYNSKI, 2016; WILKAT; RINGS; LEHNERTZ, 2019). This conflicting evidence might be explained by recent findings in (MATURANA *et al.*, 2020), which found strong evidence in favor of critical slowing down preceding seizures over varying timescales – some longer than would be observable in standard clinical settings.

Our work provides more evidence for seizures being preceded by the phenomenon of critical slowing down. But more importantly, this was observed with low-frequency probing stimulation in most model configurations. That is, some underlying dynamics were observable only when probing stimuli were used – which is related to one of the definitions of critical slowing down, which is marked by slower recoveries from perturbations. Thus, although such hallmarks do not always require stimuli to be revealed, as shown by (MATURANA *et al.*, 2020; SCHEFFER *et al.*, 2009), identifying them should be "easier" with the use of low-frequency perturbations (VERAART *et al.*, 2012).

4.1.3. ASSRs are promising diagnostic tools in epilepsy, but appear to have limited value on accurately localizing epileptogenic regions

We hypothesized that ASSRs within SOZ or EZ could help identify putative seizure foci. That is, responses to AM sound stimuli could be (i) enhanced and elicited in epileptogenic brain regions not commonly involved in auditory processing, due to epileptogenic circuits being prone to entrainment. On the other hand, (ii) impaired ASSRs could result from dysfunctional central auditory processing from epilepsy.

With no control group (considering the invasive nature of the recording method), and the highly heterogeneous nature of the SEEG data (with different epilepsies and implant schemes), defining what is an “abnormal” ASSR is not straightforward. Thus, while the low overlap between SOZ/EZ and responding (with ASSR) contacts may allow discarding the first hypothesis of abnormally high ASSRs within the EZ , evaluating the second hypothesis (of impaired ASSRs) was not possible. Having a SOZ contact within a region that consistently displayed ASSRs, such as the transverse temporal gyrus, would provide evidence to better assess this, but this was not the case.

The apparent lack of diagnostic value for accurate localizing the EZ with the ASSR may be related to one of the conclusions from chapter 2; the predictive value of active probing is somewhat localized and restricted by the propagation of the stimuli. In the case of the ASSR, the topography of the auditory response was not widespread as initially expected, which may limit the value of its predictive value for accurately highlighting epileptogenic regions. It is well known that sensorial responses may span wide cortical regions that are not usually involved in primary sensory processing (KAPLAN; ZIMMER, 2020; STRINGER *et al.*, 2019). However, this is highly dependent on context, and modulated by factors such as attention, experience, or engagement. The passive nature of our task may explain the low proportion of contacts with ASSRs (and some participants with no response at all). And of note, one participant (P08) that reported being a meditation practitioner, felt a ‘tingling’ or ‘pressure’ sensation during the task displayed one of the strongest and most widespread responses.

The diagnostic values of ASSRs should be investigated under different contexts and objectives. That is, considering the effectiveness of ASSRs for assisting the diagnosis of several neuronal disorders (BAŞAR, 2013; LEHONGRE *et al.*, 2011; ODA *et al.*, 2012; PARKER *et al.*, 2019), including the identification of lateralization of the epileptic focus in patients with epilepsy (MATSUBARA *et al.*, 2019), these steady-state responses may prove useful for assessing seizure susceptibility, or proximity to seizures.

4.1.4. 40 and 80 Hz ASSRs

For most participants, more brain regions are recruited in 40 Hz trials (and with higher ASSR values), compared to 80 Hz trials. The effects seem to be more participant-specific than region-specific, while we were expecting for the latter – with deeper brain structures being more responsive to 80 Hz trials, while cortical ones would present higher 40 Hz ASSRs.

4.1.5. Eyes-open x eyes-closed ASSR

The results show that for 80 Hz trials, eyes-closed condition elicited slightly smaller responses, while 40 Hz ASSRs were comparable between conditions, except for a few participants. The different responses between EC and EO conditions were more participant-specific than region-specific – and could not be related to the epileptogenic zones.

It was shown that the setup with speakers may be used with an additional task that would consist of presenting short AM sounds throughout the day to investigate if significant changes occur in the proximity of seizure events. The use of a 40 Hz modulation rate would be preferable in this case.

4.2.Perspectives

4.2.1. Closing the loop

There is a vast literature on seizure-suppressing or seizure-controlling stimulation methods (COTA *et al.*, 2016; FISHER; VELASCO, 2014; THEODORE; FISHER, 2004). The effectiveness of these methods is multifactorial, depending on factors such as region of stimulation, seizure type (or seizure model), and stimulation parameters

(such as frequency, amplitude, or waveform). Combining some of these methods with a seizure forecasting algorithm would enable targeted, on-demand interventions, just like in a closed-loop control system. Achieving this kind of seizure control reliably and safely is one of the ultimate goals of epilepsy therapies (NAGARAJ *et al.*, 2015).

Theoretical models are an invaluable tool for assessing the effectiveness of different combinations of seizure forecasting and control methods. Thus, the next step of this work is to incorporate seizure-controlling stimulation patterns that act upon the modified WNMM. That is, changing from active probing low-frequency stimuli that aid in the detection of upcoming seizures, to seizure-controlling stimuli.

Despite the drawback of being an invasive method, probing with electrical stimulation may be incorporated into clinical practice with seizure-suppressing DBS devices. Currently, there are 32 clinical trials with DBS and epilepsy (from clinicaltrials.gov), and some devices have already been approved by regulatory agencies and are being used in clinical practice. Thus, closing the loop between active detection of upcoming seizures (or a high risk of seizures) and acting to interrupt it could be achieved with electrical stimulation by changing the stimulation parameters; from low-frequency probing stimuli (CARVALHO, VINÍCIUS REZENDE *et al.*, 2021) to seizure-suppressing or controlling patters, such as desynchronizing ones (DE OLIVEIRA *et al.*, 2018; MESQUITA *et al.*, 2011).

4.2.2. Evaluating active probing on other models and validating with experimental data

One next step in potential is to evaluate if similar results hold for more complex networks of the modified model. That is, to evaluate the use of active probing on a larger number of neuronal populations or model subsets (instead of the 2 populations studied here), with varying network topologies (SPORNS; ZWI, 2004). Another possibility is to evaluate if similar results hold for other seizure-generating models, such as the EPILEPTON variant of the EPILEPTOR model (NAZE; BERNARD; JIRSA, 2015), or a detailed CA1 model (DEMONT-GUIGNARD *et al.*, 2009).

Another goal is to validate the results with experimental models and clinical data. One possibility is evaluating if the results here hold when using low-frequency

stimulation with a Kainic Acid model of recurrent seizures. Another is to do a model inversion with depth electrode implant data from presurgical monitoring, as in (KAROLY *et al.*, 2018). Furthermore, combining this kind of validation with bifurcation analyses would provide valuable insights of the phenomena involved in the initiation and generations of seizures.

4.2.3. Evaluating ASSRs on longer timescales

A possible new task would consist of presenting sounds to evoke ASSRs throughout the day (15-second trials every 20 minutes, for instance). This would allow to investigate if auditory steady-state responses reflect altered synchronization and/or excitability prior to the occurrence of seizures, something that has been shown in animal seizure models (PINTO, H.P.P. *et al.*, 2017).

4.2.4. Promising future for neuronal dynamics and epilepsy

Recent advances in several areas provide optimistic projections that, at least for a subset of epilepsy and seizure types, reliable seizure-forecasting methods are achievable in the near-future (FREESTONE; KAROLY; COOK, 2017). Improvements on high throughput neural recording and stimulation (LEE *et al.*, 2021), the increasing use of implantable devices and public datasets are offering additional insights into dynamics that lead to epileptic seizures. Combining this with recent advancements of non-linear dynamics and deep-learning methods is a promising way of achieving robust decoding of brain states from neuronal signals. An example of the former is delay-differential analysis (DDA) (LAINSCSEK; WEYHENMEYER; *et al.*, 2013). This framework reveals non-linear properties of underlying dynamical systems and has been used to differentiate healthy controls and Parkinson's disease patients (LAINSCSEK; HERNANDEZ; *et al.*, 2013), and has assisted in the detection of cortical chimera states that are highly predictive of seizure likelihood (LAINSCSEK *et al.*, 2019).

5.SUPPLEMENTARY MATERIAL

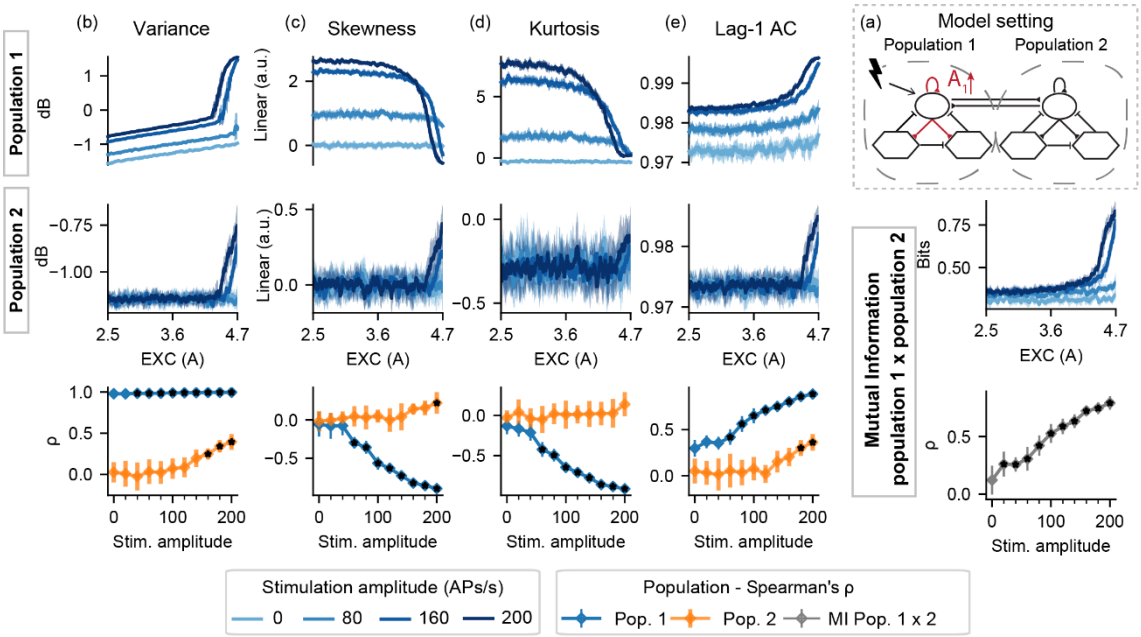

Supplementary Figure 1: Alternative model setting I-A. Stimulation of the ictogenic population, with the increase of excitability. Active probing highlights the increased dependency between activity of both populations, and improves the predictability of other features for population 1 (although variance is a good predictor with no stimuli at all).

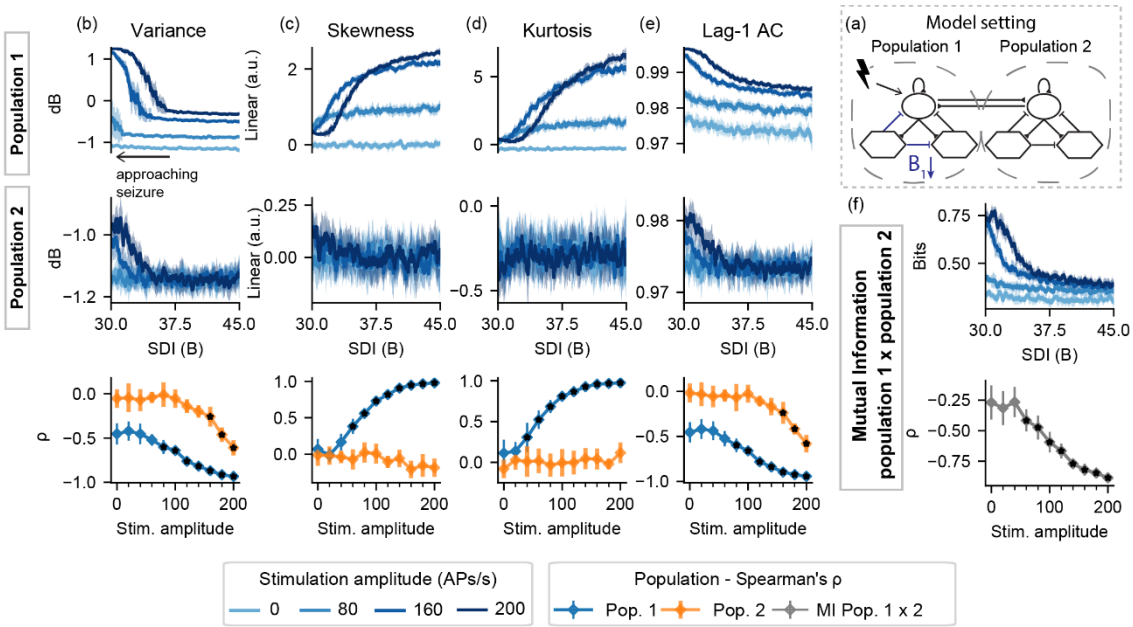

Supplementary Figure 2: Alternative model setting I-B. Stimulation of the ictogenic population, while slow inhibition is decreased. Active probing highlights the increased dependency between activity of both populations, and improves the predictability for population 1. Trends are also observed for features extracted from the second population – however, increased stimulation amplitudes are required in this case.

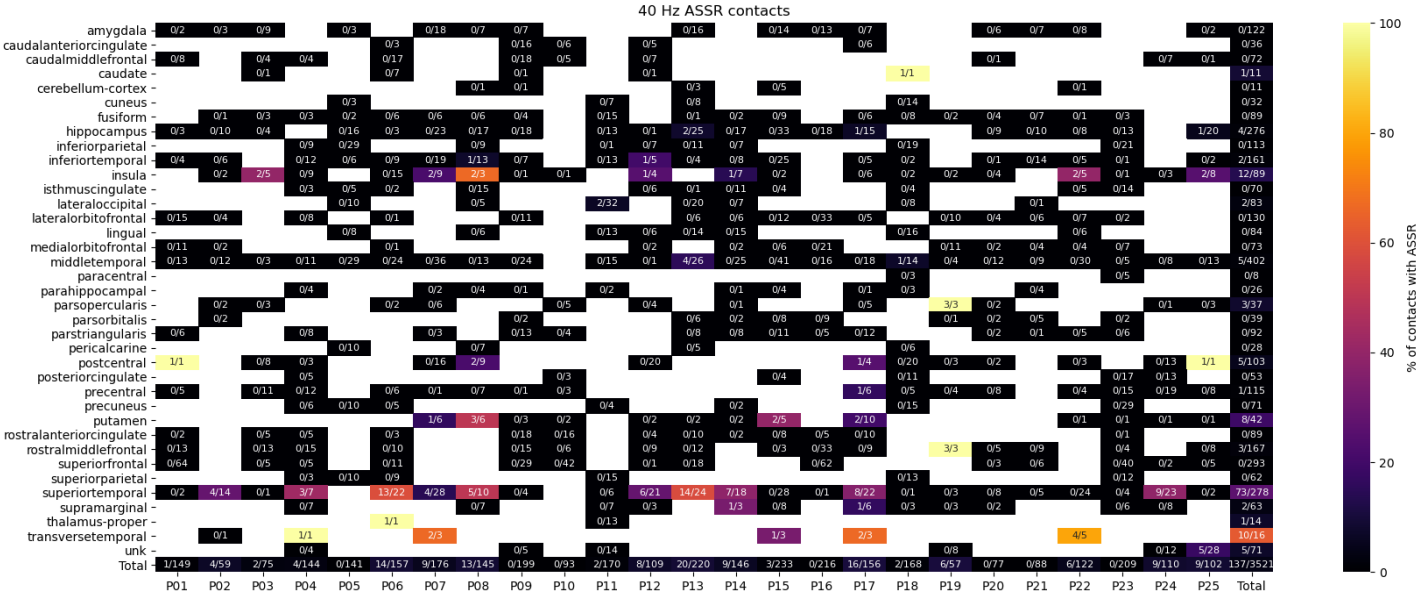

Supplementary Figure 3: 40 Hz ASSR coverage, Laplacian montage. Across patients and brain regions, the color scale shows the percentage of contacts that display the ASSR. Annotations show the exact number of contacts with ASSR, followed by the total number of implanted contacts.

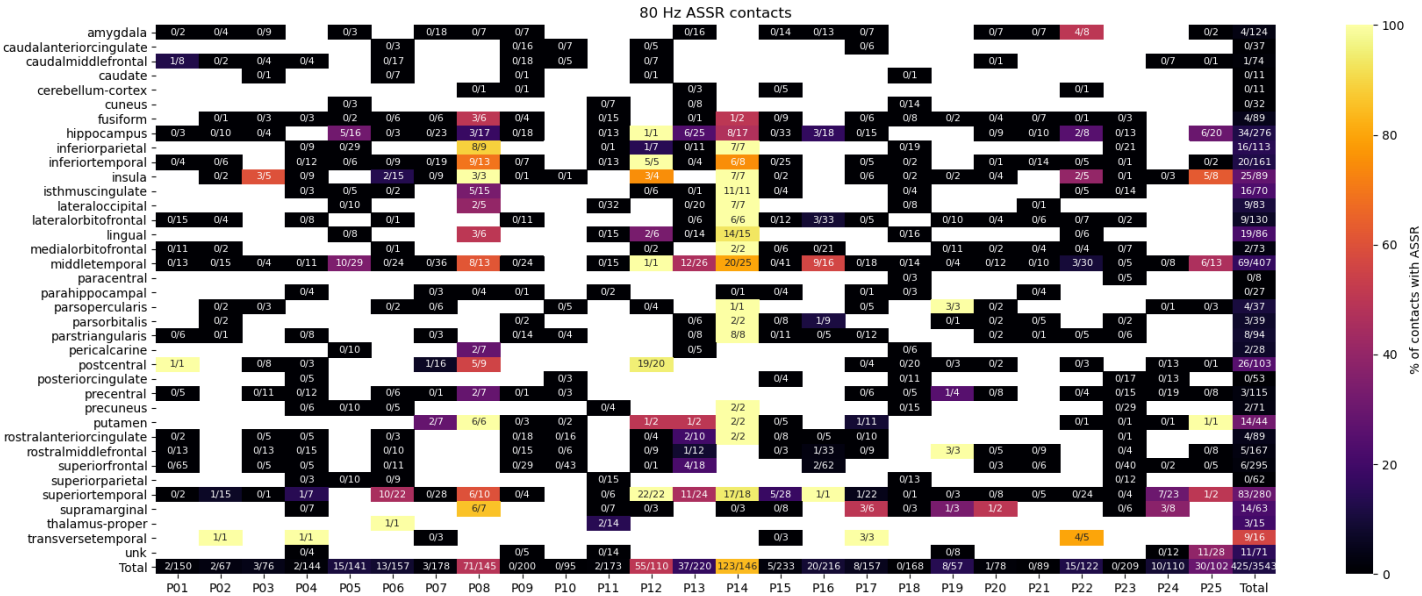

Supplementary Figure 4: 80 Hz ASSR coverage, monopolar montage. Across patients and brain regions, the color scale shows the percentage of contacts that display the ASSR. Annotations show the exact number of contacts with ASSR, followed by the total number of implanted contacts.

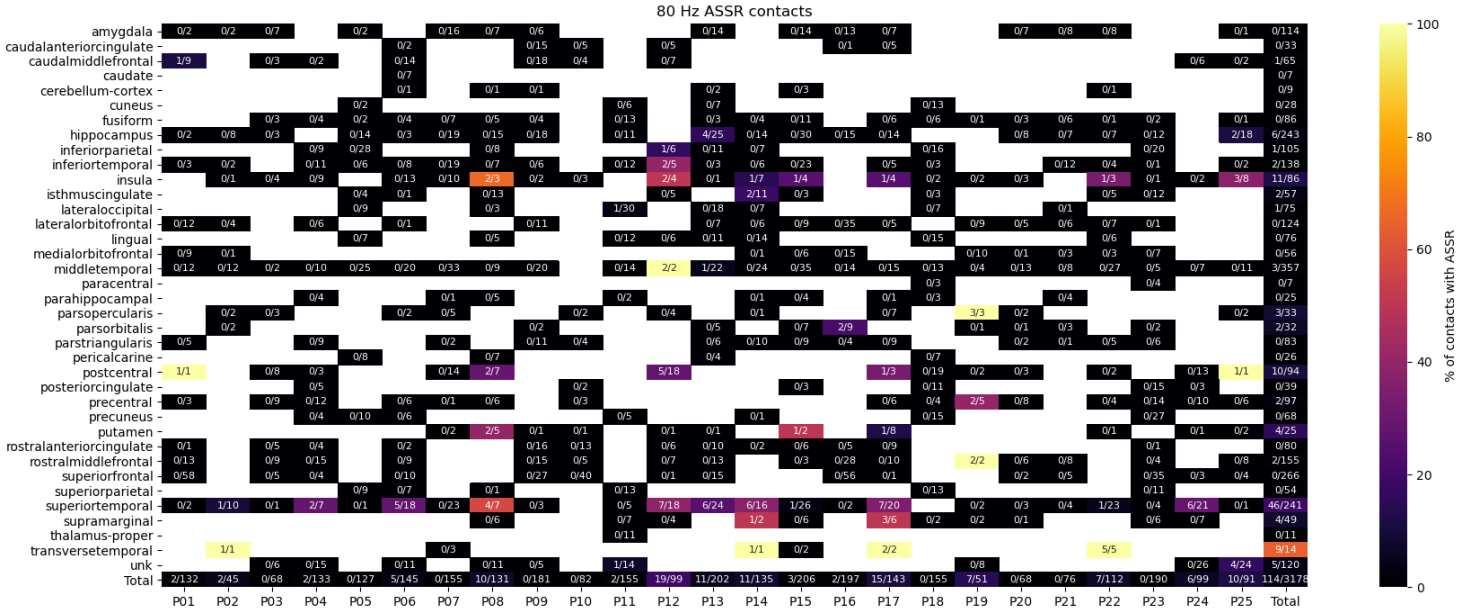

Supplementary Figure 5: 80 Hz ASSR coverage, bipolar montage.

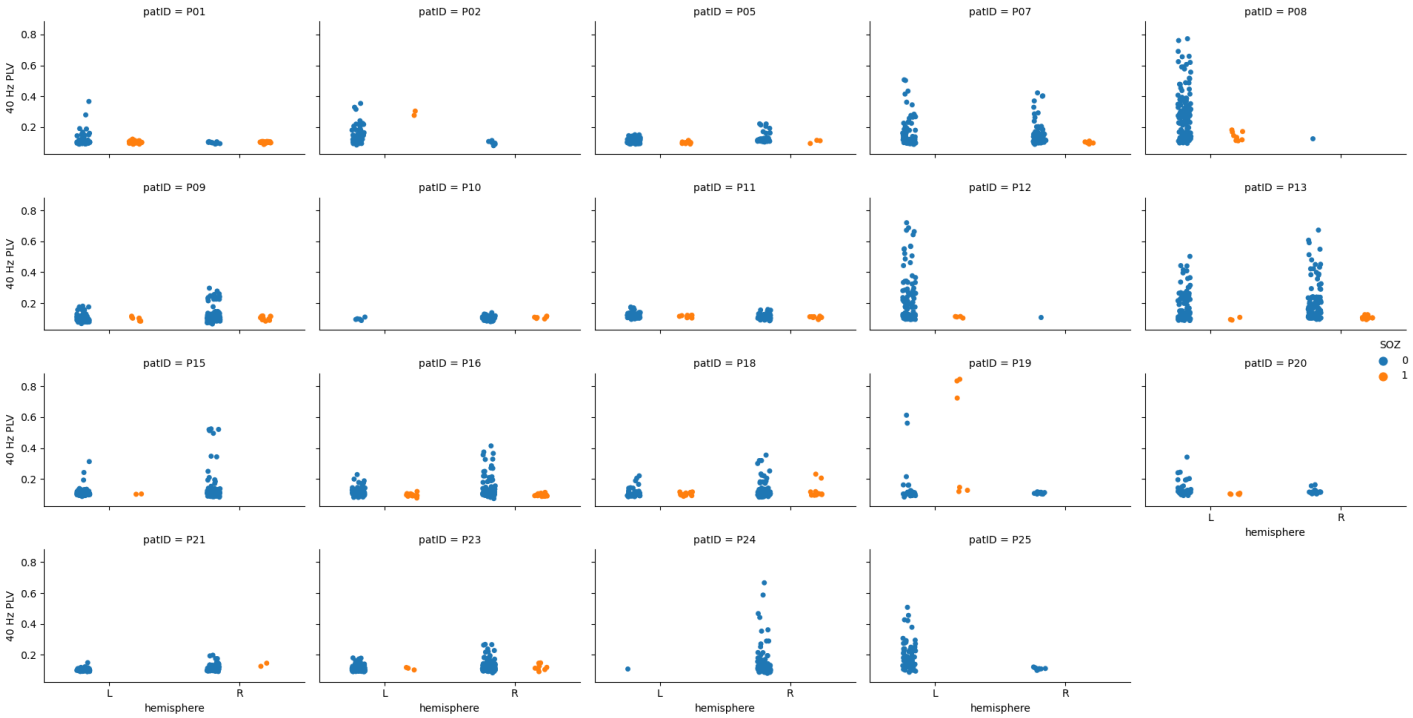

Supplementary Figure 6: 40 Hz ASSR PLV by hemisphere, monopolar montage.

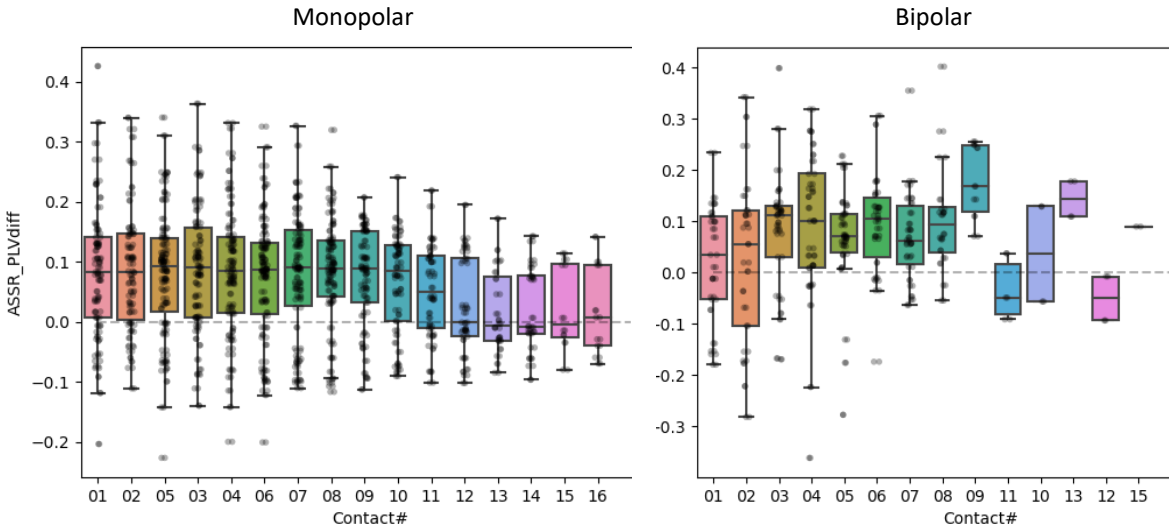

Supplementary Figure 7: ASSR PLV difference (40 Hz – 80 Hz ASSRs) by contact depth, monopolar montage. (40 – 80 Hz) trials ASSR PLVs, by contact depth – from deepest (contact #1) to more superficial contacts, from monopolar or bipolarized montages. Only significant ASSR values are considered.

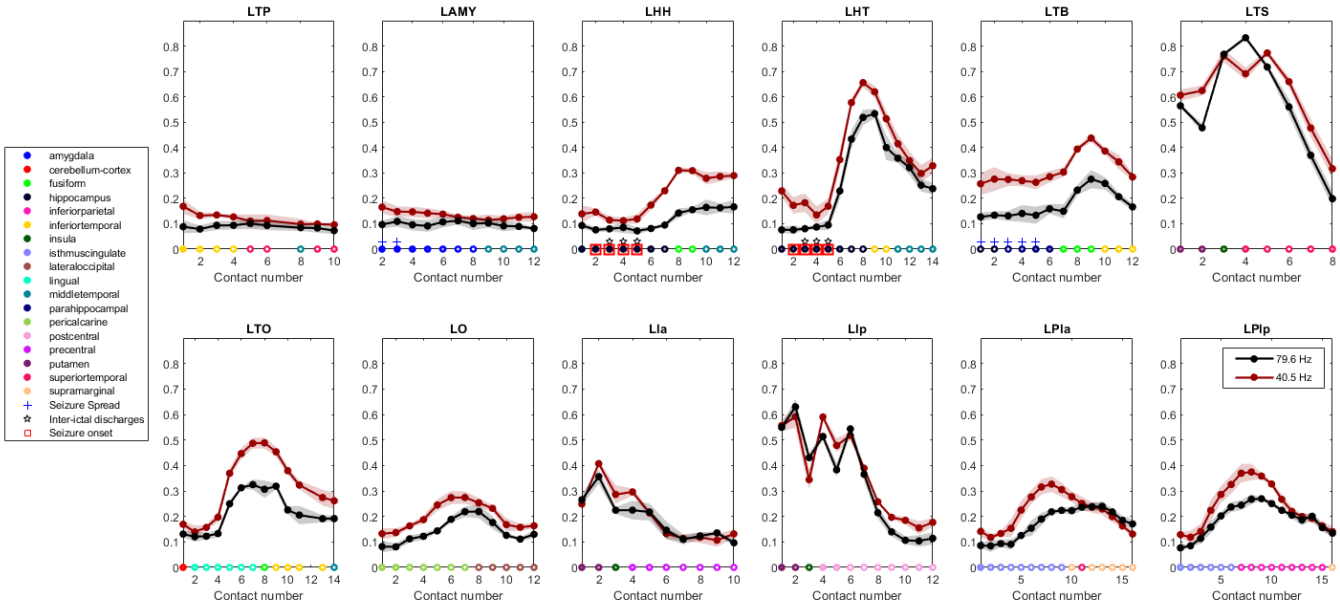

Supplementary Figure 8: 40 Hz and 80 Hz ASSR PLVs for one participant (P08). For each electrode, mean ASSR PLV values for different modulation rates across all contacts – from 1 (deepest) to most superficial contacts (10 to 16). Each contact is labeled according to the assigned brain region, with white dots indicating high probability of being within white matter. Red squares indicate SOZ contacts.

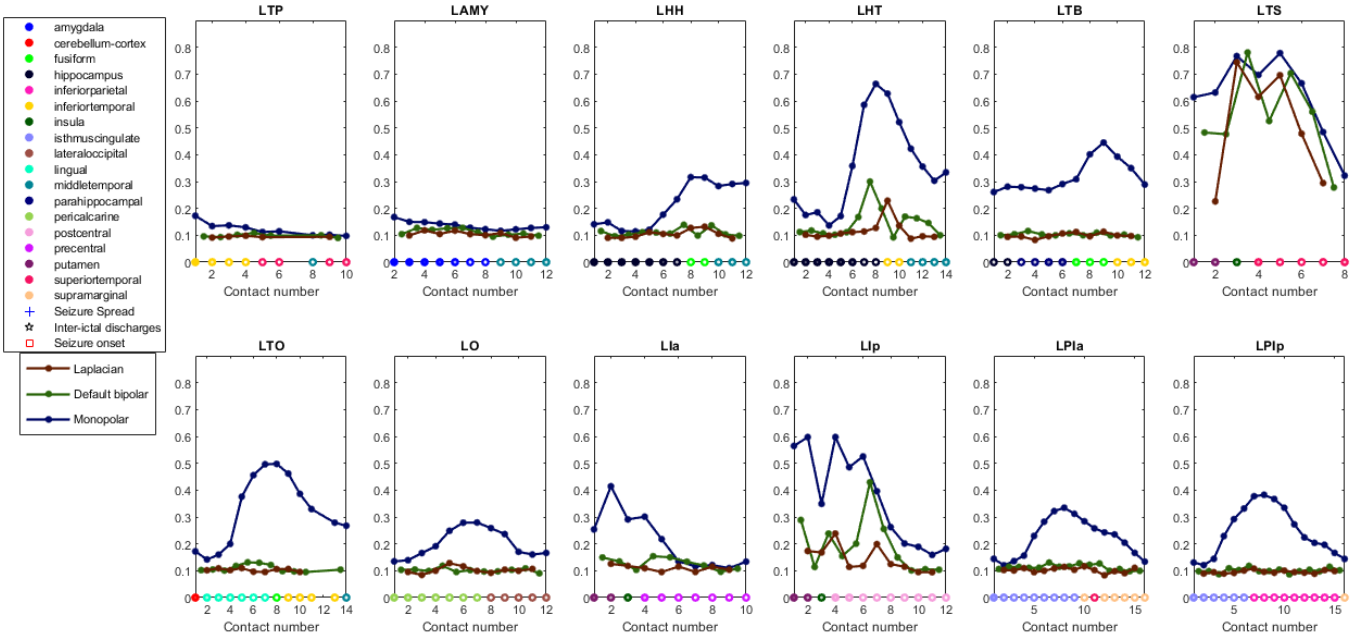

Supplementary Figure 9: 40 Hz ASSR PLV re-referencing comparisons for one participant (P08). For each electrode, ASSR PLV values for different re-referencing methods across all contacts – from 1 (deepest) to most superficial contacts (10 to 16). Each contact is labeled according to the assigned brain region, with white dots indicating high probability of being within white matter.

REFERENCES

AVOLI, M.; DE CURTIS, M.; KÖHLING, R. Does interictal synchronization influence ictogenesis? *Neuropharmacology*, v. 69, p. 37–44, jun. 2013. Disponível em: <http://linkinghub.elsevier.com/retrieve/pii/S0028390812003024>.

AXMACHER, N. *et al.* Cross-frequency coupling supports multi-item working memory in the human hippocampus. *Proceedings of the National Academy of Sciences of the United States of America*, v. 107, n. 7, p. 3228–33, 2010. Disponível em: <http://www.pubmedcentral.nih.gov/articlerender.fcgi?artid=2840289&tool=pmcentrez&rendertype=abstract>.

BADAWY, R. *et al.* The peri-ictal state: Cortical excitability changes within 24 h of a seizure. *Brain*, v. 132, n. 4, p. 1013–1021, 2009.

BADAWY, R. A. B. *et al.* Epilepsy: Ever-changing states of cortical excitability. *Neuroscience*, v. 222, p. 89–99, 2012. Disponível em: <http://dx.doi.org/10.1016/j.neuroscience.2012.07.015>.

BAJAJ, V.; PACHORI, R. B. Epileptic seizure detection based on the instantaneous area of analytic intrinsic mode functions of EEG signals. *Biomedical Engineering Letters*, v. 3, n. 1, p. 17–21, 14 abr. 2013. Disponível em: <http://link.springer.com/10.1007/s13534-013-0084-0>. Acesso em: 6 nov. 2013.

BAŞAR, E. Brain oscillations in neuropsychiatric disease. *Dialogues in Clinical Neuroscience*, v. 15, n. 3, p. 291–300, 2013.

BASTOS, A. M. *et al.* Canonical Microcircuits for Predictive Coding. *Neuron*, v. 76, n. 4, p. 695–711, 2012. Disponível em: <http://dx.doi.org/10.1016/j.neuron.2012.10.038>.

BAUD, M. O. *et al.* Multi-day rhythms modulate seizure risk in epilepsy. *Nature Communications*, v. 9, n. 1, p. 88, 8 dez. 2018. Disponível em: <http://dx.doi.org/10.1038/s41467-017-02577-y>.

BEENHAKKER, M. P.; HUGUENARD, J. R. Neurons that Fire Together Also Conspire Together: Is Normal Sleep Circuitry Hijacked to Generate Epilepsy? *Neuron*, v. 62, n. 5, p. 612–632, 2009. Disponível em: <http://dx.doi.org/10.1016/j.neuron.2009.05.015>.

BERNARD, C. Circadian/multidien Molecular Oscillations and Rhythmicity of Epilepsy (MORE). *Epilepsia*, n. June, p. 1–20, 2020.

BERTRAM, E. H. *Neuronal circuits in epilepsy: Do they matter? Experimental Neurology*. [S.l.]: Elsevier B.V. Disponível em: <http://dx.doi.org/10.1016/j.expneurol.2012.01.028>. , 2013

BERZHANSKAYA, J. *et al.* Modulation of hippocampal rhythms by subthreshold electric fields and network topology. *Journal of Computational Neuroscience*, v. 34, n. 3, p. 369–389, 2013.

BRAGIN, A.; ENGEL, J.; WILSON, C. L.; FRIED, I.; BUZSÁKI, G. High-frequency oscillations in human brain. *Hippocampus*, v. 9, n. 2, p. 137–42, 1999. Disponível em:

<http://doi.wiley.com/10.1002/(SICI)1098-1063(1999)9:2%3C137::AID-HIPO5%3E3.0.CO;2-0>.

BRAGIN, A.; ENGEL, J.; WILSON, C. L.; FRIED, I.; MATHERN, G. W. Hippocampal and entorhinal cortex high-frequency oscillations (100-500 Hz) in human epileptic brain and in kainic acid-treated rats with chronic seizures. *Epilepsia*, v. 40, n. 2, p. 127–137, 1999.

BREAKSPEAR, M. *et al.* A unifying explanation of primary generalized seizures through nonlinear brain modeling and bifurcation analysis. *Cerebral Cortex*, v. 16, n. 9, p. 1296–1313, 2006.

BRETT, T. *et al.* Detecting critical slowing down in high-dimensional epidemiological systems. *PLOS Computational Biology*, v. 16, n. 3, p. e1007679, 9 mar. 2020. Disponível em: <http://dx.doi.org/10.1371/journal.pcbi.1007679>.

BRODAL, A. *Neurological anatomy in relation to clinical medicine*. Third edit ed. New York: Oxford University Press, 1981. Disponível em: <http://doi.wiley.com/10.1002/ana.410100629>.

BUZSÁKI, G. *Rhythms of the Brain*. [S.l.]: Oxford University Press, 2006. v. 1. Disponível em: <http://www.oxfordscholarship.com/view/10.1093/acprof:oso/9780195301069.001.0001/acprof-9780195301069>. Acesso em: 5 dez. 2014.

BUZSÁKI, GYÖRGY; DRAGUHN, A. Neuronal oscillations in cortical networks. *Science (New York, N.Y.)*, v. 304, n. 5679, p. 1926–9, 25 jun. 2004. Disponível em: <http://www.sciencemag.org/content/304/5679/1926.full.pdf>.

BUZSÁKI, GYÖRGY; LOGOTHETIS, N.; SINGER, W. Scaling Brain Size, Keeping Timing: Evolutionary Preservation of Brain Rhythms. *Neuron*, v. 80, n. 3, p. 751–764, out. 2013. Disponível em: <https://linkinghub.elsevier.com/retrieve/pii/S0896627313009045>.

BUZSÁKI, GYÖRGY; WATSON, B. O. Brain rhythms and neural syntax: Implications for efficient coding of cognitive content and neuropsychiatric disease. *Dialogues in Clinical Neuroscience*, v. 14, n. 4, p. 345–367, 2012.

CANCADO, S. A. V. *Avaliação Das Respostas Auditivas Evocadas Em Regime Permanente Nos Pacientes Com Epilepsia.* 2016. Universidade Federal de Minas Gerais, 2016.

CARVALHO, VINÍCIUS R.; MORAES, M. F. D.; MENDES, E. M. A. M. On the Validity of Using Probing Stimuli for Seizure Prediction in the Epileptor Model. 2019, In: Cota V., Barone D., Dias D., Damázio L. (eds) Computational Neuroscience. LAWCN 2019. Communications in Computer and Information Science, vol 1068. Springer, Cham. <https://doi.org/10.1007/978-3-030-36636-0_20>.

CARVALHO, VINÍCIUS REZENDE *et al.* Active probing to highlight approaching transitions to ictal states in coupled neural mass models. *PLOS Computational Biology*, v. 17, n. 1, p. e1008377, 25 jan. 2021. Disponível em: <https://dx.plos.org/10.1371/journal.pcbi.1008377>.

CASALI, A. G. *et al.* A Theoretically Based Index of Consciousness Independent of Sensory Processing and Behavior. *Science Translational Medicine*, v. 5, n. 198, p. 198ra105-

198ra105, 14 ago. 2013. Disponível em: <http://stm.sciencemag.org/cgi/doi/10.1126/scitranslmed.3006294>.

CHAMPION, K. *et al.* Data-driven discovery of coordinates and governing equations. *Proceedings of the National Academy of Sciences of the United States of America*, v. 116, n. 45, p. 22445–22451, 2019.

CHANG, W. C. *et al.* Loss of neuronal network resilience precedes seizures and determines the ictogenic nature of interictal synaptic perturbations. *Nature Neuroscience*, v. 21, n. 12, p. 1742–1752, 2018. Disponível em: <http://dx.doi.org/10.1038/s41593-018-0278-y>.

CHAOVALITWONGSE, W. *et al.* Performance of a seizure warning algorithm based on the dynamics of intracranial EEG. *Epilepsy research*, v. 64, n. 3, p. 93–113, maio 2005. Disponível em: <http://www.ncbi.nlm.nih.gov/pubmed/15961284>. Acesso em: 8 nov. 2013.

CHOWDHURY, F. A.; NASHEF, L.; ELWES, R. D. C. Misdiagnosis in epilepsy: A review and recognition of diagnostic uncertainty. *European Journal of Neurology*, v. 15, n. 10, p. 1034–1042, 2008.

COSSART, R. *et al.* Dendritic but not somatic GABAergic inhibition is decreased in experimental epilepsy. *Nature Neuroscience*, v. 4, n. 1, p. 52–62, 2001.

COTA, V. R. *et al.* The epileptic amygdala: Toward the development of a neural prosthesis by temporally coded electrical stimulation. *Journal of Neuroscience Research*, v. 94, n. 6, p. 463–485, jun. 2016. Disponível em: <http://doi.wiley.com/10.1002/jnr.23741>.

DAVID, O. *et al.* Studying network mechanisms using intracranial stimulation in epileptic patients. *Frontiers in systems neuroscience*, v. 4, n. October, p. 148, 2010. Disponível em: <http://www.ncbi.nlm.nih.gov/pubmed/21060722%5Cnhttp://www.pubmedcentral.nih.gov/articlerender.fcgi?artid=PMC2972750>.

DE OLIVEIRA, J. C. *et al.* Asynchronous, bilateral, and biphasic temporally unstructured electrical stimulation of amygdalae enhances the suppression of pentylenetetrazole-induced seizures in rats. *Epilepsy Research*, v. 146, n. June 2018, p. 1–8, 2018. Disponível em: <https://doi.org/10.1016/j.eplepsyres.2018.07.009>.

DEMONT-GUIGNARD, S. *et al.* Analysis of intracerebral EEG recordings of epileptic spikes: Insights from a neural network model. *IEEE Transactions on Biomedical Engineering*, v. 56, n. 12, p. 2782–2795, 2009.

DREIFUSS, F. E. Juvenile myoclonic epilepsy: characteristics of a primary generalized epilepsy. *Epilepsia*, v. 30 Suppl 4, p. S1–S7; discussion S24-S27, 1989.

EL HOUSSAINI, K. *et al.* Seizures, refractory status epilepticus, and depolarization block as endogenous brain activities. *Physical Review E - Statistical, Nonlinear, and Soft Matter Physics*, v. 91, n. 1, p. 2–6, 2015.

ENGEL, A. K.; SINGER, W. Temporal binding and the neural correlates of sensory awareness. *Trends in Cognitive Sciences*, v. 5, n. 1, p. 16–25, 2001.

ENGEL, J. *et al.* High-frequency oscillations: What is normal and what is not? *Epilepsia*,

v. 50, n. 4, p. 598–604, 2009.

ENGEL, J. Seizures and epilepsy. *Annals of Neurology*, v. 28, n. 3, p. 398–398, set. 1989. Disponível em: <http://doi.wiley.com/10.1002/ana.410280323>. Acesso em: 29 nov. 2013.

ENGEL, J.; PEDLEY, T. *Epilepsy - A Comprehensive Textbook*. [S.l: s.n.], 1989. v. 53.

FELDMAN, D. E. The Spike-Timing Dependence of Plasticity. *Neuron*, v. 75, n. 4, p. 556–571, 2012.

FELSENSTEIN, O. *et al.* Multi-modal neuroimaging analysis and visualization tool (mmvt). *arXiv*, v. 1, n. 617, p. 1–29, 2019.

FISHER, R. S. *et al.* ILAE Official Report: A practical clinical definition of epilepsy. *Epilepsia*, v. 55, n. 4, p. 475–482, 2014. Disponível em: <http://doi.wiley.com/10.1111/epi.12550>.

FISHER, R. S.; VELASCO, A. L. Electrical brain stimulation for epilepsy. *Nature Reviews Neurology*, v. 10, n. 5, p. 261–270, 8 maio 2014. Disponível em: <http://dx.doi.org/10.1038/nrneurol.2014.59>.

FRAUSCHER, B. *et al.* High-frequency oscillations: The state of clinical research. *Epilepsia*, p. 1–14, 2017. Disponível em: <http://doi.wiley.com/10.1111/epi.13829>.

FREEMAN, W. J. A linear distributed feedback model for prepyriform cortex. *Experimental Neurology*, v. 10, n. 6, p. 525–547, dez. 1964. Disponível em: <http://www.ncbi.nlm.nih.gov/pubmed/4332108>.

FREESTONE, D. R. *et al.* A method for actively tracking excitability of brain networks using a fully implantable monitoring system. *Conference proceedings : ... Annual International Conference of the IEEE Engineering in Medicine and Biology Society. IEEE Engineering in Medicine and Biology Society. Annual Conference*, v. 2013, p. 6151–6154, 2013.

FREESTONE, D. R.; KUHLMANN, L.; *et al.* Electrical probing of cortical excitability in patients with epilepsy. *Epilepsy and Behavior*, v. 22, n. SUPPL. 1, p. S110–S118, 2011. Disponível em: <http://dx.doi.org/10.1016/j.yebeh.2011.09.005>.

FREESTONE, D. R.; BURKITT, A. N.; *et al.* Probing for cortical excitability. *Proceedings of the Annual International Conference of the IEEE Engineering in Medicine and Biology Society, EMBS*, p. 1644–1647, 2011.

FREESTONE, D. R.; KAROLY, P. J.; COOK, M. J. A forward-looking review of seizure prediction. *Current opinion in neurology*, v. 30, n. 2, p. 167–173, 2017.

FRENCH, J. A. Refractory epilepsy: Clinical overview. 2007, [S.l: s.n.], 2007. p. 3–7.

FRIDLEY, J. *et al.* Brain stimulation for the treatment of epilepsy. *Neurosurgical focus*, v. 32, n. 3, p. E13, mar. 2012. Disponível em: <http://www.ncbi.nlm.nih.gov/pubmed/24957200>. Acesso em: 14 jul. 2014.

FRIES, P. Rhythms for Cognition: Communication through Coherence. *Neuron*, v. 88, n. 1, p. 220–235, 2015. Disponível em: <http://linkinghub.elsevier.com/retrieve/pii/S0896627315008235>.

FUMEAUX, N. F. *et al.* Accurate detection of spontaneous seizures using a generalized linear model with external validation. *Epilepsia*, n. August 2019, p. 1–13, 2020.

GIRAUD, A. L.; POEPPEL, D. Cortical oscillations and speech processing: Emerging computational principles and operations. *Nature Neuroscience*, v. 15, n. 4, p. 511–517, 2012.

GODEY, B. *et al.* Neuromagnetic source localization of auditory evoked fields and intracerebral evoked potentials: A comparison of data in the same patients. *Clinical Neurophysiology*, v. 112, n. 10, p. 1850–1859, 2001.

GONZALEZ-MARTINEZ, J. A.; CHAUVEL, P. The Stereoelectroencephalography Methodology Applied to Epilepsies with a Visible Lesion. *Neurosurgery Clinics of North America*, v. 31, n. 3, p. 387–394, 2020. Disponível em: <https://doi.org/10.1016/j.nec.2020.03.010>.

GOODFELLOW, M. *et al.* Estimation of brain network ictogenicity predicts outcome from epilepsy surgery. *Scientific Reports*, v. 6, n. 1, p. 29215, 7 set. 2016. Disponível em: <http://www.nature.com/articles/srep29215>.

GRISKOVA-BULANOVA, I. *et al.* Distraction task rather than focal attention modulates gamma activity associated with auditory steady-state responses (ASSRs). *Clinical Neurophysiology*, v. 122, n. 8, p. 1541–1548, 2011. Disponível em: <http://dx.doi.org/10.1016/j.clinph.2011.02.005>.

GUÉGUIN, M. *et al.* Evidence of functional connectivity between auditory cortical areas revealed by amplitude modulation sound processing. *Cerebral Cortex*, v. 17, n. 2, p. 304–313, 2007.

HAMMOND, C.; BERGMAN, H.; BROWN, P. Pathological synchronization in Parkinson's disease: networks, models and treatments. *Trends in Neurosciences*, v. 30, n. 7, p. 357–364, 2007.

HARRIS, C. R. *et al.* Array programming with NumPy. *Nature*, v. 585, n. 7825, p. 357–362, 2020. Disponível em: <http://dx.doi.org/10.1038/s41586-020-2649-2>.

HEBBINK, J. *et al.* Pathological responses to single-pulse electrical stimuli in epilepsy: The role of feedforward inhibition. *European Journal of Neuroscience*, v. 51, n. 4, p. 1122–1136, 2020.

HEBBINK, J.; VAN GILS, S. A.; MEIJER, H. G. E. On analysis of inputs triggering large nonlinear neural responses Slow-fast dynamics in the Wendling neural mass model: Slow-fast dynamics in the Wendling neural mass model. *Communications in Nonlinear Science and Numerical Simulation*, v. 83, p. 105103, 2020. Disponível em: <https://doi.org/10.1016/j.cnsns.2019.105103>.

HERDMAN, A. T. *et al.* Intracerebral sources of human auditory steady-state responses. *Brain Topography*, v. 15, n. 2, p. 69–86, 2002.

HODGKIN, A. L.; HUXLEY, A. F. A quantitative description of membrane current and its application to conduction and excitation in nerve. *The Journal of Physiology*, v. 117, n. 4, p. 500–544, 28 ago. 1952. Disponível em:

<http://www.ncbi.nlm.nih.gov/pubmed/12991237>.

HUNTER, J. D. Matplotlib: A 2D Graphics Environment. *Computing in Science & Engineering*, v. 9, n. 3, p. 90–95, 2007. Disponível em: <http://ieeexplore.ieee.org/document/4160265/>.

IASEMIDIS, LEON D. Epileptic seizure prediction and control. *IEEE transactions on bio-medical engineering*, v. 50, n. 5, p. 549–58, maio 2003. Disponível em: <http://www.ncbi.nlm.nih.gov/pubmed/12769431>.

IASEMIDIS, LEONIDAS D. *et al.* Phase space topography and the Lyapunov exponent of electrocorticograms in partial seizures. *Brain Topography*, v. 2, n. 3, p. 187–201, 1990. Disponível em: <http://link.springer.com/10.1007/BF01140588>.

IZHIKEVICH, E. M. Neural Excitability, Spiking and Bursting. *International Journal of Bifurcation and Chaos*, v. 10, n. 06, p. 1171–1266, 2 jun. 2000. Disponível em: <http://www.worldscientific.com/doi/abs/10.1142/S0218127400000840>.

JIRSA, V. K. *et al.* On the nature of seizure dynamics. *Brain*, v. 137, n. 8, p. 2210–2230, 2014.

JIRUSKA, P. *et al.* High-Frequency Network Activity, Global Increase in Neuronal Activity, and Synchrony Expansion Precede Epileptic Seizures In Vitro. *Journal of Neuroscience*, v. 30, n. 16, p. 5690–5701, 21 abr. 2010. Disponível em: <http://www.jneurosci.org/cgi/doi/10.1523/JNEUROSCI.0535-10.2010>.

JIRUSKA, PREMYSL *et al.* Update on the mechanisms and roles of high-frequency oscillations in seizures and epileptic disorders. *Epilepsia*, v. 58, n. 8, p. 1330–1339, 2017. Disponível em: <http://doi.wiley.com/10.1111/epi.13830>.

JIRUSKA, PREMYSL; BRAGIN, A. High-frequency activity in experimental and clinical epileptic foci. *Epilepsy Research*, v. 97, n. 3, p. 300–307, dez. 2011. Disponível em: <http://linkinghub.elsevier.com/retrieve/pii/S0920121111003056>.

JIRUSKA, PREMYSL; DE CURTIS, M.; JEFFERYS, J. G. R. Modern Concepts of Focal Epileptic Networks. *International Review of Neurobiology*. [S.l: s.n.], 2014. v. 114. p. 1–7. Disponível em: <http://linkinghub.elsevier.com/retrieve/pii/B9780124186934000017>.

KALITZIN, S. *et al.* Electrical brain-stimulation paradigm for estimating the seizure onset site and the time to ictal transition in temporal lobe epilepsy. *Clinical Neurophysiology*, v. 116, n. 3, p. 718–728, 2005.

KALITZIN, S. N.; VELIS, D. N.; DA SILVA, F. H. L. Stimulation-based anticipation and control of state transitions in the epileptic brain. *Epilepsy & behavior : E&B*, v. 17, n. 3, p. 310–23, mar. 2010. Disponível em: <http://www.ncbi.nlm.nih.gov/pubmed/20163993>. Acesso em: 14 jul. 2014.

KALITZIN, STILIYAN *et al.* Enhancement of phase clustering in the EEG/MEG gamma frequency band anticipates transitions to paroxysmal epileptiform activity in epileptic patients with known visual sensitivity. *IEEE transactions on bio-medical engineering*, v. 49, n. 11, p. 1279–86, nov. 2002. Disponível em: <http://www.ncbi.nlm.nih.gov/pubmed/12450358>.

KAPLAN, H. S.; ZIMMER, M. Brain-wide representations of ongoing behavior: a universal principle? *Current Opinion in Neurobiology*, v. 64, p. 60–69, 2020. Disponível em: <https://doi.org/10.1016/j.conb.2020.02.008>.

KAROLY, P. J. *et al.* Interictal spikes and epileptic seizures: Their relationship and underlying rhythmicity. *Brain*, v. 139, n. 4, p. 1066–1078, 2016.

KAROLY, P. J. *et al.* Seizure pathways: A model-based investigation. *PLoS Computational Biology*, v. 14, n. 10, p. 1–24, 2018.

KAROLY, P. J. *et al.* The circadian profile of epilepsy improves seizure forecasting. *Brain*, v. 140, n. 8, p. 2169–2182, 2017.

KLEIN, A.; TOURVILLE, J. 101 Labeled Brain Images and a Consistent Human Cortical Labeling Protocol. *Frontiers in Neuroscience*, v. 6, n. DEC, p. 1–12, 2012.

KOZONO, N. *et al.* Auditory Steady State Response; nature and utility as a translational science tool. *Scientific Reports*, v. 9, n. 1, p. 1–10, 2019. Disponível em: <http://dx.doi.org/10.1038/s41598-019-44936-3>.

KRAMER, M. A. *et al.* Human seizures self-terminate across spatial scales via a critical transition. *Proceedings of the National Academy of Sciences*, v. 109, n. 51, p. 21116–21121, 2012. Disponível em: <http://www.pnas.org/cgi/doi/10.1073/pnas.1210047110>.

KRAMER, MARK A; CASH, S. S. Epilepsy as a Disorder of Cortical Network Organization. *The Neuroscientist*, v. 18, n. 4, p. 360–372, 10 ago. 2012. Disponível em: <http://journals.sagepub.com/doi/10.1177/1073858411422754>.

KUDELA, P.; FRANASZCZUK, P. J.; BERGEY, G. K. Model of the propagation of synchronous firing in a reduced neuron network. *Neurocomputing*, v. 26–27, p. 411–418, 1999.

KWAN, P. *et al. Long-term outcome after epilepsy surgery: Relapsing, remitting disorder? Epilepsy Currents*. [S.l: s.n.]. , 2012

LACHAUX, J. P. *et al.* Measuring phase-synchrony in brain signals. *Human Brain Mapp.*, v. 8, p. 194–208, 1999. Disponível em: <http://www.researchgate.net/publication/2499461_Measuring_Phase_Synchrony_in_Brain_Signals/file/60b7d52baa8c9a792b.pdf>. Acesso em: 5 dez. 2014.

LAINSCSEK, C. *et al.* Cortical chimera states predict epileptic seizures. *Chaos*, v. 29, n. 12, 2019.

LAINSCSEK, C.; HERNANDEZ, M. E.; *et al.* Non-Linear Dynamical Analysis of EEG Time Series Distinguishes Patients with Parkinson's Disease from Healthy Individuals. *Frontiers in Neurology*, v. 4, p. 200, 2013. Disponível em: <http://journal.frontiersin.org/article/10.3389/fneur.2013.00200/abstract>.

LAINSCSEK, C.; WEYHENMEYER, J.; *et al.* Non-Linear Dynamical Classification of Short Time Series of the Rössler System in High Noise Regimes. *Frontiers in Neurology*, v. 4, 2013. Disponível em: <http://journal.frontiersin.org/article/10.3389/fneur.2013.00182/abstract>.

LE VAN QUYEN, M. *et al.* Anticipating epileptic seizures in real time by a non-linear analysis of similarity between EEG recordings. *NeuroReport*, v. 10, n. 10, p. 2149–2155, 1999.

LECUN, Y.; BENGIO, Y.; HINTON, G. Deep learning. *Nature*, v. 521, n. 7553, p. 436–444, 2015.

LEE, J. *et al.* Neural recording and stimulation using wireless networks of microimplants. *Nature Electronics*, v. 4, n. 8, p. 604–614, 2021. Disponível em: <http://dx.doi.org/10.1038/s41928-021-00631-8>.

LEHNERTZ, K. Non-linear time series analysis of intracranial EEG recordings in patients with epilepsy--an overview. *International journal of psychophysiology : official journal of the International Organization of Psychophysiology*, v. 34, n. 1, p. 45–52, out. 1999. Disponível em: <http://www.ncbi.nlm.nih.gov/pubmed/10555873>.

LEHNERTZ, KLAUS; ELGER, C. Can epileptic seizures be predicted? Evidence from nonlinear time series analysis of brain electrical activity. *Physical Review Letters*, p. 5019–5022, 1998. Disponível em: <http://prl.aps.org/abstract/PRL/v80/i22/p5019_1>. Acesso em: 23 mar. 2014.

LEHONGRE, K. *et al.* Article Altered Low-Gamma Sampling in Auditory Cortex Accounts for the Three Main Facets of Dyslexia. *Neuron*, v. 72, p. 1080–1090, 2011.

LEROUSSEAU, J. P. *et al.* Persistent neural entrainment in the human cortex is frequency selective. v. 01, p. 1–35, 2019.

LHATOO, S. D. *et al.* Big data in epilepsy: Clinical and research considerations. Report from the Epilepsy Big Data Task Force of the International League Against Epilepsy. *Epilepsia*, n. October 2019, p. 1–15, 2020.

LI, G. *et al.* Optimal referencing for stereo-electroencephalographic (SEEG) recordings. *NeuroImage*, v. 183, p. 327–335, dez. 2018. Disponível em: <https://doi.org/10.1016/j.neuroimage.2018.08.020>.

LIÉGEOIS-CHAUVEL, C. *et al.* Evoked potentials recorded from the auditory cortex in man: evaluation and topography of the middle latency components. *Electroencephalography and Clinical Neurophysiology/ Evoked Potentials*, v. 92, n. 3, p. 204–214, 1994.

LIÉGEOIS-CHAUVEL, CATHERINE *et al.* Temporal envelope processing in the human left and right auditory cortices. *Cerebral Cortex*, v. 14, n. 7, p. 731–740, 2004.

LOPES DA SILVA, F H *et al.* Model of brain rhythmic activity. The alpha-rhythm of the thalamus. *Kybernetik*, v. 15, n. 1, p. 27–37, 31 maio 1974. Disponível em: <http://www.ncbi.nlm.nih.gov/pubmed/4853232>.

LOPES DA SILVA, FERNANDO H *et al.* Dynamical diseases of brain systems: different routes to epileptic seizures. *IEEE transactions on bio-medical engineering*, v. 50, n. 5, p. 540–8, 2003. Disponível em: <http://www.ncbi.nlm.nih.gov/pubmed/12769430>.

LOPES, M A; LEE, K. E.; GOLTSEV, A. V. Neuronal network model of interictal and recurrent ictal activity. *Physical Review E*, v. 96, n. 6, p. 1–8, 2017.

LOPES, MARINHO A. *et al.* An optimal strategy for epilepsy surgery: Disruption of the rich-club? *PLoS computational biology*, v. 13, n. 8, p. e1005637, 2017.

LOZANO, A. M.; LIPSMAN, N. Probing and Regulating Dysfunctional Circuits Using Deep Brain Stimulation. *Neuron*, v. 77, n. 3, p. 406–424, 2013. Disponível em: <http://dx.doi.org/10.1016/j.neuron.2013.01.020>.

LYTTON, W. W. Computer modelling of epilepsy. *Nature Reviews Neuroscience*, v. 9, n. 8, p. 626–637, 2008.

MARTIN, K. *et al.* Ketogenic diet and other dietary treatments for epilepsy. *Cochrane Database of Systematic Reviews*, 9 fev. 2016. Disponível em: <http://doi.wiley.com/10.1002/14651858.CD001903.pub3>.

MARTINERIE, J. *et al.* Epileptic seizures can be anticipated by non-linear analysis. *Nature medicine*, v. 4, n. 10, p. 1173–6, out. 1998. Disponível em: <http://www.ncbi.nlm.nih.gov/pubmed/9771751>.

MARTIS, R. J. *et al.* Application of empirical mode decomposition (emd) for automated detection of epilepsy using EEG signals. *International journal of neural systems*, v. 22, n. 6, p. 1250027, dez. 2012. Disponível em: <http://www.ncbi.nlm.nih.gov/pubmed/23186276>. Acesso em: 6 nov. 2013.

MATSUBARA, T.; OGATA, K.; *et al.* Altered neural synchronization to pure tone stimulation in patients with mesial temporal lobe epilepsy: An MEG study. *Epilepsy & Behavior*, v. 88, p. 96–105, nov. 2018. Disponível em: <https://doi.org/10.1016/j.yebeh.2018.08.036>.

MATSUBARA, T.; UEHARA, T.; *et al.* Hemispheric difference in temporal perception between 40- and 80-Hz auditory steady-state responses: MEG and ECoG studies. *Clinical Neurophysiology*, v. 129, n. 2018, p. e63–e64, maio 2018. Disponível em: <http://www.embase.com/search/results?subaction=viewrecord&from=export&id=L622820079%0Ahttp://dx.doi.org/10.1016/j.clinph.2018.04.160>.

MATSUBARA, T. *et al.* Monaural 40-Hz auditory steady-state magnetic responses can be useful for identifying epileptic focus in mesial temporal lobe epilepsy. *Clinical Neurophysiology*, v. 130, n. 3, p. 341–351, 2019. Disponível em: <https://doi.org/10.1016/j.clinph.2018.11.026>.

MATURANA, M. I. *et al.* Critical slowing down as a biomarker for seizure susceptibility. *Nature Communications*, v. 11, n. 1, p. 2172, 1 dez. 2020. Disponível em: <http://dx.doi.org/10.1038/s41467-020-15908-3>.

MCKINNEY, W. Data Structures for Statistical Computing in Python. 2010, [S.l: s.n.], 2010. p. 56–61. Disponível em: <https://conference.scipy.org/proceedings/scipy2010/mckinney.html>.

MEDEIROS, D. D. C. *et al.* Temporal Rearrangement of Pre-ictal PTZ Induced Spike Discharges by Low Frequency Electrical Stimulation to the Amygdaloid Complex. *Brain Stimulation*, v. 7, n. 2, p. 170–178, 25 mar. 2014. Disponível em: <http://www.ncbi.nlm.nih.gov/pubmed/24332185>. Acesso em: 22 dez. 2013.

MEISEL, C. *et al.* Failure of adaptive self-organized criticality during epileptic seizure attacks. *PLoS Computational Biology*, v. 8, n. 1, 2012.

MEISEL, C. *et al.* Intrinsic excitability measures track antiepileptic drug action and uncover increasing/decreasing excitability over the wake/sleep cycle. *Proceedings of the National Academy of Sciences*, v. 112, n. 47, p. 14694–14699, 2015. Disponível em: <http://www.pnas.org/lookup/doi/10.1073/pnas.1513716112>.

MERCIER, M. R. *et al.* Evaluation of cortical local field potential diffusion in stereotactic electro-encephalography recordings: A glimpse on white matter signal. *NeuroImage*, v. 147, p. 219–232, fev. 2017. Disponível em: <http://dx.doi.org/10.1016/j.neuroimage.2016.08.037>.

MESQUITA, M. B. S. *et al.* Distinct temporal patterns of electrical stimulation influence neural recruitment during PTZ infusion: an fMRI study. *Progress in biophysics and molecular biology*, v. 105, n. 1–2, p. 109–18, mar. 2011. Disponível em: <http://www.ncbi.nlm.nih.gov/pubmed/21044644>. Acesso em: 22 dez. 2013.

MILANOWSKI, P.; SUFFCZYNSKI, P. Seizures Start without Common Signatures of Critical Transition. *International Journal of Neural Systems*, v. 26, n. 8, p. 1–15, 2016.

MINA, F. *et al.* Model-guided control of hippocampal discharges by local direct current stimulation. *Scientific Reports*, v. 7, n. 1, p. 1–13, 2017. Disponível em: <http://dx.doi.org/10.1038/s41598-017-01867-1>.

MIRSKI, M. A. *et al.* Anticonvulsant effect of anterior thalamic high frequency electrical stimulation in the rat. *Epilepsy Research*, v. 28, n. 2, p. 89–100, 1997.

MORMANN, F. *et al.* Seizure prediction: the long and winding road. *Brain : a journal of neurology*, v. 130, n. Pt 2, p. 314–33, fev. 2007. Disponível em: <http://www.ncbi.nlm.nih.gov/pubmed/17008335>. Acesso em: 11 dez. 2013.

MOSER, E. I. *et al.* Coordination in Brain Systems. *Dynamic Coordination in the Brain: From Neurons to Mind. Strüngmann Forum Report*, n. November 2015, p. 193–214, 2010.

NAGARAJ, V. *et al.* Future of seizure prediction and intervention: Closing the loop. *Journal of Clinical Neurophysiology*, v. 32, n. 3, p. 194–206, 2015.

NAZE, S.; BERNARD, C.; JIRSA, V. Computational Modeling of Seizure Dynamics Using Coupled Neuronal Networks: Factors Shaping Epileptiform Activity. *PLoS Computational Biology*, v. 11, n. 5, p. 1–21, 2015.

NEGAHBANI, E. *et al.* Noise-Induced Precursors of State Transitions in the Stochastic Wilson–Cowan Model. *Journal of Mathematical Neuroscience*, v. 5, n. 1, p. 1–27, 2015.

O'DONNELL, B. F. *et al.* The auditory steady-state response (ASSR): a translational biomarker for schizophrenia. *Supplements to Clinical Neurophysiology*. [S.l: s.n.], 2013. v. 62. p. 101–112. Disponível em: <http://linkinghub.elsevier.com/retrieve/pii/B9780702053078000065>.

O'SULLIVAN-GREENE, E. *et al.* Probing to Observe Neural Dynamics Investigated with Networked Kuramoto Oscillators. *International Journal of Neural Systems*, v. 27, n. 01,

p. 1650038, fev. 2017. Disponível em: <http://www.worldscientific.com/doi/abs/10.1142/S0129065716500386>.

ODA, Y. *et al.* Gamma Band Neural Synchronization Deficits for Auditory Steady State Responses in Bipolar Disorder Patients. *PLoS ONE*, v. 7, n. 7, p. e39955, 5 jul. 2012. Disponível em: <http://www.ncbi.nlm.nih.gov/pubmed/24783449>.

PARKER, D. A. *et al.* Auditory steady-state EEG response across the schizo-bipolar spectrum. *Schizophrenia Research*, v. 209, n. 2019, p. 218–226, 2019. Disponível em: <https://doi.org/10.1016/j.schres.2019.04.014>.

PAZ, J. T.; HUGUENARD, J. R. Microcircuits and their interactions in epilepsy: is the focus out of focus? *Nature neuroscience*, v. 18, n. 3, p. 351–9, 2015. Disponível em: <http://www.pubmedcentral.nih.gov/articlerender.fcgi?artid=4561622&tool=pmcentrez&rendertype=abstract>.

PEDREGOSA, F. *et al.* Scikit-learn: Machine Learning in Python. *Journal of Machine Learning Research*, v. 12, p. 2825–2830, 2 jan. 2012. Disponível em: <http://arxiv.org/abs/1201.0490>.

PELED, N. *et al. Invasive Electrodes Identification and Labeling*. . [S.l: s.n.]. Disponível em: <https://github.com/pelednoam/ieil>. , 2017

PENA, R. R. *et al.* Home-cage odors spatial cues elicit theta phase/gamma amplitude coupling between olfactory bulb and dorsal hippocampus. *Neuroscience*, v. 363, p. 97–106, nov. 2017. Disponível em: <http://dx.doi.org/10.1016/j.neuroscience.2017.08.058>.

PENFIELD, WILDER & JASPER, H. *Epilepsy and the functional anatomy of the human brain,*. [S.l: s.n.], 1954.

PERUCCA, P.; DUBEAU, F.; GOTMAN, J. Intracranial electroencephalographic seizure-onset patterns: Effect of underlying pathology. *Brain*, v. 137, n. 1, p. 183–196, 2014.

PICTON, T.W. *et al.* Human auditory evoked potentials. I: Evaluation of components. *Electroencephalography and Clinical Neurophysiology*, v. 36, p. 179–190, jan. 1974. Disponível em: <http://www.sciencedirect.com/science/article/pii/0013469474901552>. Acesso em: 29 abr. 2015.

PICTON, TERENCE W. *et al.* Human Auditory Steady-State Responses: The Effects of Recording Technique and State of Arousal. *Anesthesia and Analgesia*, v. 97, n. 5, p. 1396–1402, 2003.

PICTON, TERENCE W *et al.* Human auditory steady-state responses. *International journal of audiology*, v. 42, n. 4, p. 177–219, jun. 2003. Disponível em: <http://www.ncbi.nlm.nih.gov/pubmed/12790346>. Acesso em: 16 jun. 2015.

PINTO, H.P.P. *et al.* Auditory processing assessment suggests that Wistar audiogenic rat neural networks are prone to entrainment. *Neuroscience*, v. 347, 2017.

PINTO, HYORRANA PRISCILA PEREIRA *et al.* Auditory processing assessment suggests that Wistar audiogenic rat neural networks are prone to entrainment. *Neuroscience*, v.

347, p. 48–56, 2017.

PINTO, HYORRANA PRISCILA PEREIRA *et al.* Seizure Susceptibility Corrupts Inferior Colliculus Acoustic Integration. *Frontiers in Systems Neuroscience*, v. 13, n. 1, p. 105–121, 6 nov. 2019. Disponível em: <https://www.frontiersin.org/article/10.3389/fnsys.2019.00063/full>.

PITKÄNEN, A.; SCHWARTZKROIN, P. A.; MOSHÉ, S. L. *Models of Seizures and Epilepsy*. [S.l.]: Elsevier, 2006. Disponível em: <http://linkinghub.elsevier.com/retrieve/pii/B9781845692155500474>.

POCKETT, S.; TAN, S. M. The auditory steady-state response is not a suitable monitor of anesthesia. *Anesthesia and Analgesia*, v. 95, n. 5, p. 1318–1323, 2002.

POELMANS, H. *et al.* Hemispheric asymmetry of auditory steady-state responses to monaural and diotic stimulation. *JARO - Journal of the Association for Research in Otolaryngology*, v. 13, n. 6, p. 867–876, 2012.

PRIME, D. *et al.* Considerations in performing and analyzing the responses of cortico-cortical evoked potentials in stereo-EEG. *Epilepsia*, v. 59, n. 1, p. 16–26, jan. 2018. Disponível em: <http://doi.wiley.com/10.1111/epi.13939>.

PROIX, T. *et al.* Permittivity Coupling across Brain Regions Determines Seizure Recruitment in Partial Epilepsy. *Journal of Neuroscience*, v. 34, n. 45, p. 15009–15021, 2014. Disponível em: <http://www.jneurosci.org/cgi/doi/10.1523/JNEUROSCI.1570-14.2014>.

PROIX, TIMOTHÉE *et al.* Individual brain structure and modelling predict seizure propagation. *Brain*, v. 140, n. 3, p. 641–654, 21 mar. 2017. Disponível em: <https://academic.oup.com/brain/article-lookup/doi/10.1093/brain/awx004>.

QUIAN QUIROGA, R.; PANZERI, S. Extracting information from neuronal populations: information theory and decoding approaches. *Nature Reviews Neuroscience*, v. 10, n. 3, p. 173–185, mar. 2009. Disponível em: <http://www.nature.com/articles/nrn2578>.

RAMGOPAL, S. *et al.* Seizure detection, seizure prediction, and closed-loop warning systems in epilepsy. *Epilepsy and Behavior*, v. 37, p. 291–307, 2014. Disponível em: <http://dx.doi.org/10.1016/j.yebeh.2014.06.023>.

ROSENOW, F.; LÜDERS, H. Presurgical evaluation of epilepsy. *Brain*, v. 124, n. Pt 9, p. 1683–700, 1 set. 2001. Disponível em: <http://www.pediatricneurosciences.com/text.asp?2008/3/1/74/40593>.

ROSS, B. *et al.* Frequency specificity of 40-Hz auditory steady-state responses. *Hearing Research*, v. 186, n. 1–2, p. 57–68, dez. 2003. Disponível em: <https://linkinghub.elsevier.com/retrieve/pii/S0378595503002995>.

ROSS, B. C. Mutual Information between Discrete and Continuous Data Sets. *PLoS ONE*, v. 9, n. 2, p. e87357, 19 fev. 2014. Disponível em: <https://dx.plos.org/10.1371/journal.pone.0087357>.

SACKELLARES, J. C. Current Review in Clinical Science - Seizure Prediction. *Epilepsy Currents*, v. 8, n. 3, p. 55–59, 2008.

SANCHEZ-CARPINTERO, R. *et al.* Abnormal brain gamma oscillations in response to auditory stimulation in Dravet syndrome. *European Journal of Paediatric Neurology*, v. 24, n. xxxx, p. 134–141, jan. 2020. Disponível em: <https://doi.org/10.1016/j.ejpn.2019.12.004>.

SANZ PERL, Y. *et al.* Perturbations in dynamical models of whole-brain activity dissociate between the level and stability of consciousness. *PLOS Computational Biology*, v. 17, n. 7, p. e1009139, 2021.

SCHARFMAN, H. E. The neurobiology of epilepsy. *Current Neurology and Neuroscience Reports*, v. 7, n. 4, p. 348–354, 2007.

SCHAWORONKOW, N.; VOYTEK, B. Enhancing oscillations in intracranial electrophysiological recordings with data-driven spatial filters. *PLOS Computational Biology*, v. 17, n. 8, p. e1009298, 2021. Disponível em: <http://dx.doi.org/10.1371/journal.pcbi.1009298>.

SCHEFFER, M. *et al.* Anticipating Critical Transitions. *Science*, v. 338, n. 6105, p. 344–348, 19 out. 2012. Disponível em: <https://www.sciencemag.org/lookup/doi/10.1126/science.1225244>.

SCHEFFER, M. *et al.* Early-warning signals for critical transitions. *Nature*, v. 461, n. 7260, p. 53–59, 2009. Disponível em: <http://dx.doi.org/10.1038/nature08227>.

SCHELTER, B.; TIMMER, J.; SCHULZE-BONHAGE, A. *Seizure prediction in epilepsy: from basic mechanisms to clinical applications*. [S.l: s.n.], 2008. Disponível em: <http://link.springer.com/chapter/10.1007/0-306-48610-5_12>. Acesso em: 4 set. 2014.

SCHRATER, P.; KORDING, K.; BLOHM, G. Modeling in Neuroscience as a Decision Process. 2019, Brentwood, Tennessee, USA: Cognitive Computational Neuroscience, 2019. Disponível em: <https://ccneuro.org/2019/Papers/ViewPapers.asp?PaperNum=1176>.

SEGAL, M. A correlation between hippocampal responses to interhemispheric stimulation, hippocampal slow rhythmic activity and behaviour. *Electroencephalography and Clinical Neurophysiology*, v. 45, n. 3, p. 409–411, set. 1978. Disponível em: <https://linkinghub.elsevier.com/retrieve/pii/001346947890192X>.

SILVA, F. L. DA; NIEDERMEYER, E. *Electroencephalography: Basic Principles, Clinical Applications, and Related Fields*. Fifth edit ed. [S.l.]: Lippincott Williams & Wilkins, 2010. Disponível em: <http://www.amazon.com/Electroencephalography-Principles-Clinical-Applications-Related-ebook/dp/B0080KAWAA>.

SINHA, N. *et al.* Predicting neurosurgical outcomes in focal epilepsy patients using computational modelling. *Brain*, v. 140, n. 2, p. 319–332, 2017.

SPORNS, O.; ZWI, J. D. The small world of the cerebral cortex. *Neuroinformatics*, v. 2, n. 2, p. 145–162, 2004.

STACEY, W. C.; LITT, B. Technology insight: neuroengineering and epilepsy-designing devices for seizure control. *Nature clinical practice. Neurology*, v. 4, n. 4, p. 190–201, abr. 2008. Disponível em:

<http://www.pubmedcentral.nih.gov/articlerender.fcgi?artid=2904395&tool=pmcentrez&rendertype=abstract>. Acesso em: 8 nov. 2013.

STALEY, K. J.; DUDEK, F. E. Interictal Spikes and Epileptogenesis. *Epilepsy Currents*, v. 6, n. 6, p. 199–202, 2006.

STEAD, M. *et al.* Microseizures and the spatiotemporal scales of human partial epilepsy. *Brain*, v. 133, n. 9, p. 2789–2797, 2010.

STRINGER, C. *et al.* Spontaneous behaviors drive multidimensional, brainwide activity. *Science*, v. 364, n. 6437, 2019.

SUFFCZYNSKI, P. *et al.* Active paradigms of seizure anticipation: Computer model evidence for necessity of stimulation. *Physical Review E - Statistical, Nonlinear, and Soft Matter Physics*, v. 78, n. 5, p. 1–9, 2008.

TALAIRACH, J. *et al.* Functional stereotaxic investigations in epilepsy. Methodological remarks concerning a case. *Revue neurologique*, v. 105, p. 119–30, ago. 1961. Disponível em: <http://www.ncbi.nlm.nih.gov/pubmed/13919300>.

THEODORE, W.; FISHER, R. Brain stimulation for epilepsy. *The Lancet Neurology*, v. 3, n. February, p. 111–118, 2004. Disponível em: <http://www.sciencedirect.com/science/article/pii/S1474442203006641>. Acesso em: 8 nov. 2013.

TORT, A. B. L. *et al.* Dynamic cross-frequency couplings of local field potential oscillations in rat striatum and hippocampus during performance of a T-maze task. *Proceedings of the National Academy of Sciences of the United States of America*, v. 105, n. 51, p. 20517–20522, 2008.

TRAUB, R. D. *et al.* Single-column thalamocortical network model exhibiting gamma oscillations, sleep spindles, and epileptogenic bursts. *Journal of neurophysiology*, v. 93, n. 4, p. 2194–232, 10 nov. 2005. Disponível em: <http://jn.physiology.org/cgi/doi/10.1152/jn.00983.2004>.

VALENTIN, A. Responses to single pulse electrical stimulation identify epileptogenesis in the human brain in vivo. *Brain*, v. 125, n. 8, p. 1709–1718, 1 ago. 2002. Disponível em: <https://academic.oup.com/brain/article-lookup/doi/10.1093/brain/awf187>.

VALENTÍN, A. *et al.* Single pulse electrical stimulation for identification of structural abnormalities and prediction of seizure outcome after epilepsy surgery: a prospective study. *The Lancet Neurology*, v. 4, n. 11, p. 718–726, 2005. Disponível em: <http://linkinghub.elsevier.com/retrieve/pii/S1474442205702003>.

VAN DIESSEN, E. *et al.* Functional and structural brain networks in epilepsy: What have we learned? *Epilepsia*, v. 54, n. 11, p. 1855–1865, 2013.

VARELA, F. *et al.* The brainweb: phase synchronization and large-scale integration. *Nature reviews. Neuroscience*, v. 2, n. 4, p. 229–239, 2001. Disponível em: <http://www.ncbi.nlm.nih.gov/pubmed/11283746>.

VERAART, A. J. *et al.* Recovery rates reflect distance to a tipping point in a living system. *Nature*, v. 481, n. 7381, p. 357–359, 2012.

VIRTANEN, P. *et al. SciPy 1.0--Fundamental Algorithms for Scientific Computing in Python*. . [S.l: s.n.]. , 2019

VONCK, K. *et al.* A decade of experience with deep brain stimulation for patients with refractory medial temporal lobe epilepsy. *International Journal of Neural Systems*, v. 23, n. 1, 2013.

WANG, Y. *et al.* Interictal intracranial electroencephalography for predicting surgical success : The importance of space and time. n. May, p. 1–10, 2020.

WANG, Y. C. *et al.* Probing circuit of Papez with stimulation of anterior nucleus of the thalamus and hippocampal evoked potentials. *Epilepsy Research*, v. 159, n. October 2019, p. 106248, 2020. Disponível em: <https://doi.org/10.1016/j.eplepsyres.2019.106248>.

WELCH, P. The use of fast Fourier transform for the estimation of power spectra: A method based on time averaging over short, modified periodograms. *IEEE Transactions on Audio and Electroacoustics*, v. 15, n. 2, p. 70–73, jun. 1967. Disponível em: <http://148.204.64.201/paginas anexas/voz/articulos interesantes/IEEE DSP/IEEE DSP/55.pdf>. Acesso em: 21 mar. 2014.

WENDLING, F. *et al.* Brain (Hyper)Excitability Revealed by Optimal Electrical Stimulation of GABAergic Interneurons. *Brain Stimulation*, v. 9, n. 6, p. 919–932, 2016. Disponível em: <http://dx.doi.org/10.1016/j.brs.2016.07.001>.

WENDLING, FABRICE *et al. Computational models of epileptiform activity*. *Journal of Neuroscience Methods*. [S.l.]: Elsevier B.V. Disponível em: <http://dx.doi.org/10.1016/j.jneumeth.2015.03.027>. , 2016

WENDLING, FABRICE *et al.* Epileptic fast activity can be explained by a model of impaired GABAergic dendritic inhibition. *European Journal of Neuroscience*, v. 15, n. 9, p. 1499–1508, 2002.

WENDLING, FABRICE *et al.* Epileptic fast intracerebral EEG activity: evidence for spatial decorrelation at seizure onset. *Brain*, v. 126, n. Pt 6, p. 1–18, 2003.

WENDLING, FABRICE *et al.* Interictal spikes, fast ripples and seizures in partial epilepsies - combining multi-level computational models with experimental data. *European Journal of Neuroscience*, v. 36, n. 2, p. 2164–2177, 2012.

WENDLING, FABRICE *et al.* Interictal to ictal transition in human temporal lobe epilepsy: Insights from a computational model of intracerebral EEG. *Journal of Clinical Neurophysiology*, v. 22, n. 5, p. 343–356, 2005.

WICHMANN, T.; DELONG, M. R. Deep Brain Stimulation for Neurologic and Neuropsychiatric Disorders. *Neuron*, v. 52, n. 1, p. 197–204, 2006.

WILKAT, T.; RINGS, T.; LEHNERTZ, K. No evidence for critical slowing down prior to human epileptic seizures. *Chaos*, v. 29, n. 9, 2019.

WILSON, H. R.; COWAN, J. D. Excitatory and Inhibitory Interactions in Localized Populations of Model Neurons. *Biophysical Journal*, v. 12, n. 1, p. 1–24, dez. 1972. Disponível em: <http://linkinghub.elsevier.com/retrieve/pii/0014488664900494>.

WORLD HEALTH ORGANIZATION. *Fact Sheet about Epilepsy*. Disponível em: <http://www.who.int/mediacentre/factsheets/fs999/en/>. Acesso em: 17 mar. 2015.

ZIJLMANS, M. *et al.* High-frequency oscillations as a new biomarker in epilepsy. *Annals of Neurology*, v. 71, n. 2, p. 169–178, 2012.

ZWEIPHENNING, W. J. E. M. *et al.* Increased gamma and decreased fast ripple connections of epileptic tissue: A high-frequency directed network approach. *Epilepsia*, n. December 2017, p. epi.16296, 2019. Disponível em: <https://onlinelibrary.wiley.com/doi/abs/10.1111/epi.16296>.

ZWILLINGER, D.; KOKOSKA, S. *CRC Standard Probability and Statistics Tables and Formulae*. New York: Chapman & Hall, 2000.

APPENDIX

PLOS COMPUTATIONAL BIOLOGY

RESEARCH ARTICLE

Active probing to highlight approaching transitions to ictal states in coupled neural mass models

Vinícius Rezende Carvalho[1,2,3], **Márcio Flávio Dutra Moraes**[2,4], **Sydney S. Cash**[3], **Eduardo Mazoni Andrade Marçal Mendes**[1,2,4]*

1 Programa de Pós-Graduação em Engenharia Elétrica, Universidade Federal de Minas Gerais, Belo Horizonte, Brazil, **2** Núcleo de Neurociências, Departamento de Fisiologia e Biofísica, Instituto de Ciências Biológicas, Universidade Federal de Minas Gerais, Belo Horizonte, Brazil, **3** Department of Neurology, Massachusetts General Hospital and Harvard Medical School, Boston, Massachusetts, United States of America, **4** Centro de Tecnologia e Pesquisa em Magneto-Ressonância, Escola de Engenharia, Universidade Federal de Minas Gerais, Belo Horizonte, Brazil

* emmendes@cpdee.ufmg.br

Check for updates

OPEN ACCESS

Citation: Carvalho VR, Moraes MFD, Cash SS, Mendes EMAM (2021) Active probing to highlight approaching transitions to ictal states in coupled neural mass models. PLoS Comput Biol 17(1): e1008377. https://doi.org/10.1371/journal.pcbi.1008377

Editor: Peter Neal Taylor, Newcastle University, UNITED KINGDOM

Received: October 1, 2020

Accepted: December 2, 2020

Published: January 25, 2021

Peer Review History: PLOS recognizes the benefits of transparency in the peer review process; therefore, we enable the publication of all of the content of peer review and author responses alongside final, published articles. The editorial history of this article is available here: https://doi.org/10.1371/journal.pcbi.1008377

Copyright: © 2021 Carvalho et al. This is an open access article distributed under the terms of the Creative Commons Attribution License, which permits unrestricted use, distribution, and reproduction in any medium, provided the original author and source are credited.

Data Availability Statement: All Python scripts are available at https://github.com/vrcarva/WNMM_probing.

Abstract

The extraction of electrophysiological features that reliably forecast the occurrence of seizures is one of the most challenging goals in epilepsy research. Among possible approaches to tackle this problem is the use of active probing paradigms in which responses to stimuli are used to detect underlying system changes leading up to seizures. This work evaluates the theoretical and mechanistic underpinnings of this strategy using two coupled populations of the well-studied Wendling neural mass model. Different model settings are evaluated, shifting parameters (excitability, slow inhibition, or inter-population coupling gains) from normal towards ictal states while probing stimuli are applied every 2 seconds to the input of either one or both populations. The correlation between the extracted features and the ictogenic parameter shifting indicates if the impending transition to the ictal state may be identified in advance. Results show that not only can the response to the probing stimuli forecast seizures but this is true regardless of the altered ictogenic parameter. That is, similar feature changes are highlighted by probing stimuli responses in advance of the seizure including: increased response variance and lag-1 autocorrelation, decreased skewness, and increased mutual information between the outputs of both model subsets. These changes were mostly restricted to the stimulated population, showing a local effect of this perturbational approach. The transition latencies from normal activity to sustained discharges of spikes were not affected, suggesting that stimuli had no pro-ictal effects. However, stimuli were found to elicit interictal-like spikes just before the transition to the ictal state. Furthermore, the observed feature changes highlighted by probing the neuronal populations may reflect the phenomenon of critical slowing down, where increased recovery times from perturbations may signal the loss of a systems' resilience and are common hallmarks of an impending critical transition. These results provide more evidence that active probing approaches highlight information about underlying system changes involved in ictogenesis and may be able to play a role in assisting seizure forecasting methods which can